IZMIR KATIP CELEBI UNIVERSITY ★ GRADUATE SCHOOL OF NATURAL AND APPLIED SCIENCES

MODELING AND EXPERIMENTAL STUDY OF TURBULENT NEWTONIAN FLUID IN FULLY ECCENTRIC ANNULUS CONSIDERING TEMPERATURE AND PIPE ROTATION EFFECTS

Ph.D. DISSERTATION

Erman ÜLKER

Department of Civil Engineering

Thesis Advisor: Assoc. Prof. Mehmet SORGUN

OCTOBER 2017

IZMIR KATIP CELEBI UNIVERSITY ★ GRADUATE SCHOOL OF NATURAL AND APPLIED SCIENCES

MODELING AND EXPERIMENTAL STUDY OF TURBULENT NEWTONIAN FLUID IN FULLY ECCENTRIC ANNULUS CONSIDERING TEMPERATURE AND PIPE ROTATION EFFECTS

Ph.D. DISSERTATION

Erman ÜLKER
(D130104001)

Department of Civil Engineering

Thesis Advisor: Assoc. Prof. Mehmet SORGUN

OCTOBER 2017

İZMİR KATİP ÇELEBİ ÜNİVERSİTESİ ★ FEN BİLİMLERİ ENSTİTÜSÜ

SICAKLIK VE BORU DÖNME HIZI DİKKATE ALINARAK AYRI
MERKEZLİ BORULAR ARASINDAN AKAN TÜRBÜLANSLI NEWTONIAN
AKIŞKANIN MODELLENMESİ VE DENEYSEL ÇALIŞMASI

DOKTORA TEZİ

Erman ÜLKER
(D130104001)

İnşaat Mühendisliği Bölümü

Tez Danışmanı: Doç. Dr. Mehmet SORGUN

EKİM 2017

Erman ÜLKER, a **Ph.D.** student of **IZMIR KATIP CELEBI UNIVERSITY Graduate School of Natural and Applied Sciences**, D130104001, successfully defended the **dissertation** entitled "**MODELING AND EXPERIMENTAL STUDY OF TURBULENT NEWTONIAN FLUID IN FULLY ECCENTRIC ANNULUS CONSIDERING TEMPERATURE AND PIPE ROTATION EFFECTS**", which he prepared after fulfilling the requirements specified in the

Thesis Advisor : **Assoc. Prof. Mehmet SORGUN**   ....
Izmir Katip Celebi University

Jury Members : **Professor Birol KAYA**   ....
Dokuz Eylul University

 Assoc. Prof. İsmail SOLMUŞ   ....
Ataturk University

 Assoc. Prof. Mustafa DOĞAN   ....
Dokuz Eylul University

 Asst. Prof. Ziya Haktan KARADENİZ   ....
Izmir Katip Celebi University

Date of Submission :
Date of Defense   :

To my family,

FOREWORD

In the following dissertation, I have tried to give a new perspective for modeling of temperature effect on frictional pressure loss of Newtonian fluid in an annulus including inner pipe rotation. The introduced model brings a different approach compared to the other theoretical and experimental approaches.

It has been a remarkable experience working on this kind of subject for my dissertation. This Ph.D. dissertation was prepared at İzmir Katip Çelebi University under the supervision of Assoc. Prof. Mehmet Sorgun. I would like to give my heartful gratitude to him for his guidance, motivation and invaluable advice throughout my education.

I would like to also give my sincere thanks to my family, my relatives, and persons who always encourage me by being at my side no matter what.

I believe that I presented an useful study which brings one of the precursor touches that incorporates a different reasoning process in contradistinction to former approaches.

October 2017   Erman ÜLKER

TABLE OF CONTENTS

ABBREVIATIONS AND NOMENCLATURE

RPM	: Revolution Per Minute $[T^{-1}]$	
Re	: Reynolds Number	
Ta	: Taylor Number	
Pr	: Prandtl Number	
c_p	: Specific Heat $[L^2 \Theta^{-1} T^{-2}]$	
k	: Thermal Conductivity $[M L \Theta^{-1} T^{-3}]$	
g	: Gravitational Acceleration $[M L^{-2}]$	
ω	: Pipe Rotation Speed $[T^{-1}]$	
H	: Slot Height $[L]$	
D_i	: Inner Pipe Diameter $[L]$	
D_o	: Outer Pipe Diameter $[L]$	
t	: Time $[T]$	
P	: Pressure $[M L^{-1} T^{-2}]$	
u, v, w	: Velocity Components in x,y,z Directions $[L T^{-1}]$	
ρ	: Density $[M L^{-3}]$	
τ_{ij}	: Stress Tensor $[M L^{-1} T^{-2}]$	
$\bar{u}, \bar{v}, \bar{w}$	: Mean Velocity Components $[L T^{-1}]$	
$\acute{u}, \acute{v}, \acute{w}$	: Fluctuating Velocity Components $[L T^{-1}]$	
r_i	: Inner Pipe Radius $[L]$	
r_o	: Outer Pipe Radius $[L]$	
υ	: Kinematic Viscosity $[L^2 T^{-1}]$	
θ	: Angle	
μ	: Dynamic Viscosity $[M L^{-1} T^{-1}]$	
l_m	: Mixing Length $[L]$	
μ_t	: Turbulent Viscosity $[M L^{-1} T^{-1}]$	
κ	: von Karman Constant	
A	: van Driest's Damping Constant	

LIST OF TABLES

LIST OF FIGURES

MODELING AND EXPERIMENTAL STUDY OF TURBULENT NEWTONIAN FLUID IN FULLY ECCENTRIC ANNULUS CONSIDERING TEMPERATURE AND PIPE ROTATION EFFECTS

SUMMARY

In this work, the effect of temperature on the pressure loss of Newtonian fluid in a fully eccentric annulus with pipe rotation is investigated. For this purpose, initially comprehensive experimental study has been conducted at Izmir Katip Celebi University (IKCU), Fluid Mechanics and Hydraulics Laboratory of Civil Engineering Department. Effect of temperature has been observed for flow velocities from 0.7 m/s to 3.4 m/s, for pipe rotations from 0 rpm to 120 rpm, and for temperatures is from 20 °C to 65 °C. The pressure loss within the test section is recorded. An increase in the liquid temperature results in a decrease in pressure gradient. On the other hand, the influence of temperature on pressure gradient becomes more significant, as the Reynolds number is raised. Variation of Taylor number causes negligible changes on frictional pressure losses for all temperature conditions considered. By using regression analysis of the dataset obtained from the experimental work, a simple empirical frictional pressure losses correlation taking into account of temperature effect is proposed. The proposed correlation could estimate the frictional pressure gradient within an error range of $\pm 5\%$.

Numerical methods frequently are used to solve turbulent flow problems due to the trouble in solving Navier-Stokes equations. Navier-Stokes equations including inner pipe rotation and temperature effects are solved via two different numerical techniques. Firstly, a developed numerical method presents the discretization of the equation with finite difference method and solved iteratively by fixing the nonlinear terms. Secondly, Newton-Raphson method is used to linearize the equation and then solve iteratively. The efficiency of the proposed scheme is compared with the

obtained solutions of the Newton-Raphson method. The proposed numerical method is computationally expensive, however, it may allow tackling the non-linearity of challenging problems in hydraulics. Moreover, a mechanistic model including proposed numerical method is developed in order to determine frictional pressure gradient for fully developed turbulent flow through fully eccentric horizontal annulus including pipe rotation and temperature. The computational frameworks are developed in MATLAB. A mathematical model is confirmed by the experimental study. Results show that computational fluid model is capable of estimating frictional pressure gradient with an error of less than 16.2%.

Keywords: frictional pressure loss, inner pipe rotation, temperature, correlation, mechanistic model

SICAKLIK VE BORU DÖNME HIZI DİKKATE ALINARAK AYRI MERKEZLİ BORULAR ARASINDAN AKAN TÜRBÜLANSLI NEWTONIAN AKIŞKANIN MODELLENMESİ VE DENEYSEL ÇALIŞMASI

ÖZET

Bu çalışmada iç içe geçmiş farklı merkezli (tam eksantrik) iki boru arasında akan Newton tipi akışkanlarda içteki borunun dönmesi durumunda sıcaklığın basınç farkına etkisi araştırılmıştır. Bu amaçla, İzmir Katip Çelebi Üniversitesi (İKÇÜ) İnşaat Mühendisliği Bölümü Akışkanlar Mekaniği ve Hidrolik Laboratuvarı'nda kapsamlı bir deneysel çalışma yapılmıştır. Sıcaklığın etkisi akışkan hızının 0.7 m/s ile 3.4 m/s arasında olduğu durumda, boru dönme hızının 0 ile 120 devir/dakika arasında olduğu durumda, ve 20 °C ile 65 °C sıcaklık aralığında gözlemlenmiştir. Deney düzeneğindeki basınç farkları kaydedilmiştir. Akışkan sıcaklığındaki artış basınç gradyeninde düşüşe yol açmaktadır. Bununla beraber, Reynolds Sayısı'nın artmasıyla birlikte sıcaklığın basınç gradyeni üzerindeki etkisi daha önemli hale gelmektedir. Diğer yandan ise, farklı Taylor Sayısı'nın deney aralığındaki bütün sıcaklık değerlerinde sürtünmeyle ilgili basınç kaybında ihmal edilebilir bir etkisi olduğu görülmüştür. Deneysel çalışmadan elde edilen verilerin regresyon analizi ile incelenmesi sonucunda, basınç kayıplarını sıcaklığın etkisini de dikkate alan basit bir ampirik denklem önerilmiştir. Önerilen denklem basınç gradyenini ±%5 hata payı ile tahmin edebilmektedir.

Navier-Stokes denklemlerinin çözümündeki zorluk sebebiyle, sayısal metotlar türbülanslı akış problemlerinde sıklıkla kullanılır. İçteki borunun dönmesi ve sıcaklık etkilerini içeren Navier-Stokes denklemleri iki farklı sayısal teknikle çözülmüştür. İlk olarak, önerilen sayısal metot, sonlu farklar metodu ile denklemin ayrıştırılmasını ve lineer olmayan terimlerin sabitlenerek iteratif olarak çözümlenmesini içerir.

İkincisi ise, Newton-Raphson metodu ile denklemin doğrusallaştırılması ve daha sonra iteratif olarak çözümünü içerir. Önerilen metodun verimliliği, Newton-Raphson metodundan elde edilen çözümler ile karşılaştırılmıştır. Önerilen sayısal metodun hesaplaması daha uzun sürmesine rağmen, hidrolikteki lineer olmayan meşakatli problemlerin üstesinden gelmeye yarayabilir. Ek olarak, boru dönmesini içeren iç içe geçmiş farklı merkezli borular arasından geçen tam gelişmiş türbülanslı akışlardaki sürtünmeye bağlı basınç farkını belirleyebilmek için önerilen sayısal metodu içeren bir mekanistik model geliştirilmiştir. Sayısal hesaplamalar MATLAB'ta geliştirilen kodlarla yapılmıştır. Yapılan sayısal hesaplamalar deneysel sonuçlarla teyit edilmiştir. Elde edilen sonuçlar, hesaplamalı akışkanlar modelinin sürtünmeye bağlı basınç farkını %16.2'den daha az bir hata ile tahmin edebildiğini göstermiştir.

Anahtar Kelimeler: basınç kaybı, içteki boru dönmesi, sıcaklık, korelasyon, mekanistik model

1. INTRODUCTION

1.1 Description of The Problem

Flow through annulus has many applications in civil engineering as well as other engineering branches such as petroleum engineering, mechanical engineering, etc. Some examples of these applications are cleaning of geothermal, oil and gas wells and heat exchanger, which is a device for transferring heat from one medium to another.

Among the annular flow used in technology, drilling oil wells is the most popular research area for the scientists. However, there are many crucial applications, which requires annular flow characteristics as well. For instance, processing industrial waste with slurries and suspensions, mass transport in blood through veins, and extrude plastics and polymers. The mathematical insight of those applications is far from trivial. Comprehensive understanding of the physical behavior of fluid flow requires in order getting accurate solutions. Just recently, it has been gradually available to predict all features of the annular flow including its affecting parameters such as flow velocity, rotating cylinder, eccentricity.

It is well known that temperature is a property that plays a significant role in changing liquid rheology. Increasing liquid temperature causes decreasing in viscosity. For instance, the viscosity of water at 62 °C is almost half of the viscosity of water at room temperature. It is common to assume that viscosity of liquids decreases linearly with increasing temperature. However, there are generally significant increases in the suspension viscosity, yield point and the gelling tension of the liquid due to accumulation when the temperature reach or pass the critical temperature of the liquid.This causes instability of the liquid. Therefore, the above assumption of viscosity relation with temperature for the non-Newtonian fluid may

not be valid. For this reason, it is necessary to conduct an intensive investigation of temperature effect on liquids.

Additional parameter on the fluid flow brings more complexity and requires experimental study in order to understand physical behavior of the corresponding parameters. Several factors can affect hydraulics and characteristics of the annular flow such as flow rate, flow regime, fluid rheology, geometry of annulus, inner pipe rotation, etc. Since annular flow characteristics gained attention, there has been a significant number of scientific studies for investigating those parameters effects on annular flow performance. However, there have been limited studies, which investigated the combined effect of those parameters while the fluid temperature varies.

The main objective of this present study is to better understand the effects of temperature on characteristics and hydraulics of the fully developed fluid flow in fully eccentric annuli including inner pipe rotation. The experimental study consists of Newtonian fluid –water- for turbulent flow regime. Experiments carried out with and without inner pipe rotation with varying fluid temperature at different flow rates. Accurate estimation of frictional pressure loss makes the determination of necessary hydraulic power available. In another word, the pump pressure is a function of frictional pressure loss. Therefore, determining pressure losses is essential to save energy, cost and also catastrophic events such as hole closure, tools loss etc. Therefore, pressure losses should be foreknown. The focus of this study is to determine pressure loss in an annulus. For that reason, frictional pressure loss along the test section of the flow loop was measured by using sensitive pressure transmitter for each experiment. Obtaining an empirical correlation for field use due to lack of time and instant measures is also necessary. In the present study, an empirical equation for determining pressure losses is presented and three dimensionless parameters that are effective on the pressure loss determination are used in the equation due to obtaining a general approach. For enhanced knowledge of the fully developed turbulent flow through annulus including inner pipe rotation and temperature variation effect, a mathematical model is also developed and solved numerically.

1.2 Literature Review

Determining frictional pressure loss has an importance of any design applications that require fluid flow. Misreading of pressure loss causes malfunction of the applications. For some cases, it can cause fatal incidents. Therefore, frictional pressure loss has been investigated and tried to develop general information by including additional parameters that have significant impact on pressure loss variation. In order to link the present study, previously published papers that are concerned about the hydraulics and characteristics of fluid flow through annular ducts are presented in this section. An interested scholar can be found a good start with this background.

1.2.1 Flow through concentric annuli

The start off the point of turbulence study is Leonardo Da Vinci's drawings in the fifteenth century. Almost four hundred years later, the study of turbulence took again researchers attention. First, Boussinesq [1] proposed eddy viscosity idea and his hypothesis "turbulent stresses are linearly dependent to mean strain rates". This hypothesis has been still used in most of the turbulence models.

Right after Boussinesq, Reynolds Osborne [2] conducted an experimental study. This study led him to identify the only physical parameter that helps to generalize the determination of the fluid in transition to turbulence.

According to Reynolds' experiment, turbulent flow exists for the fluid flow through pipes at Reynolds number above 4000. However, Prengle and Rothfus [3] observed the first disturbance eddy starts at 2200 to 2300 Reynolds number for annular flow.

Later, scientist and researchers have paid attention to annular flow and the first attempts to study annular flow was for concentric annulus due to its simplicity. The representation of concentric annulus can be seen Figure 1.1.

3
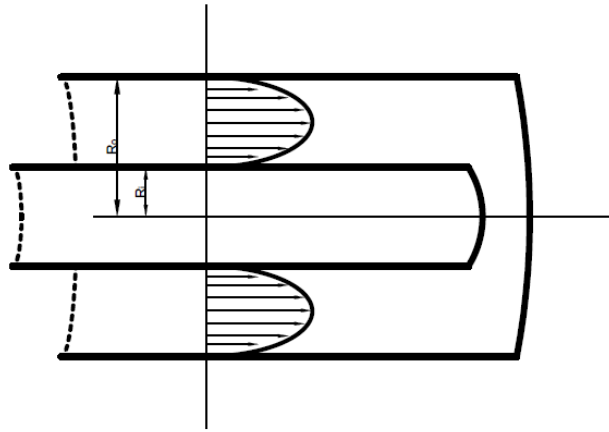
Figure 1.1 : Representation of annular flow in concentric annulus

Bird and Fredrickson [4] proposed an empirical model for predicting volumetric flow rate and frictional pressure loss of non-Newtonian fluids through the concentric annulus.

Rofthus et al. [5] proposed a model in order to estimate velocity profile for turbulent flow of water through concentric annuli. He conducted experiments on different radius ratio and compared his model with his experimental data. He concluded that his proposed model establish reasonably good annular velocity profile by comparing annuli.

Skelland [6] proposed an empirical solution for Bingham plastic fluid flow through the concentric annulus. Although he presented an exact solution of volumetric flow rate, the equation is big and not practical to use in the field.

Quarmby {7] conducted an experimental study on fully developed turbulent flow in concentric annuli. He concluded that the radius of maximum velocity decreases with Reynolds number below 50,000. On the other hand, it is independent of radius ratio above Re = 50,000.

A year later, Klump and Kwasnoski [8] developed an eddy diffusivity model in order to predict velocity distribution for the air of turbulent flow through concentric annuli.

They compared their model with previous experimental studies and models. They obtained good agreement with them, although their models are simpler than previous models.

Meter and Bird [9] used previous experimental results from literature and proposed a friction factor based on Reynolds number by using Prandtl mixing length. They stated that mixing length friction factor expression gives better prediction than hydraulic radius procedure.

Hanks and Larsen [10] presented an algebraic solution for volumetric flow rate and pressure drop of power-law fluid in laminar regime through the concentric annulus. They stated that their mathematical model is valid for all flow behavior index and annulus aspect ratio.

Later, Leung [11] figured out that previous models of friction factors prediction scatter away from accurate results for small gaps. His empirical equation gives the friction factor of turbulent flow at Reynolds number above 7,000 within 5 percent error margin.

Nouri et al. [12] conducted an experimental study on Newtonian and non-Newtonian fluids in both concentric and eccentric annulus. They concluded that the friction factor coefficient variation with Reynolds number implies if there is concentric annular flow rather than smooth pipe flow, the flow resistance increases around 8% in concentric annuli.

Gucuyener and Mehmetoğlu [13] conducted a study to develop a simple mathematical model which has an analytical solution to find volumetric flow rate of yield pseudo-plastic fluids flow through the concentric annulus.

Escudier and Gouldson [14] conducted an experimental study in order to understand the effect of inner pipe rotation on pressure drop in the concentric annulus. They concluded that the inner pipe rotation is negligible on the pressure loss when the flow is turbulent for both Newtonian and non-Newtonian fluids. However, inner pipe rotation is moderately effective when the flow is in laminar regime.

Gucuyener and Mehmetoğlu [15] conducted another study on yield pseudo-plastic fluids flow characterization in the concentric annulus. They concluded that transition

in flow regime is very sensitive to the geometry of the conduits and rheology of the fluids.

Filip and David [16] analyzed non-Newtonian fluid flow through concentric annulus including the effects of geometry, kinematic and rheologic behavior of fluids while the inner pipe moving axially. They proposed a semi-analytical model to predict volumetric flow rate. They compared their result with Robertson–Stiff model and obtained relatively good results.

Enhancing computer technology enabled Chung and Sung [17] investigation of the effect of inner wall rotation on the velocity profile with LES (Large Eddy Simulation) method. Their simulation emphasized that the mean velocity is getting lower slowly when the flow is approaching the wall while the inner pipe rotates.

Sorgun and Ozbayoglu [18] proposed a mechanistic model in order to have a general solution for estimating the friction factor of Newtonian turbulent flow through concentric annuli. The results showed that proposed model can predict within 10% error margin.

Kelessidis et al. [19] compared their experimental data for laminar, transition, and turbulent flow through concentric annulus with the previously proposed models to determine pressure losses. They concluded that API correlations obtain much higher pressure drop than their indicated data when in transition to the turbulent regime. They solved the problem by adding a correction factor.

As it can be analyzed that the application of fluid flow through concentric annulus has been studied widely in analytically, experimentally and computationally. Annular flow in the concentric annulus is a preliminary study for enhanced complex geometry or any additional parameters that brings complexity to solution of fluid flow problem in the annulus. Due to its symmetric geometry, authors prefer to approach concentric annulus first in order to step ahead to more complex geometries. Those mentioned studies cover most of the attempts to understand the annular flow in the concentric annulus.

1.2.2 Flow through eccentric annuli

In applications of fluid flow through the annulus, the geometry is rarely concentric. Most of them lose the alignment of the center body and become eccentric due to gravity, roughness etc. The representation of eccentric annulus can be seen in Figure 1.2. Fluid flow in an eccentric annulus has been taken great attention of researchers over the years. The effect of eccentricity on velocity profile and frictional pressure loss was studied by following researchers.
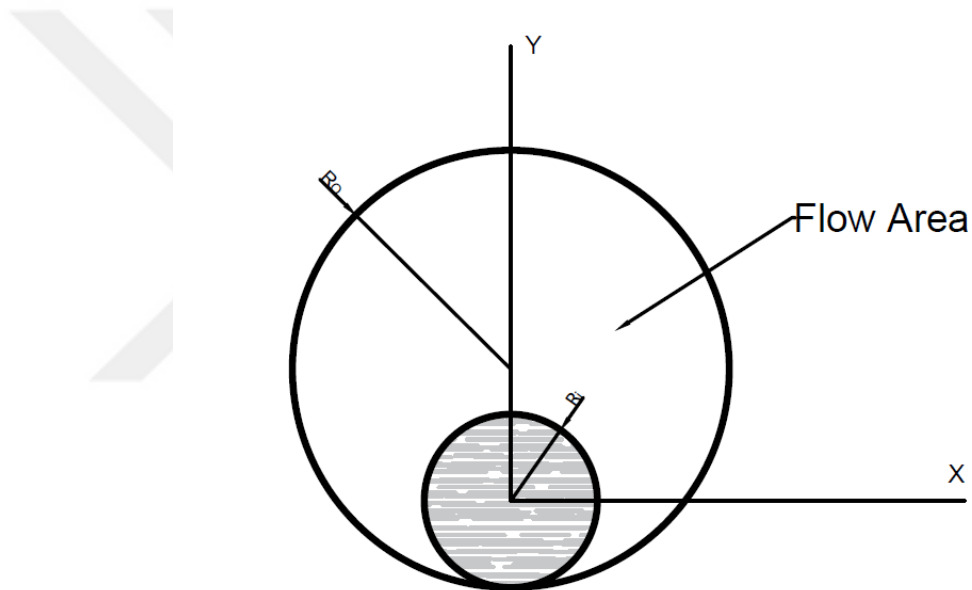
Figure 1.2 : Representation of eccentric annulus

Deissler [20] investigated an analytical model for turbulent heat and mass transfer in smooth tubes. He accounted the effect of kinematic viscosity in the region close to the wall and he obtained good agreement with experimental results. After his previous work, Deissler and Taylor [21] conducted an analytical study to describe the velocity profile of turbulent flow through eccentric annular geometries.

Wolffe and Clump [22] conducted an experimental study on determining velocity lines and locus of maximum velocity for turbulent flow of air. They compared their experimental results with the calculated solution of Navier-Stokes equation with Heyda's assumption [23] for analytical solution of laminar flow in annuli containing eccentricity. Wolffe and Clump also compared theirs with Deissler and Taylor's study [21]. They concluded that their study well matches with the previous analytical solution of Navier Stokes equation under certain assumptions.

Johnson and Sparrow [24, 25] conducted experimental work on turbulent flow in the eccentric annulus and they reported that circumferential pressure gradient is quite larger than that for concentric annulus. Also, they observed that friction factor decreases with increasing eccentricity.

Rehme [26] proposed a correlation of friction factor prediction for turbulent flow in channels with non-circular cross-sections. He concluded that this prediction method is better than all previous attempts and it can be used on other shapes of channels such as eccentric annulus.

Kacker [27] conducted an experimental study of fully turbulent flow in the circular pipe containing one or two eccentrically located rods. He developed a correlation to estimate friction factor. The correlation predicts the experimental data with 2% error margin for both one and two rods geometries.

Usui and Tsuruta [28] analyzed the equation of motion for fully turbulent flow in an eccentric annulus with using Kirchoff transformation. They explained the dependence of eccentricity on friction factor at high Reynolds number range.

Tosun [29] proposed an approximate solution axial laminar flow through the eccentric annulus and he compared his results with previously published experimental works. An approximate solution is relatively good agreement with the data in the literature. He and his group [30, 31] expanded the study for non-Newtonian fluids applying on Power law, Bingham plastic and Sutterby models. Those studies were concluded that proposed approximate solution well matches with previous experimental studies.

Ogino et al. [32] also investigated momentum equation for fully developed turbulent flow in the eccentric annulus. They used bipolar coordinate transform in order to model eccentric annulus geometry.

Haciislamoglu and Langlinais [33] investigated the effect of eccentricity on frictional pressure losses without inner pipe rotation and obtained pressure losses reduction as much as 60%.

Nouri et al. [12] conducted an experimental study on Newtonian and non-Newtonian fluids in both concentric and eccentric annulus. They concluded that the flow resistance decreases as the eccentricity is increased when it is compared with smooth pipe flow.

One year later, Nouri and Whitelaw [34] introduced rotational effect in the same study and their results showed that the effect of rotation on frictional pressure losses decreases with increase in Reynolds number after the flow is in transition. Decreasing of rotational effect on frictional pressure losses continues until they are same as without rotation case. Numerical and analytical approaches have been done for modeling turbulent flow.

The study of Haciislamoglu and Langlinais [33] was conducted under laminar flow regime. Corresponding to this study, Erge et al. [35] conducted another experimental study of turbulent flow in the eccentric annulus. They concluded that eccentricity significantly reduces the frictional pressure loss in turbulent flow as well.

Erge et al. [36] conducted an experimental, analytical and numerical study of the effect of eccentricity on frictional pressure loss. They concluded that frictional pressure loss in fully eccentric annulus has up to 50% discrepancy than the results which is calculated with Narrow Slot approach.

Recently, Rushd et al. [37] investigated eccentricity, roughness and rotation effects on frictional pressure loss. They conducted an experimental study and developed a CFD model in ANSYS validated by experimental results. Their CFD analysis showed that effect of roughness and eccentricity are more prominent than the effect of inner pipe rotation.

1.2.3 Flow through annuli including pipe rotation effect

Coleman and Nole [38] developed an expression for determining axial pressure drop, discharge rate and angular velocity for incompressible fluid flow through concentric annulus with inner pipe rotation. Their study is one of the classical studies for helical flow.

Walker and Al-Rawi [39] conducted an experimental study in order to validate the model proposed by Coleman and Noll [38] and also Fredrickson and Bird [4] for laminar helical flow to predict pressure drop with inner pipe rotation. They observed that decrease in pressure drop while increasing inner pipe rotation. The result shows similarity with the previous study.

Luo and Peden [40] proposed a method of solving the dimensionless equations, which were derived for obtaining an analytical solution of helical flow in the concentric annulus. Those dimensionless equations consist of three dimensionless parameters such as inner pipe rotation rate, ratio of inner and outer pipe diameter and fluid behavior index.

Delwiche et al. [41] studied theoretical of rotation effects in the eccentric annulus with comparing field study. They concluded that inner pipe rotation increases frictional pressure loss up to 100% at 500 RPM.

Marken et al. [42] investigated combination effects of eccentricity, inner pipe motion and fluid temperature on flow regime which contributes to determine pressure losses. They concluded that combined effect of those three parameters makes a significant change in pressure losses. Increasing inner pipe rotation increases pressure losses. However, the variation of fluid temperature couldn't be determined because of complexity and not easily implemented into the classical models.

Cui and Liu [43] solved numerically the governing equations of the helical flow of the non-Newtonian fluid in eccentric annuli by using the finite difference method. Numerically calculated flow rates are compared with the flow rates that measured in the experiments.

McCann et al. [44] experimentally investigated pipe rotation and eccentricity effect on pressure losses of non-Newtonian fluid flow in the annulus. They proposed a

simple correlation for estimating pressure losses for fluid flow through concentric annulus including inner pipe rotation and eccentric annulus without inner pipe rotation. They observed that increasing inner pipe rotation increases pressure losses in turbulent flow and decreases in laminar flow.

Hansen et al. [45] asserted a hydraulic model that included the effect of eccentricity, pipe rotation, and fluid rheology. Furthermore, they performed an experimental study for providing data in order to confirm and complement the pressure loss model.

Escudier et al. [46] conducted an experimental and computational study of the fully developed laminar flow of Newtonian fluid through eccentric annulus including inner pipe rotation. They transformed N-S equations from rectangular coordinate to non-orthogonal coordinate and solved it numerically. According to their results, they reported that increase in inner pipe rotation rate causes increases in frictional pressure loss.

Wan et al [47] investigated inner pipe rotation effect on Newtonian and non-Newtonian fluid flow in eccentric annuli by using numerical SIMPLE approach. They concluded that frictional pressure loss always increase with pipe rotation rate when the eccentricity is high (greater than 0.9)

Ooms and Kampman-Reinhartz [48] studied analytical, numerical and experimental study of influencing inner pipe rotation and eccentricity of Newtonian fluid flow through the annulus. In this study, they reported that there are insignificant effects of inner pipe rotation at high flow rates. Domination of inertial effect on rotation effect is given as an explanation of the insignificant effect of inner pipe rotation.

Fang and Manglik [49] conducted a comprehensive theoretical study of effects of inner pipe rotation, radius ratio and eccentricity on frictional pressure loss of Newtonian fluid. They employed the stream function and vorticity formulation for fully developed laminar flow and solved it numerically. According to their result, inner pipe rotation increases axial pressure drop. This effect is more pronounced at medium eccentricity (between 0.5 and 0.6).

Diaz et al. [50] conducted an experimental study and proposed a new model to estimate frictional pressure losses with pipe rotation in the concentric annulus. They

extended Tao and Donovan's method [51] by applying narrow slot approach. They concluded that their model comparison with experimental results shows good agreement.

Hemphill and Ravi [52, 53] developed a model with using advanced engineering approach by coupling axial and radial velocities. They concluded that pipe rotation can lower the pressure drop. However, pipe rotation can raise pressure drop after a certain rate. Furthermore, they stated that changing pipe radius ratio causes a change in pressure drop as well.

Alizadehdakhel et al. [54] determined pressure drop by using the ANN and computational fluid dynamics (CFD) and compared the performance. They stated the CFD has better result than ANN for their model.

Ahmed et al. [55] investigated the effect of pipe rotation on equivalent circulation density. Results indicated that pressure loss ratio is affected by various parameters including pipe rotation speed, pipe eccentricity, fluid properties, diameter ratio and flow regime.

Neto et al. [56] simulated rotating and non-rotating turbulent flows of Newtonian fluids in concentric and eccentric annular sections using computational fluid dynamics (CFD) with different turbulence models based on the RANS approach.

Sorgun et al. [57] studied and developed a mathematical model to predict flow characteristics of Newtonian fluids in a concentric annulus. To obtain velocity field, Navier-Stokes equations are numerically solved using the finite differences techniques.

Furthermore, Bicalho et al. [58] concluded from his experimental study that annular pressure drop is effected by CG concentration, fluid flow rate, eccentricity and inner pipe rotation.

Erge et al [59] conducted another CFD analysis for estimating pressure losses in an eccentric annulus including inner pipe rotation. They obtained good agreement with their experimental data and the empirical results. ANN has been used widely to solve complicated fluid mechanics problems.

With developing new technologies enhance us to use computer intelligence such as artificial neural networks (ANN) and any other computational applications. Rushd et al [37] implemented a CFD model in ANSYS CFX in order to investigate the effect of eccentricity, rotational speed, and equivalent hydrodynamic roughness. They obtained the results within 30% error margin.

Rooki and Rakhshkhorshid [60] estimated the pressure loss of drilling fluids inside the horizontal annulus using the ANN. They obtained their prediction within 5.93% error margin.

Additional to his previous study, Rooki [61] investigated the prediction capability of GRNN (General Regression Neural Network) by comparing his experimental data. The study was indicated that GRNN can predict pressure losses with high accuracy.

1.2.4 Flow through annuli including temperature effect

There are many parameters that incorporate to change annular frictional pressure losses such as flow rate, fluid properties (density and viscosity), annulus geometry, flow regime, pipe rotation, and pipe eccentricity as stated previously. In addition to all those parameters, temperature also has a significant role in determining annular frictional pressure losses. If the ambient temperature of the fluid is changed, the rheological properties of the fluid and flow performances vary. In many cases, significant differences are observed when theoretical calculations and measurements for pressure losses are compared. There has been some attempt to investigate temperature effects on flow through ducts.

Syrjala [62] conducted a study to provide accurate heat transfer prediction for non-Newtonian fluid flow through the rectangular duct by finite element method. On the other hand, Naccache and Mendes [63] solved the mass, momentum and energy equations for the same problem as Syrjala [51] but using finite volume technique. Then, Moraga et al. [64] investigated heat transfer for annular flow by using finite volume technique as well.

Peixinho et al. [65] experimentally investigated temperature effect on dynamics of the flow in the circular pipe for transition regime. Farias et al. [66] conducted another

13

experimental study of heat transfer coefficient of flow through the concentric pipe in laminar regime.

Sheela-Francisca et al. [67] developed a semi-analytical solution for temperature distribution through a channel under the assumption of Coutte-Poiseuille flow in laminar flow regime. As well as experimental study of heat transfer analysis for flows through ducts,

Lian-Cun et al. [68], Carmona et al [69], Prasad et al. [70], Li et al. [71] studied theoretical phenomena of the heat transfer through ducts and developed CFD solutions. Pinho and Coelho [72] and Yavuz et al. [73] studied analytical solution of heat transfer in the concentric annulus.

Han et al. [74] did closer attempt to the present work. They investigated temperature effect including rotation effect in eccentric annulus both experimentally and numerically. However, their results are limited to Newtonian laminar flow.

It can be realized that adding the additional parameters to fluid flow makes the problem more challenging. Enhancing information about annular flow leads the researcher to investigate effects of substantial parameters. In this study, turbulence Newtonian fluid flow through fully eccentric annulus including inner pipe rotation and temperature effects has studied both experimentally and computationally. When all previous attempts are analyzed, it has been seen that the solution of the problem considering all those combined effects is still a gap in the literature.

1.3 Scope of The Present Study

In the present study, the temperature effects on annular frictional pressure losses with inner pipe rotation in a fully eccentric annulus are investigated experimentally. Experiments were done in the flow loop constructed in IKCU Civil Engineering Department's Hydraulics and Fluid Mechanics Laboratory. Firstly, experimental results were gathered and compared how the flow hydraulics and characteristics change with various flow variables such as axial flow rate, inner pipe rotation rate. Then, the effects of those variables on frictional pressure loss were again observed when the temperature of the fluid differs. By using regression analysis of the dataset

obtained from the experimental work, a simple empirical frictional pressure losses correlation taking into account of temperature effect was proposed due to ease of determining pressure loss for field use. Moreover, the mathematical model of momentum equation for fully developed turbulent flow in fully eccentric annuli including the effects of temperature and inner pipe rotation was developed in order to have a general solution.

Within this dissertation, one can find the theory of fully developed turbulent flow through eccentric annulus including inner pipe rotation in Chapter 2. Experimental setup and process can be found at Chapter 3 in details. In Chapter 4, derivation of mathematical modeling of momentum equation of fully turbulent flow with or without inner pipe rotation in Cartesian Coordinates can be found. Evaluation of the data from experiments, mechanistic models, and the empirical equation can be found in Chapter 5.

2. THEORY

2.1 Basic Equations For Turbulent Pipe Flow

This part of the present study is aimed to present governing equations of motion for turbulent flow. The fundamental mathematical model of fluid flow motion is given by the Navier Stokes equations in closed form as;

- Continuity Equation

$$\frac{\partial \rho}{\partial t} + \frac{\partial \rho u_i}{\partial x_i} = 0 \tag{1}$$

- Momentum Equation

$$\rho \left(\frac{\partial u_j}{\partial t} + u_i \frac{\partial u_j}{\partial x_i} \right) = -\frac{\partial P}{\partial x_j} - \frac{\partial \tau_{ij}}{\partial x_i} + \rho g_j \tag{2}$$

In the closed form of Navier-Stokes equations shown above, velocity term consists of mean velocity component and fluctuating component for turbulent flow case. Therefore, velocity term in these equations should be written in the form of;

$$u = \bar{u} + u' \tag{3}$$

where $\bar{u}$ represents mean velocity component and u' represents fluctuating component of the fluid flow.

As an old-fashioned way for mathematical modeling of turbulent flow is modifying Navier-Stokes equations by satisfying mean value parameters such as $\bar{u}$ and $\bar{p}$ and approaching to the real value of velocity and pressure. However, in Reynolds Averaged Navier-Stokes equations (RANS), the modified NS equations for the mean values should be obtained by taking mean values of NS equations in order to get

Averaged NS equations. Replacing all variables in momentum equation with their mean and fluctuating component, also taking their time average gives the well-known RANS equation as in closed form of;

$$\rho\left(\frac{\partial \overline{u}_j}{\partial t}+\frac{\partial}{\partial x_i}\left(\overline{u_i u_j}+\overline{u'_i u'_j}\right)\right)=-\frac{\partial P}{\partial x_j}-\frac{\partial}{\partial x_i}\overline{\tau}_{ij}+\rho g_j \tag{4}$$

After this point mean velocity (e.g. $\overline{u}$) replace the same latter without bar (e.g. u) for simplicity. In Cartesian coordinate, Bird et al. [78] expanded the closed form of equation of motion for turbulent flow including pipe rotation as;

For x-momentum equation;

$$\rho\left(\frac{\partial u}{\partial t}+u\frac{\partial u}{\partial x}+v\frac{\partial u}{\partial y}+w\frac{\partial u}{\partial z}\right)=$$
$$-\frac{\partial P}{\partial x}+\left[\frac{\partial}{\partial x}\tau_{xx}+\frac{\partial}{\partial y}\tau_{yx}+\frac{\partial}{\partial z}\tau_{zx}\right]+\rho g_x-\frac{\partial\left(\rho u'^2\right)}{\partial x}-\frac{\partial\left(\rho u'v'\right)}{\partial y}-\frac{\partial\left(\rho u'w'\right)}{\partial z}+\rho\omega^2 y \tag{5}$$

For y-momentum equation;

$$\rho\left(\frac{\partial v}{\partial t}+u\frac{\partial v}{\partial x}+v\frac{\partial v}{\partial y}+w\frac{\partial v}{\partial z}\right)=$$
$$-\frac{\partial P}{\partial y}+\left[\frac{\partial}{\partial x}\tau_{xy}+\frac{\partial}{\partial y}\tau_{yy}+\frac{\partial}{\partial z}\tau_{zy}\right]+\rho g_y-\frac{\partial\left(\rho u'v'\right)}{\partial x}-\frac{\partial\left(\rho v'^2\right)}{\partial y}-\frac{\partial\left(\rho v'w'\right)}{\partial z} \tag{6}$$

For z-momentum equation;

$$\rho\left(\frac{\partial w}{\partial t}+u\frac{\partial w}{\partial x}+v\frac{\partial w}{\partial y}+w\frac{\partial w}{\partial z}\right)=$$
$$-\frac{\partial P}{\partial z}+\left[\frac{\partial}{\partial x}\tau_{xz}+\frac{\partial}{\partial y}\tau_{yz}+\frac{\partial}{\partial z}\tau_{zz}\right]+\rho g_z-\frac{\partial\left(\rho u'w'\right)}{\partial x}-\frac{\partial\left(\rho v'w'\right)}{\partial y}-\frac{\partial\left(\rho w'^2\right)}{\partial z} \tag{7}$$

2.2 Fluid Properties

For Newtonian fluids, momentum transport term in general form can be expressed as;

$$\tau_{ij} = -\mu \left(\frac{\partial u_i}{\partial x_j} + \frac{\partial u_j}{\partial x_i} \right) + \frac{2}{3} \mu \delta_{ij} \frac{\partial u_k}{\partial x_k} \tag{8}$$

where δ_{ij} is Kronecker delta.

τ_{yx} represents the y component of the stress acting on the surface whose outward normal is located in the positive x-direction. For Newtonian fluids, the constitutive equation of stress tensor is;

$$\tau_{yx} = \mu \left[\frac{\partial v}{\partial x} + \frac{\partial u}{\partial y} \right] \tag{9}$$

2.3 Geometry and Narrow Slot Approach

In the present study, experiments were conducted for flow in the fully eccentric annulus. Therefore, the height of the slot should be determined according to the eccentric annulus. Iyoho and Azar [79] proposed a model for determining the height of eccentric annulus. Unlike concentric annulus, they stated that the height of eccentric annulus varies with respect to pipe angle.

It is hard to display and understand flow behavior in an eccentric annulus. Therefore, Vaughn [80] approached the flow through an eccentric annulus as slot flow. The equivalent slot representation of eccentric annulus is slightly different when it is compared with concentric annulus due to variable slot height. The slot equivalents for both concentric and eccentric annulus can be displayed in Figure 2.1.
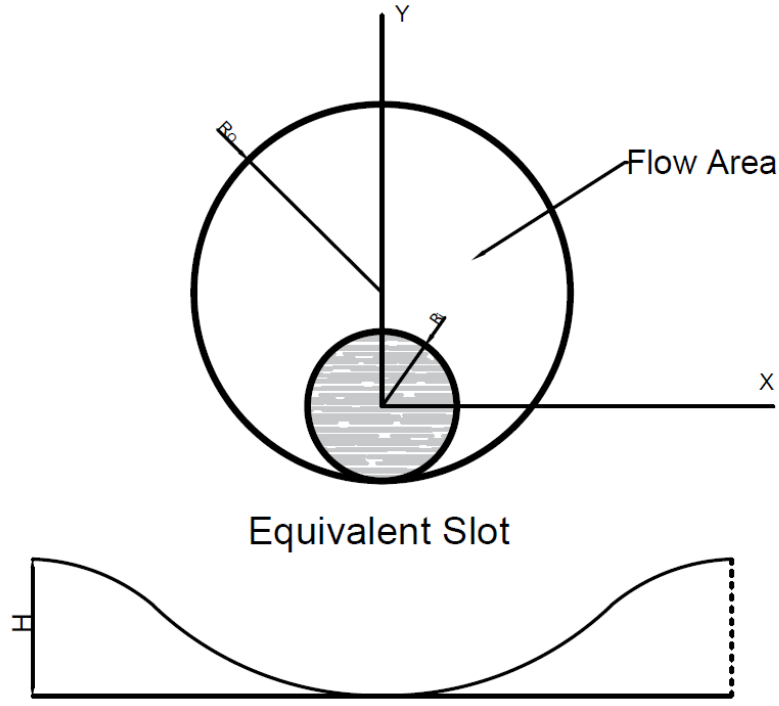
Figure 2.1 : Representation of equivalent slot for eccentric annulus

This approach overcomes the complexity of using bipolar coordinates, conformal transformation, and iterative computations. Iyaho and Azar [79] used Vaughn's [80] slot flow approach without his simplifying assumptions and obtained good accuracy with previous investigator's analytical studies in which complex coordinates or transformations were used. Therefore, Vaughn's approach has been used in the present study. The detail of narrow slot approach has been presented in the Appendix B. The final formula to determine the slot height for fully eccentric annulus is;

$$H = \frac{1}{2}\sqrt{r_o^2 - (r_o - r_i)^2 \operatorname{Sin}^2 \theta} - r_i + \operatorname{Cos}\theta \qquad (10)$$

After the numerical solution of the momentum equation, $u(y,\theta)$ can be found. However, the data of the experiment only provides the flow rate and therefore average annular fluid velocity. The relation between average annular velocity and point velocity at coordinates (y,θ) can be formulated as;

$$u(y,\theta) = u_a \left(\frac{u(y,\theta)}{u_a} \right)_{emp} \tag{11}$$

$\left(\dfrac{u(y,\theta)}{u_a} \right)_{emp}$ is a dimensionless ratio and the value can be obtained from experimental study data of Iyaho and Azar [79]. The angle, which frictional pressure losses measurements are taken, is about 90° as it can be seen in Figure 3.3. $\left(\dfrac{u(y,\theta)}{u_a} \right)_{emp}$ value for 90° is 0.67 according to Iyaho and Azar's [79] study. In the present study, numerical solution of momentum equation gives point velocity of the fluid at coordinates (y,θ). However, one can obtain average annular velocity by using flow rate measured from the flowmeter. Therefore, it is needed to divide point velocity to $\left(\dfrac{u(y,\theta)}{u_a} \right)_{emp}$ ratio in order to obtain average annular fluid velocity.

Taking the angle as 90° simplifies the slot height formula as;

$$H = \frac{1}{2} \sqrt{r_o^2 - \left(r_o - r_i \right)^2} - r_i \tag{12}$$

3. EXPERIMENTAL STUDY

Experiments of Newtonian fluid flow through fully eccentric annulus including inner pipe rotation and temperature effects are conducted at Izmir Katip Celebi University. One can find detailed experimental setup and procedure in the following section.

3.1 Experimental Setup

A flow loop was constructed at Izmir Katip Celebi University, Fluid Mechanics & Hydraulics Laboratory. The specifications of the experimental setup are given in Table 3.1.

Table 3.1 : Test parameter values during the experiments

Experiment Specifications	Values
Inner – Outer Pipe Diameter	40 – 80 mm
Flow Loop length	10 m
Flow velocity	0.7 – 3.6 m/s
Temperature	20 - 60 °C
Inner pipe rotation speed	0 – 120 rpm

Flow loop, 10 m long, has been formed from 80 mm outer pipe and 40 mm inner pipe. Inner pipe has been fixed concentrically at both ends and full eccentric annulus has been obtained at the test section due to gravity.

The flowmeter was assembled 210 cm away from the pump in order to prevent misreading due to pump wake. The diameter of the flowmeter is 125 mm. Due to

contraction and end effects, a 70 cm extension pipe was placed after flowmeter. The flowmeter has 0.15% – 0.55% uncertainty of reading the flow rate till the flow rate and temperature reaches 700 m^3/h and 80 °C, respectively. ETRANS-DP pressure transmitter was used to measure pressure losses and the uncertainty of pressure transmitter in full scale is below 0.07% for temperature from 0°C to 70°C. Pressure transmitter has been placed 7 m away from the entrance in order to maintain fully developed flow at the test section. The test section is 0.5 m in length. The data from flowmeter and pressure transmitter has been taken by DT80 Data logger to electronic media for every 5 seconds during experiments. Pictures of the flow loop are shown in figures below.

Figure 3.1 : Flow loop used in this study

An electrical motor unit has been connected to the flow loop end, which is shown in Figure 3.2. The motor has been fixed to the system with a shaft that can avoid leaking as well. This shaft is directly connected to inner pipe which is stabilized concentrically at that point in order to avoid any harm to the AC motor.

Figure 3.2 : Motor for pipe rotation and its control unit

AC motor has the capability of provide maximum 1382 rpm with the frequency of 50 Hz with spending 2.2 kW power. Due to fully eccentric nature of the system throughout most of the flow loop, it causes cracks on the plexiglass tube at high inner pipe rotation. Therefore, leakage of the flow loop arises and that causes misreading of pressure gradient. For this reason, a digital controller of the inner pipe rotation rate has been used and it is shown in Figure 3.3.

Figure 3.3 : Inner pipe rotation rate control unit

The test section is 50 cm long and the angle of both orifice with respect to center of the outer pipe has been tried to fix at same value. Moreover, both orifice have small device in which the closure member of pressure transmitter is either rotated or moved transversely or longitudinally in the waterway so as to control or stop leakage. Moreover, the side of these orifices have been applied special thermal silicon elastomer in order to avoid leakage at higher fluid temperature. Figure 3.4 shows the test section and the position of the orifices.
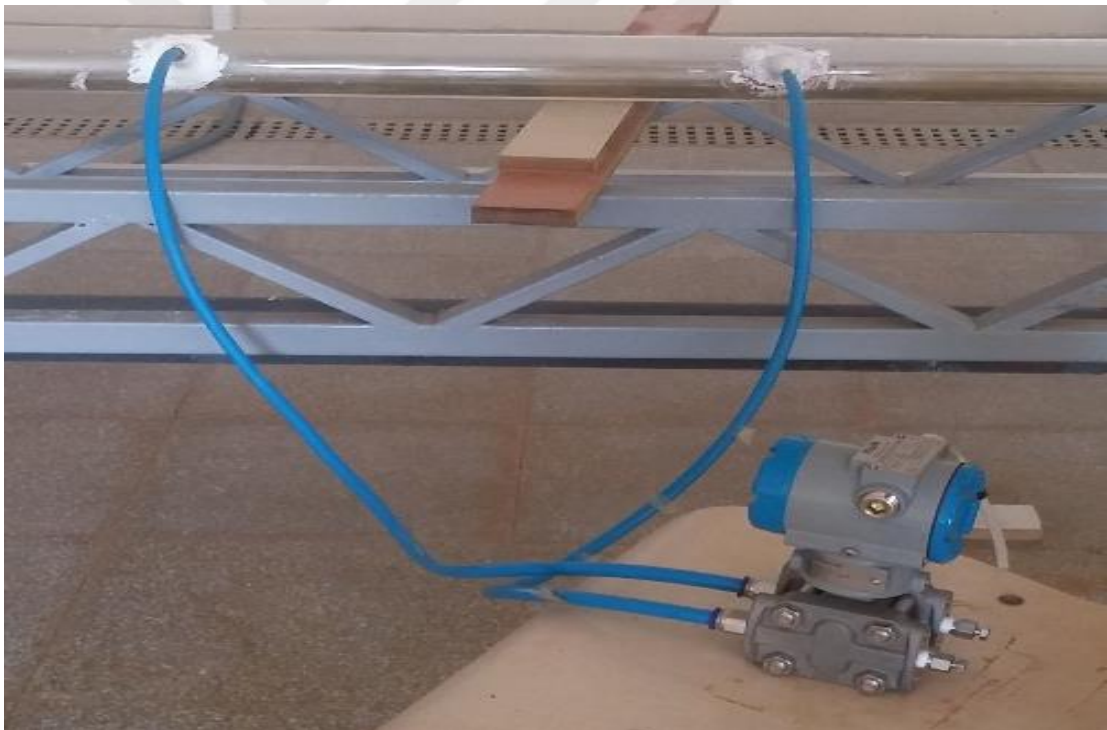
Figure 3.4 : Test section and pressure transmitter

ETRANS-M 210 electromagnetic flowmeter has been used for determining flow rate in the system. It can read maximum 100 m3/h flow rate. Due to brittle nature of the plexiglass, it has been avoided to allow the flow rate over 32 m3/h. The flowmeter can read truly when it is fully loaded and away from both pump effect and end effect. Due to these reasons, the flowmeter has been assembled 2.25 m away from the pump and 1 m away from the beginning section of the flowloop.

Figure 3.5 : Flowmeter

A 10-HP centrifugal pump has been used with butterfly type control valve in order to provide controlled circulation flow rate in the flow loop. Pump has occasionally stroke and change the flow rate because of mechanical malfunction of the valve. Flow rate has to be fixed then wait for a period in order to obtain straight and constant flow. Butterfly valve can resist up to 75 °C, it losses its property and lead to uncontrollable flowrate above this temperature.

Figure 3.6 : Pump motor and butterfly valve

Same AC motor as inner pipe rotation has been used for stirring fluid in the feeding tank. Stirring the fluid in the feeding tank is necessary in order to have a homogenous temperature in the system. Also, heater unit has been controlled by digitally and the system shuts down itself when the demand fluid temperature is reached. Continuously heating fluid inside tank causes shortcut and loss of tools. Therefore, controlling the temperature digitally and stirring the fluid while heating the fluid is important. Figure 3.7 shows the location of the stirring motor and heating controller unit on the feeding tank.

Figure 3.7 : Heater control unit and stirring motor

In the test system, the input and output effects were taken into account and the pressure loss measurements were made using pressure transmitters. The pressure gradient was defined as the function of temperature and other parameters. A Newtonian fluid, water, has been used in the experiment. The experiments were repeated at least 2 times.

When the feeding tank is filled with water, the thermostatic heater is turned on in order to increase the temperature of the water in the feeding tank. The fluid used in the experiment is returned to the fluid feeding tank, which is kept at a constant temperature between the pipes at a constant temperature. Furthermore, 230 V DV motor on the tank for stirring the water and the digital controller of the heater is switched on in order to make the water to reach necessary temperature. As soon as the temperature of the water is read as the desired value by using a thermocouple, the heater is automatically turned off. In contrast, the heater is automatically turned on when the temperature of the water dropped below the desired value. For this reason, the temperature of the water remains constant during experiments. After the desired temperature of the water is obtained, the butterfly valve is opened to release the fluid to the system.

When the system is completely filled with water, a motor pump that has 10 HP is switched on. To make rotation pipes ready for rotating, 230 V DC motor is turned on. Also, a 0-50V / 0-20 A switching power supply is turned on in order to switch on ETRANS-M 210 electromagnetic flowmeter and ETRANS-DP pressure transmitter that are connected to a desktop PC via a DT80 data logger. Water is arranged to desired flow value in the system by using the butterfly valve and flowmeter. Then, the digital controller of the inner pipe rotation motor is set to the desired value of rotational speed. The water is let to run within the system for a certain time till the flow becomes steady and isothermal in the entire system. As soon as the readings are

stable, experiment data is started to record. Input parameters are changed accordingly and repeated previous steps until data is collected for all desired parameters.

3.2 Experimental Test Procedure

A Newtonian fluid, water, has been used in the experiment. Inner pipe has been fixed concentrically at both ends and full eccentric annulus has been obtained at the test section. Schematic diagram and picture of the flow loop are shown in Figure 3.8. The following procedure is used for the tests:

- Fill the feeding tank with water

- Start the thermostatic heater for increasing the temperature of the fluid in the feeding tank

- Set the heater to desired value by digital controller

- Start 230 V DC motor on the tank for stirring the fluid in the tank in order to have homogenous temperature distribution in the fluid

- Open the butterfly valve to release the fluid to the system

- Start 10 HP pump

- Wait till the flow is steady and isothermal in the entire system

- Set flow rate to desired value

- Start 230 V DC motor for rotating inner pipe

- Set inner pipe rotation rate to desired value

- Start data acquisition system

- Start 0-50V / 0-20 A switching power supply

- Connect ETRANS-M 210 electromagnetic flowmeter to the power supply

- Connect ETRANS-DP pressure transmitter to the power supply

- Start recording data

- As soon as the readings are stable, change one of the input parameters (flow rate, inner pipe rotation rate, temperature)

- Repeat the previous step until data is collected for all desired parameters.

- Stop recording data

- Disconnect flowmeter and pressure transmitter

- Stop power supply

- Stop the motor for inner pipe rotation

- Stop the pump

- Stop the motor for stirring the fluid inside the feeding tank

- Stop the heater
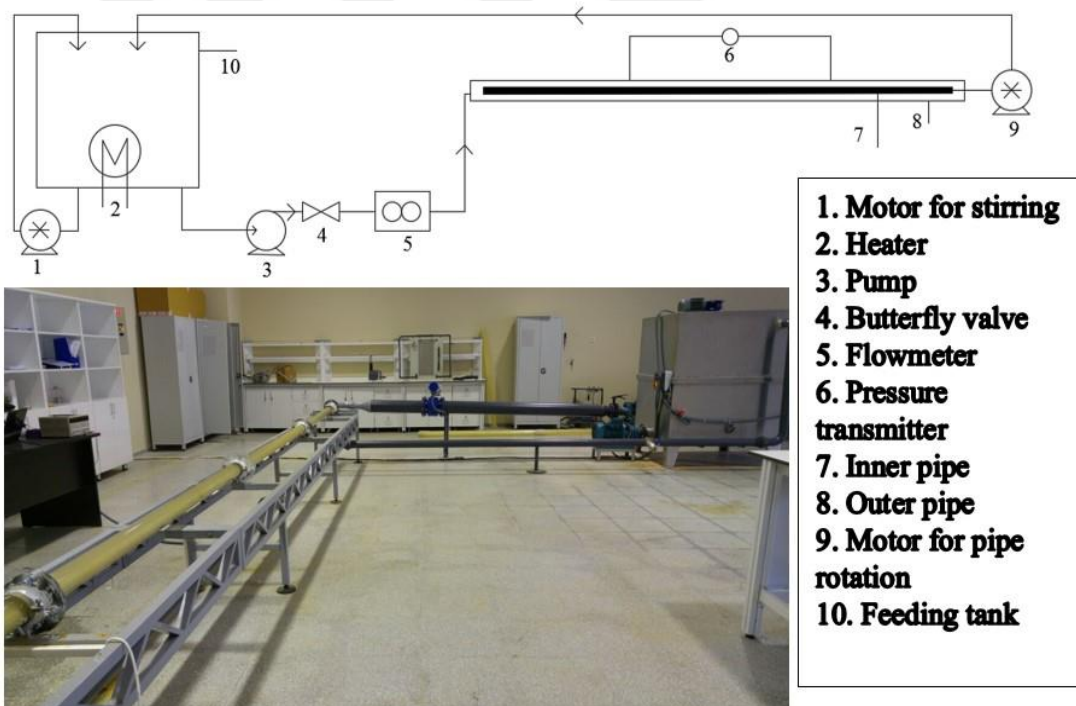
Figure 3.8 : Schematic diagram and picture of the flow loop

3.3 Experimental Test Matrix and Validation

The test matrix for the experiment of fully developed turbulent flow of Newtonian fluid including temperature and inner pipe rotation through fully eccentric annulus is presented in Table 3.2.

Table 3.2 : Test matrix for Newtonian fluid flow through eccentric annulus

Flow Rate (m^3/h)	Inner Pipe Rotation Rate (RPM)	Fluid Temperature (°C)			
7 m^3/h	0	23	40	50	60
	30	23	40	50	60
	60	23	40	50	60
	90	23	40	50	60
	120	23	40	50	60
10 m^3/h	0	23	40	50	60
	30	23	40	50	60
	60	23	40	50	60
	90	23	40	50	60
	120	23	40	50	60
13 m^3/h	0	23	40	50	60
	30	23	40	50	60
	60	23	40	50	60
	90	23	40	50	60
	120	23	40	50	60
16 m^3/h	0	23	40	50	60
	30	23	40	50	60
	60	23	40	50	60
	90	23	40	50	60
	120	23	40	50	60
19 m^3/h	0	23	40	50	60
	30	23	40	50	60
	60	23	40	50	60
	90	23	40	50	60
	120	23	40	50	60
22 m^3/h	0	23	40	50	60
	30	23	40	50	60
	60	23	40	50	60
	90	23	40	50	60
	120	23	40	50	60

	0	23	40	50	60
	30	23	40	50	60
25 m³/h	60	23	40	50	60
	90	23	40	50	60
	120	23	40	50	60
	0	23	40	50	60
	30	23	40	50	60
28 m³/h	60	23	40	50	60
	90	23	40	50	60
	120	23	40	50	60
	0	23	40	50	60
	30	23	40	50	60
31 m³/h	60	23	40	50	60
	90	23	40	50	60
	120	23	40	50	60

It is necessary to calibrate the experimental study for obtaining correct experimental data. For this purpose, the flow loop were run for water at room temperature and without inner pipe rotation for various flow rates. Pressure drop values are recorded and compare with calculated theoretical values for smooth pipe. Figure 3.9 shows that the measured and calculated pressure drop values are in good agreement.
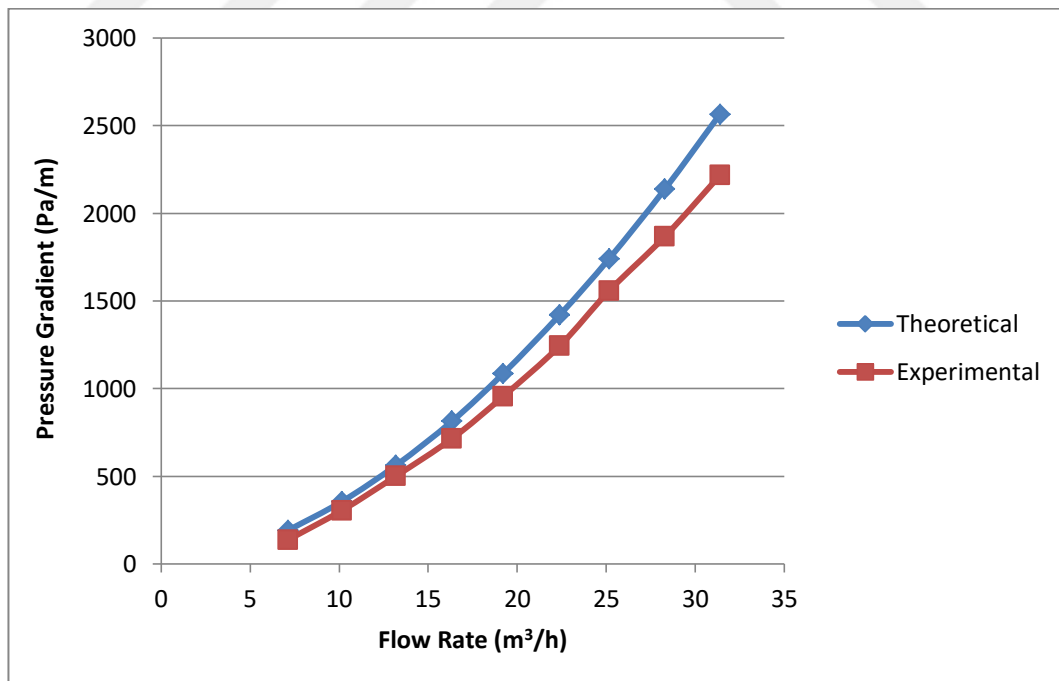
Figure 3.9 : Experimental setup verification by comparing experimental and calculated pressure drop

4. A MATHEMATICAL MODEL OF TURBULENT FLOW OF NEWTONIAN FLUID IN FULLY ECCENTRIC ANNULUS INCLUDING PIPE ROTATION AND TEMPERATURE

In order to have comprehensive understanding of the present problem, the mathematical background should be well presented and compared. Due to this reason, the following section is presented for the interested researcher to follow the steps of the mathematical insight of the present study.

4.1 Equation of Motion in Cartesian Coordinate

In Cartesian coordinate, Bird et al. [79] expanded the closed form of equation of motion for turbulent flow including pipe rotation as;

For x-momentum equation;

$$\rho\left(\frac{\partial u}{\partial t} + u\frac{\partial u}{\partial x} + v\frac{\partial u}{\partial y} + w\frac{\partial u}{\partial z}\right) =$$
$$-\frac{\partial P}{\partial x} + \left[\frac{\partial}{\partial x}\tau_{xx} + \frac{\partial}{\partial y}\tau_{yx} + \frac{\partial}{\partial z}\tau_{zx}\right] + \rho g_x - \frac{\partial\left(\rho u'^2\right)}{\partial x} - \frac{\partial\left(\rho u'v'\right)}{\partial y} - \frac{\partial\left(\rho u'w'\right)}{\partial z} + \rho\omega^2 y \tag{13}$$

For y-momentum equation;

$$\rho\left(\frac{\partial v}{\partial t} + u\frac{\partial v}{\partial x} + v\frac{\partial v}{\partial y} + w\frac{\partial v}{\partial z}\right) =$$
$$-\frac{\partial P}{\partial y} + \left[\frac{\partial}{\partial x}\tau_{xy} + \frac{\partial}{\partial y}\tau_{yy} + \frac{\partial}{\partial z}\tau_{zy}\right] + \rho g_y - \frac{\partial\left(\rho u'v'\right)}{\partial x} - \frac{\partial\left(\rho v'^2\right)}{\partial y} - \frac{\partial\left(\rho v'w'\right)}{\partial z} \tag{14}$$

34

For z-momentum equation;

$$\rho\left(\frac{\partial w}{\partial t}+u\frac{\partial w}{\partial x}+v\frac{\partial w}{\partial y}+w\frac{\partial w}{\partial z}\right)=$$
$$-\frac{\partial P}{\partial z}+\left[\frac{\partial}{\partial x}\tau_{xz}+\frac{\partial}{\partial y}\tau_{yz}+\frac{\partial}{\partial z}\tau_{zz}\right]+\rho g_z-\frac{\partial\left(\rho u'w'\right)}{\partial x}-\frac{\partial\left(\rho v'w'\right)}{\partial y}-\frac{\partial\left(\rho w'^2\right)}{\partial z} \tag{15}$$

4.2 Assumptions

> **The equation of motion is free of z-direction and its velocity component. Therefore, the equation of motion reduces to;**

For x-momentum equation;

$$\rho\left(\frac{\partial u}{\partial t}+u\frac{\partial u}{\partial x}+v\frac{\partial u}{\partial y}\right)=-\frac{\partial P}{\partial x}+\left[\frac{\partial}{\partial x}\tau_{xx}+\frac{\partial}{\partial y}\tau_{yx}\right]+\rho g_x-\frac{\partial\left(\rho u'^2\right)}{\partial x}-\frac{\partial\left(\rho u'v'\right)}{\partial y}+\rho\omega^2 y \tag{16}$$

For y-momentum equation

$$\rho\left(\frac{\partial v}{\partial t}+u\frac{\partial v}{\partial x}+v\frac{\partial v}{\partial y}\right)=-\frac{\partial P}{\partial y}+\left[\frac{\partial}{\partial x}\tau_{xy}+\frac{\partial}{\partial y}\tau_{yy}\right]+\rho g_y-\frac{\partial\left(\rho u'v'\right)}{\partial x}-\frac{\partial\left(\rho v'^2\right)}{\partial y} \tag{17}$$

> **Flow is in x-direction and it is fully developed.**

There is no variation within the parameters along the x-direction except pressure term which drives the fluid motion. Mathematical representation of 2nd assumption is $\left(\frac{\partial}{\partial x}=0, v=0\right)$. After 2nd assumption, equation of motions is reduced to;

$$\rho\left(\frac{\partial u}{\partial t}\right)=-\frac{\partial P}{\partial x}+\left[\frac{\partial}{\partial y}\tau_{yx}\right]+\rho g_x-\frac{\partial\left(\rho u'v'\right)}{\partial y}+\rho\omega^2 y \tag{18}$$

35

> ➤ **Flow is in steady state and there is no gravitational acceleration component in x-direction.**

Mathematical representation of 3rd assumption is $\left(\dfrac{\partial}{\partial t} = 0, g_x = 0 \right)$. Final form of momentum equation can be written as;

$$0 = -\frac{\partial P}{\partial x} + \left[\frac{\partial}{\partial y} \tau_{yx} \right] - \frac{\partial (\rho u' v')}{\partial y} + \rho \omega^2 y \tag{19}$$

4.3 The Mixing Length Theory

J. Boussinesq [1] introdeced a mixing coefficient of viscosity for turbelent flow along with laminar flow. which is called Reynolds stress term ;

$$\tau_t = -\rho u' v' = \mu_t \frac{\partial u}{\partial y} \tag{20}$$

So, total momentum equation for Newtonian fluids in a narrow slot can be written;

$$\frac{\partial}{\partial y} \left[(\mu + \mu_t) \frac{\partial u}{\partial y} \right] = \frac{\partial P}{\partial x} + \rho \omega^2 y \tag{21}$$

According to Prandtl's Mixing Length Hypothesis, turbelent viscosity can be written as;

$$\mu_t = \rho l_m^2 \frac{\partial u}{\partial y} \tag{22}$$

The mixing length can be expressed with van Driest formula;

$$l_m = \kappa y \tag{23}$$

where κ is von Karman constant and its value is 0.4. Viscous effect is significant at close to the wall and mixing length goes to zero at the wall. In order to count this behaviour, viscous damping function could be added to van Driest's formula;

$$l_m = \kappa y \left(1 - e^{-\frac{y^+}{A}} \right) \tag{24}$$

36

where $y^+ = \dfrac{y\sqrt{\tau_w \rho}}{\mu}$ and $\tau_w = -H\dfrac{\partial P}{\partial x}$. Here A is van Driest's damping constant and it can be assigned 26 for smooth surfaces without suction or blowing. H is half width of the channel.

4.4 The Mathematical Model of Momentum Equation in Cartesian Coordinate

Dynamic viscosity and density of water is only function of temperature. Viscosity and density of water for different temperature are available in literature. Temperature dependence water viscosity is given by a correlation as;

$$\mu(T) = 2.414 x 10^{-5} \, x 10^{\frac{247.8}{T-140}} \tag{25}$$

where T is in Kelvin. Moreover, temperature dependence of water density can be obtained from the correlation proposed by George S. Kell [81] as;

$$\rho(T) = \frac{a_0 + a_1 T + a_2 T^2 + a_3 T^3 + a_4 T^4 + a_5 T^5}{1 + bT} \tag{26}$$

where T is in Celsius and the coefficients are;

$a_1 = 17.801161 x 10^{-3}, a_2 = -7.942501 x 10^{-6}, a_3 = -52.56328 x 10^{-9},$
$a_4 = 137.6891 x 10^{-12}, a_5 = -364.4647 x 10^{-15}, b = 17.735441 x 10^{-3}$

It is now obvious that both l_m and μ_t are function of y. For this reason, chain rule should be applied in order to write open form and applied finite difference alghoritm. Chain rule method will be applied step by step to the final version of momentum equation for slot flow as follows;

$$\frac{\partial}{\partial y}\left[(\mu + \mu_t)\frac{\partial u}{\partial y} \right] = \frac{\partial P}{\partial x} - \rho \omega^2 y \tag{27}$$

$$\mu \frac{\partial^2 u}{\partial y^2} + 2\rho l_m \frac{\partial l_m}{\partial y}\left(\frac{\partial u}{\partial y}\right)^2 + 2\rho l_m^2 \frac{\partial u}{\partial y}\frac{\partial^2 u}{\partial y^2} = \frac{\partial P}{\partial x} - \rho\omega^2 y \tag{28}$$

$$\left(\mu + 2\mu_t\right)\frac{\partial^2 u}{\partial y^2} + 2\rho l_m \frac{\partial l_m}{\partial y}\left(\frac{\partial u}{\partial y}\right)^2 = \frac{\partial P}{\partial x} - \rho\omega^2 y \tag{29}$$

So the final form of momentum equation before the discretization for finite difference is;

$$\left(\mu + 2\mu_t\right)\frac{\partial^2 u}{\partial y^2} + 2\rho l_m \frac{\partial l_m}{\partial y}\left(\frac{\partial u}{\partial y}\right)^2 = \frac{\partial P}{\partial x} - \rho\omega^2 y \tag{30}$$

with boundary conditions of;

$$u(y=0)=0 \quad \text{and} \quad \frac{du}{dy}(y=H)=0 \tag{31}$$

4.5 Numerical Solution Approach

In order to discretize of derivatives of the final equation, central difference scheme is used;

$$\frac{\partial f}{\partial y} = \frac{u_{i+1} - u_{i-1}}{2\Delta y} \tag{32}$$

$$\frac{\partial^2 f}{\partial y^2} = \frac{u_{i+1} - 2u_i + u_{i-1}}{\left(\Delta y\right)^2} \tag{33}$$

To progress the computer programming, derivative operators are needed to put into matrix form by using the above formulas with accounting boundary conditions. Then, it leads to

$$\frac{\partial}{\partial y} = D_1 = \frac{1}{2\Delta y} \begin{pmatrix} 0 & 1 & 0 & 0 & \cdots & 0 & 0 & 0 \\ -1 & 0 & 1 & 0 & \cdots & 0 & 0 & 0 \\ 0 & -1 & 0 & 1 & \cdots & 0 & 0 & 0 \\ \vdots & \vdots & \vdots & \vdots & \ddots & \vdots & \vdots & \vdots \\ 0 & 0 & 0 & 0 & \cdots & -1 & 0 & 1 \\ 0 & 0 & 0 & 0 & \cdots & 0 & -1 & 1 \end{pmatrix} \tag{34}$$

$$\frac{\partial^2}{\partial y^2} = D_2 = \frac{1}{(\Delta y)} \begin{pmatrix} -2 & 1 & 0 & 0 & \cdots & 0 & 0 & 0 \\ 1 & -2 & 1 & 0 & \cdots & 0 & 0 & 0 \\ 0 & 1 & -2 & 1 & \cdots & 0 & 0 & 0 \\ \vdots & \vdots & \vdots & \vdots & \ddots & \vdots & \vdots & \vdots \\ 0 & 0 & 0 & 0 & \cdots & 1 & -2 & 1 \\ 0 & 0 & 0 & 0 & \cdots & 0 & -1 & 1 \end{pmatrix} \tag{35}$$

where D_1 and D_2 are $N-1 \times N-1$ matrices in which N represents the number of discretization in the numerical solution. Therefore, the final version of the discretized momentum equation for slot flow is as follows;

$$\left(\vec{\mu} + 2\vec{\mu}_t \right) D_2 \vec{u} + 2\rho \vec{l}_m D_1 \vec{l}_m \left(D_1 \vec{u} \right)^2 = \vec{P}_x \tag{36}$$

Due to the symmetricity of the computational domain, Eq. (36) has been solved by using two approaches on the interval $[0, H]$.

4.5.1 The proposed numerical method

The initial guess of the velocity profile is obtained by considering laminar where the turbulent viscosity is assigned zero. This guess is assigned like the old value of the velocity. In the iterative process, obtaining the new numerical solution the nonlinear term is frozen by using the old solution. Then, to get the final solution, the accuracy of the solution is checked by a given tolerance. If the tolerance is not held, then return to the iterative loop by assigning the new solution as the old solution. Otherwise, the new solution is assigned as the pre-final solution. Then, the pre-final solution is compared with experimental data. If the error between the pre-final solution and experimental data is less than the given tolerance then the pre-final solution is assigned as the final one. Otherwise, the program returns to assign initial

guess of the pressure gradient. The flow chart of this program can be seen in Figure 4.1.
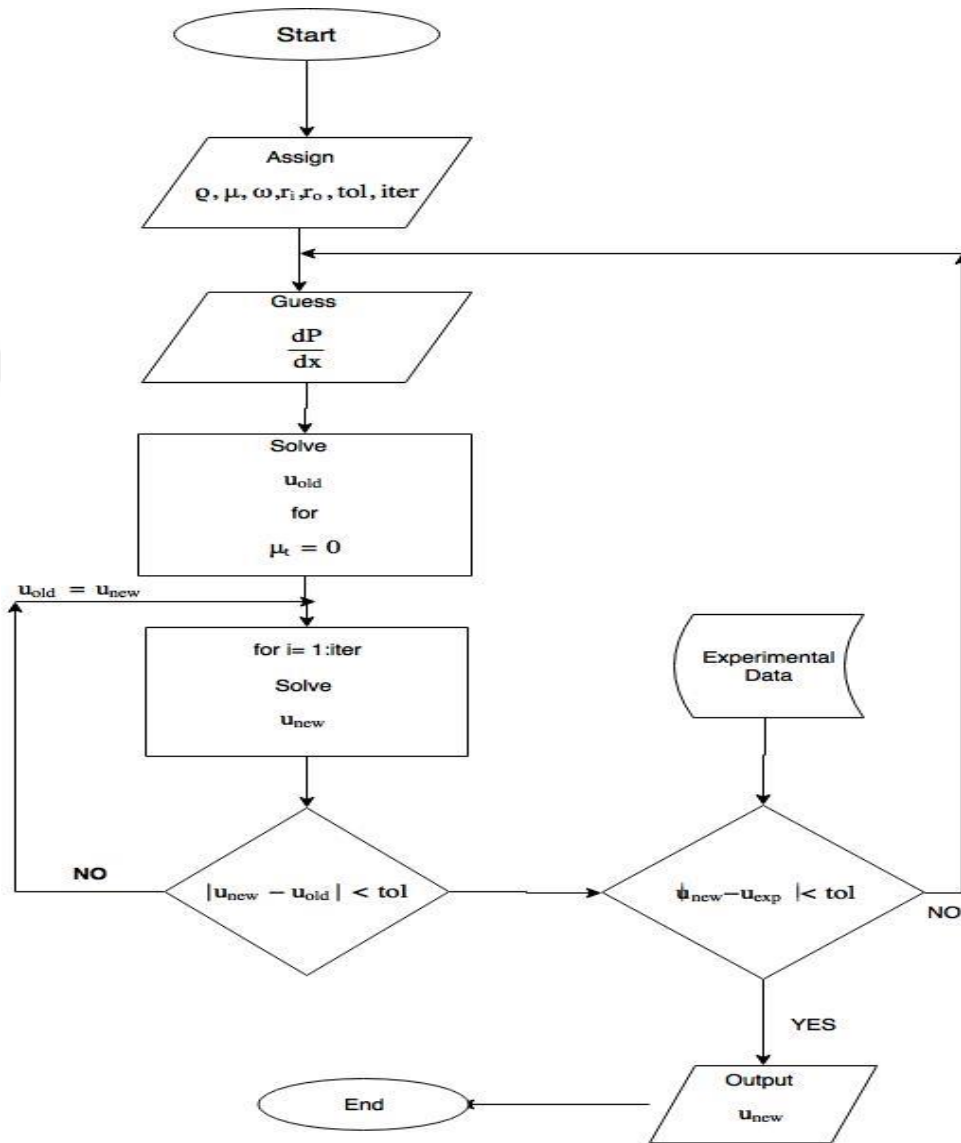
Figure 4.1 : Flow chart of the computer code with proposed method

4.5.2 Newton-Raphson method

It is the most known solver for finding the root for $F(\vec{u}) = 0$. The process of Newton's algorithms is defined as

$$\vec{u}_{n+1} = u_n - (F'(\vec{u}_n))^{-1}F(\vec{u}_n) \tag{37}$$

where $F: \mathbb{R}^n \rightarrow \mathbb{R}^n$ and $F(\vec{u}) \in C^2(\mathbb{R}^n)$. By fixing $\vec{u}_n$ Equation (45) becomes a linear equation even though $F(u)$ is nonlinear. It is worth mentioned that the choice of initial guess, $\vec{u}_0 \in \mathbb{R}^n$, is a key point for both avoiding the singularity problem of $(F'(\vec{u}_n))^{-1}$ and the convergence of the method. After doing tedious the following equation is obtained;

$$F(\vec{u}_n) = (\mu + 2\mu_t)D_2\vec{u}_n + 2\rho l_m D_1 l_m (D_1\vec{u})^2 - \vec{P}_x. \tag{38}$$

Here, $F'(u)$ denotes the derivative of $F(u)$ with respect to u. Thus, the derivative of $F(u)$ in operator form is as follows:

$$F'(\vec{u}) = (\mu + 2\mu_t)D_2 + 2\rho l_m (D_1 l_m (2D_1\vec{u}) + l_m D_2\vec{u})D_1 \tag{39}$$

The operator forms defined in Eq. (38) and Eq. (39) are substituted into Newton-Raphson method given in Eq. (37). This equation is solved for u_{n+1}. In the computational process of the second approach, the initialization of the velocity, u_0, is assigned as zero vector and this initialization vector is called the old solution. In the iterative process, solve Eq. (30) for getting the new solution of the velocity. Then, check the error of the solutions between the new and the old solutions by a given tolerance. If the tolerance is not held, then return to the iterative loop by assigning the new solution as the old solution. Otherwise, the new solution is assigned as pre-final solution. Then, the pre-final solution is compared with experimental data. If the error between the pre-final solution and experimental data is less than the given

41

tolerance then the pre-final solution is assigned as the final one. Otherwise, the program returns to assign initial guess of the pressure gradient. The flow chart of this program can be seen in Figure 4.2.
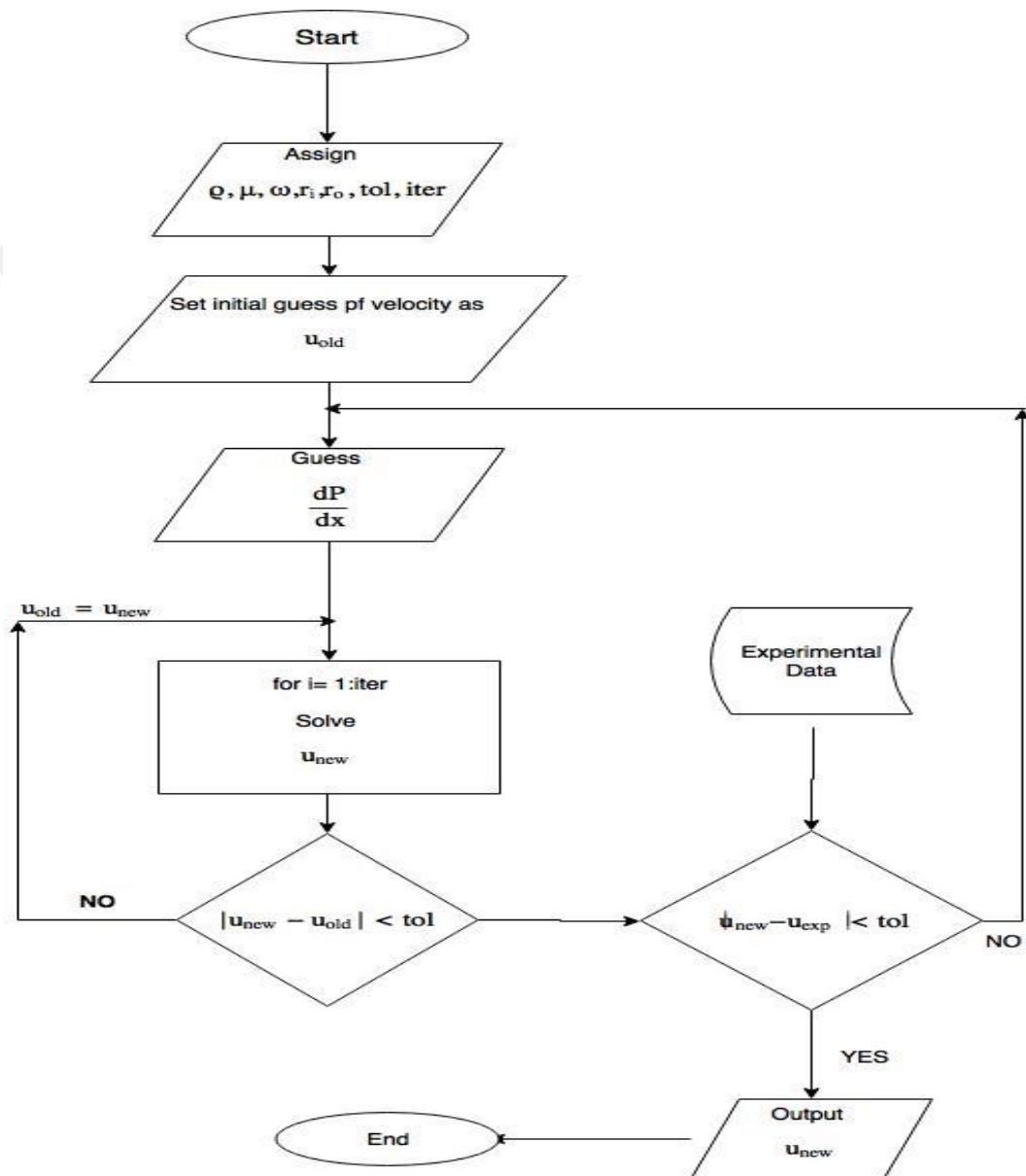
Figure 4.2 : Flow chart of the computer code with Newton's approach

4.5.3 Grid independent test

When the numerical solver is run for low velocity without temperature and inner pipe rotation effects, 140 and more grid size makes the solution independent of grid increment. However, the solver needs more discretization number when inner pipe rotation and temperature play in the role during the fluid flow. Fortunately, 1000 grid number size is efficient for making the solver independent of any grid number of the solution. Therefore, the grid number is fixed to 1000 for all cases.
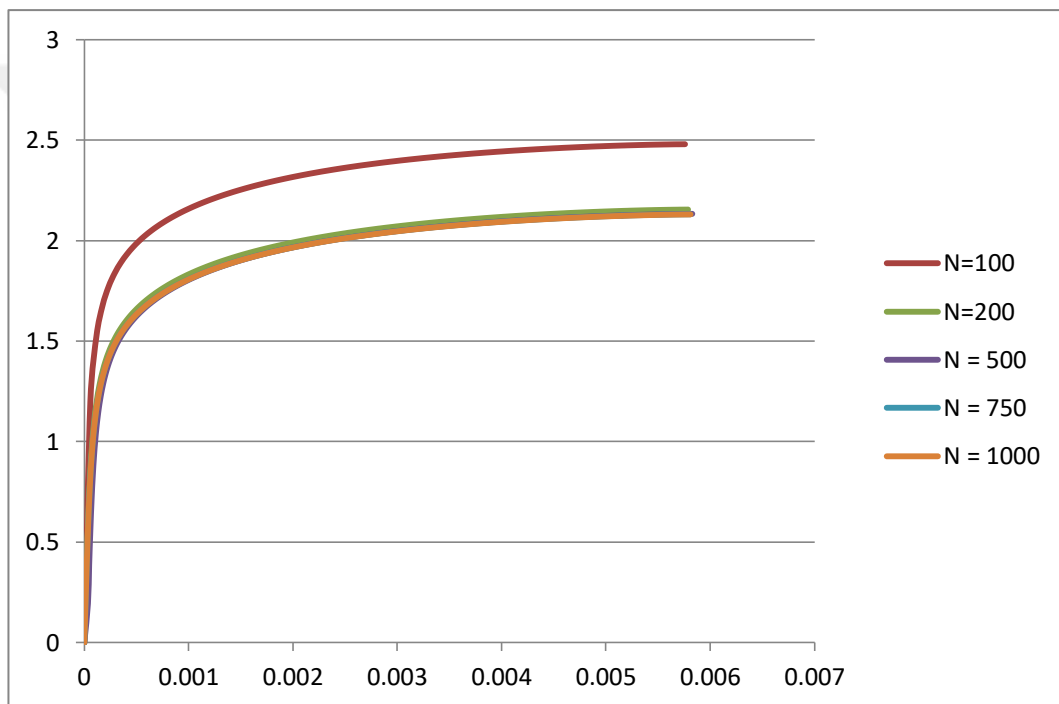
Figure 4.3 : Velocity profile for various grid number

4.5.4 Comparison of the both method

The computer codes are tested for 60 rpm inner pipe rotation and random pressure gradient. In Table 4.1, it can be seen that the discrepancy between Newton's method and the proposed numerical method is insignificant.

Table 4.1 : Comparison of two numerical approaches

Average Velocity (m/s)	Pressure Gradient (Pa/m)	Pressure Gradient (Pa/m)	Pressure Gradient (Pa/m)
	Newton's Method	Proposed Method	Experimental Result
0.74	203.608	203.612	145.737
1.09	354.112	354.108	312.074
1.41	526.893	526.881	510.901
1.73	732.615	732.622	731.447
2.40	1254.433	1254.456	1258.121
2.71	1539.298	1539.32	1578.124
3.36	2236.169	2236.179	2239.762

Therefore, other important parameter-computational cost-is checked for the same procedure. Table 4.2 shows time elapsed values for each method to predict average velocity at same input parameters. It is seen that proposed method takes relatively longer time than Newton's method

Table 4.2 : Computational cost for two models used in the present study for calculating frictional pressure losses at same input parameters

Predicting Average Velocity (seconds)	
Newton's Method	Proposed Method
8.8	20
8.6	28
8.7	34
9.3	39
9.4	43
9.5	56
10.6	69

5. RESULTS AND DISCUSSION

After conducting the experimental study for various flow rate, inner pipe rotation rate, and temperature, all the experimental data is gathered and ready to investigate the efficiency of the numerical study and proposed empirical equation. Following section is based on the empirical and numerical study of the present study.

5.1 Empirical Correlation for Determining Pressure Loss

To develop a general correlation for predicting annular frictional pressure loss by using experimental data, it is necessary to use dimensionless parameters which affect flow properties. In order to have dimensionless parameters, Buckingham-π theorem is used for the pressure gradient function as follows;

$$\frac{dP}{dL} = f\left(V, D, k, \mu, \rho, c_p, \omega\right) \tag{40}$$

In this problem, the repeating variables are V, D, k, μ. Therefore, we have three dimensionless parameters. After applying Buckingham-π theorem, dimensionless groups are specified as;

$$\Pi_1 = \frac{\mu}{\rho V D} \tag{41}$$

$$\Pi_2 = \frac{c_p \mu}{k} \tag{42}$$

$$\Pi_3 = \frac{\omega D}{V} \tag{43}$$

Obtained dimensionless groups from Buckingham-π theorem leads to decide what well known dimensionless parameters are used. As the inner pipe rotates, the flow has an oscillatory flow pattern and Taylor vortices, that cause destabilization of the flow due to the shear instability of axial flow and centrifugal instability. Two dimensionless parameters characterize the annular flow with inner pipe rotation. Those are Reynolds number and Taylor number. The Reynolds number for the annular flow and the generalized Taylor number for annular flow with inner pipe rotation are expressed as following equations [64] [65]

$$\text{Re} = \frac{U\left(D_o - D_i\right)}{\nu} \tag{44}$$

and

$$Ta = R_i\left(R_o - R_i\right)^3 \left(\frac{\omega}{\nu}\right)^2 \tag{45}$$

where is ρ density, U is flow velocity, ν is kinematic viscosity, ω is angular velocity, D_o and D_i are outer and inner pipe diameter, R_o and R_i are outer and inner pipe radius, respectively.

Moreover, there should be one more dimensionless parameter that reflects temperature effect on frictional pressure loss. Prandtl number is a dimensionless parameter found in energy equation and is expressed as follows:

$$\text{Pr} = \frac{c_p \mu}{k} \tag{46}$$

where c_p is specific heat, k is thermal conductivity, and μ is the dynamic viscosity of the fluid. Prandtl number is a temperature depended function. As temperature increases, Prandtl number decreases.

Uncertainty analysis has been used for determining the uncertainty corresponding to experimental data. General uncertainty analysis using the Taylor series method has been used. The maximum uncertainty values in Reynolds number, Taylor number, and Prandtl number were calculated as 1.8 %, 3.8 % and 0.5 %, respectively. Uncertainty analysis is presented in Appendix A in details.

The effect of variation of dimensionless parameters mentioned previously on frictional pressure losses is shown in Figure 5.1 – Figure 5.3. In Figure 5.1, it is seen that frictional pressure gradient increases as Reynolds number is increased. It can be expressed from the Darcy-Weisbach equation that pressure drop is a function of velocity squared. Moreover, Darcy friction factor is also a function of the Reynolds number. Therefore, an expected behavior pressure gradient along the flow direction shows an increase with the increasing value of Reynolds number. Prandtl number is the inverse proportion to temperature. Figure 5.2 shows that increasing temperature decreases pressure gradient. It is the fact that increasing temperature causes a decrease in viscosity, and hence decreasing the pressure gradient. Ahmed and Miska [75] indicated that pressure drop as a function of rotational speed is small compared to that in axial flow rate. Hence, a new dimensionless parameter (pressure loss gradient ratio) is introduced. This new parameter can be obtained by dividing pressure gradient at the current situation with the value of pressure gradient at room temperature without inner pipe rotation. If Figure 5.3 is analyzed, it can be seen that as temperature of water in fully eccentric annulus increases, pressure gradient decreases. On the other hand, the influence of temperature on pressure gradient becomes more severe as the Reynolds number is increased. As seen from Figure.5.4, the variation of Taylor number causes negligible change on frictional pressure losses for all temperature conditions investigated.
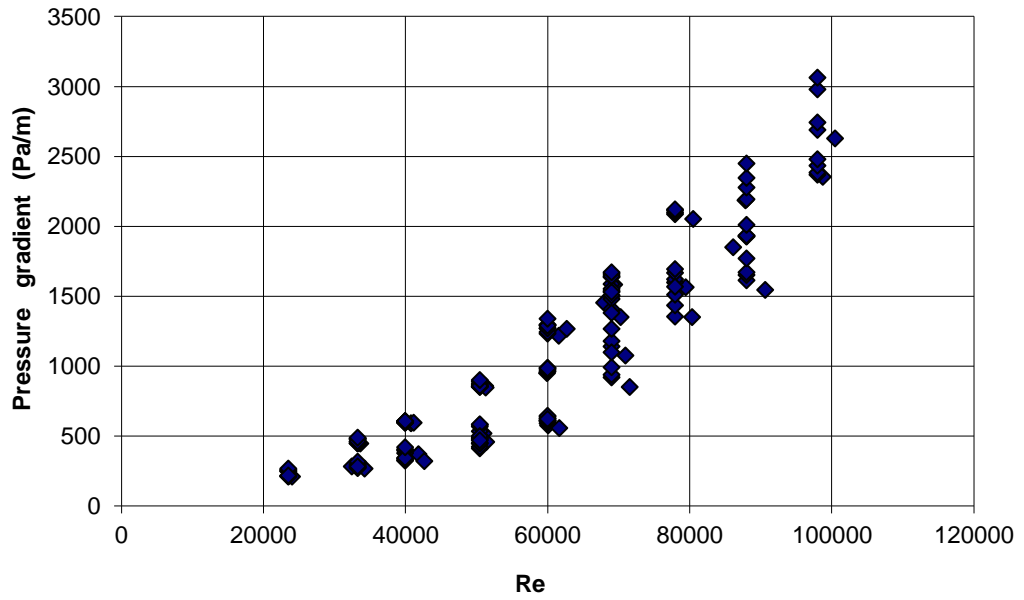
Figure 5.1 : Annular frictional pressure gradient (Pa/m) with respect to Reynolds number
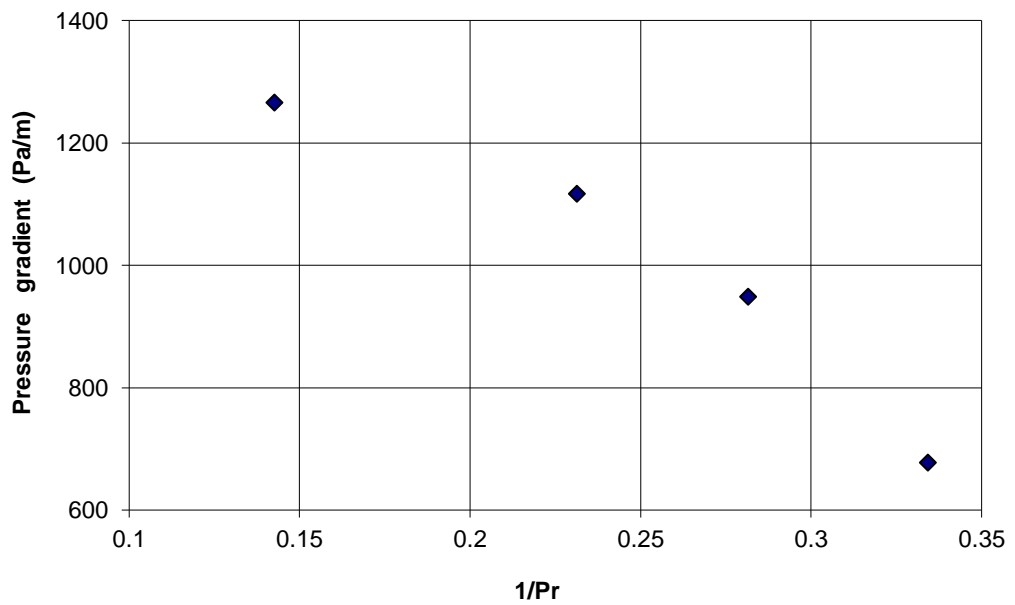
Figure 5.2 : Annular frictional pressure gradient (Pa/m) with respect to inverse of Prandtl number at Re = 60000 and Ta = 0
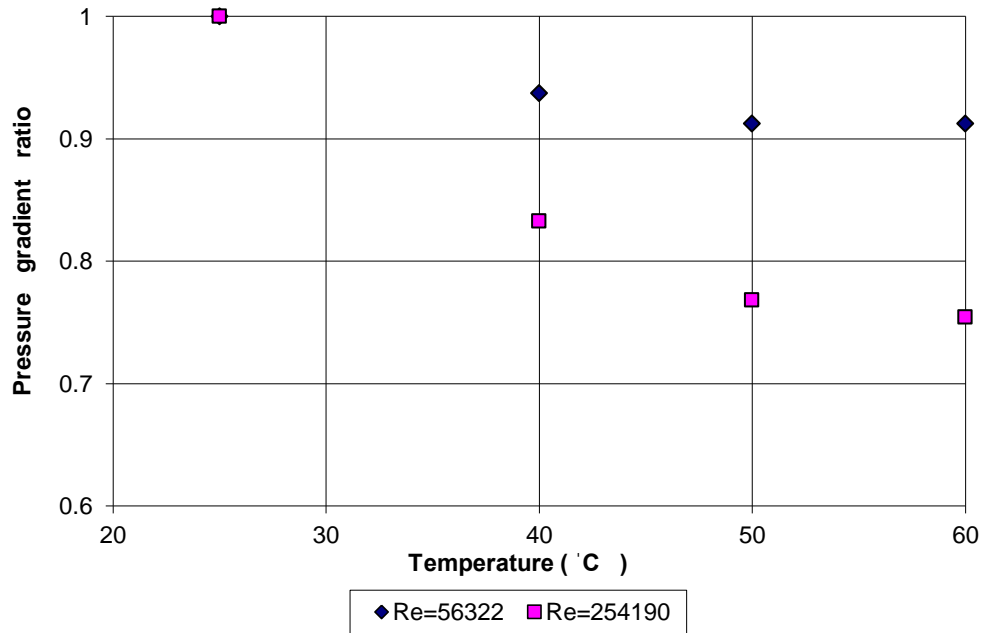
Figure 5.3 : Temperature effect on pressure gradient for different Reynolds number
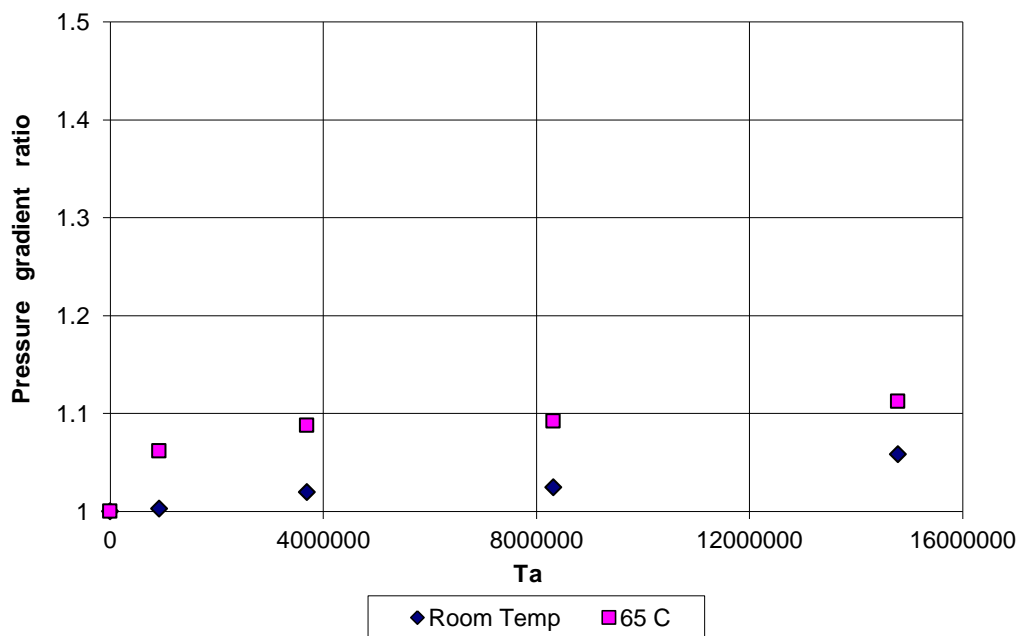
Figure 5.4 : Annular frictional pressure gradient ratio with respect to Taylor number at Re = 60,000 for different temperature values

50

With knowledge of those parameters' effects and experimental data, a simple correlation for annular frictional pressure losses is obtained by regression analysis. First, the pressure gradient is plotted as a function of Reynolds number shown in Figure 5.5.
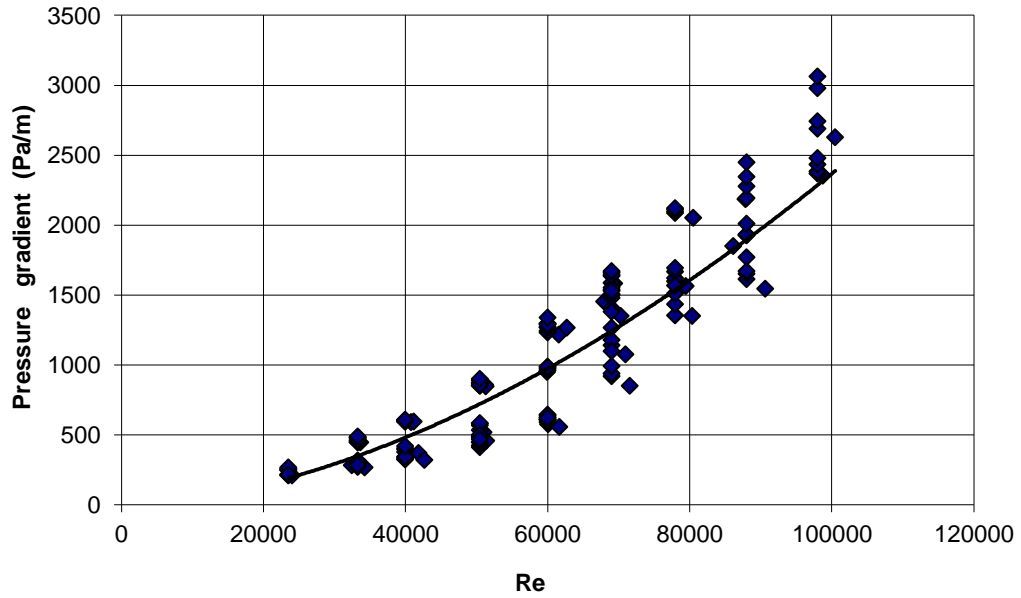
Figure 5.5 : Annular frictional pressure gradient with respect to Reynolds number

A regression analysis to fit a straight line through these points is given by;

$$\frac{dP}{dL} = A_0 \, \mathrm{Re}^{1.74} \tag{47}$$

where A_0 is a function of other parameters such as Taylor and Prandtl numbers.

Next step is plotting A_0 as a function of Taylor number on the semi-log scale. Figure 5.6 shows regression analysis to fit linear line through corresponding points.

51
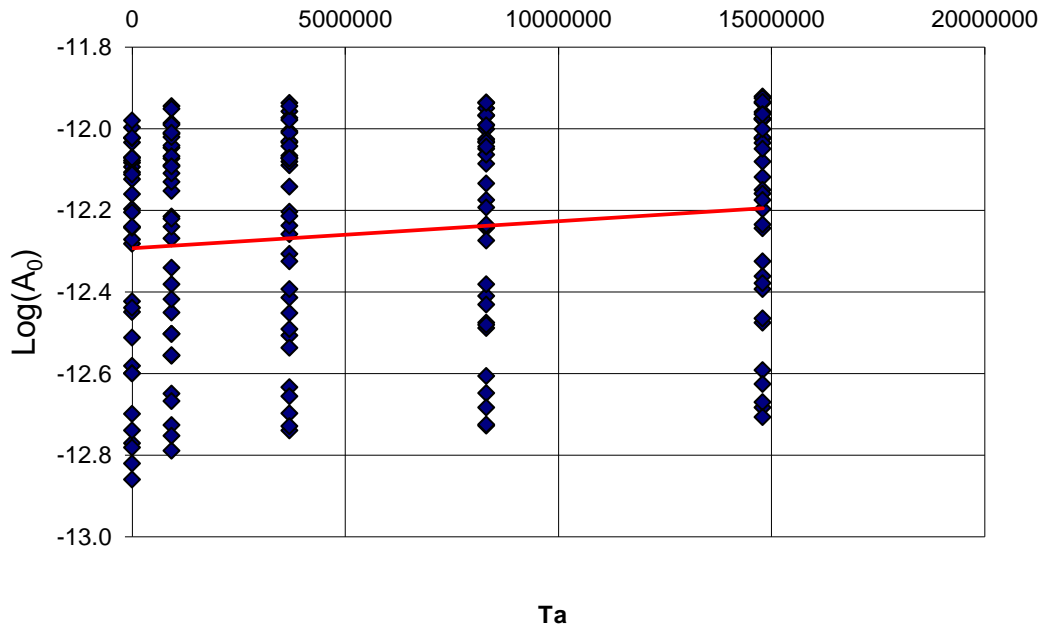
Figure 5.6 : A_0 with respect to Taylor number on semi-log scale

The following function should be obtained with the regression analysis;

$$\ln\left\{\frac{\left[dP/dL\right]}{\mathrm{Re}^{1.74}}\right\} = B + B_1 Ta \tag{48}$$

Equation (48) can be reformulated as the following equation:

$$\frac{\left[dP/dL\right]}{\mathrm{Re}^{1.74}} = B_{01} e^{7 x 10^{-9} Ta} \tag{49}$$

where B_{01} is a function of Prandtl number. In order to find the last coefficient to obtain a simple correlation for determining pressure gradient in an annulus, one more

regression analysis should be made. Figure 5.7 presents a regression analysis to fit a straight line through the corresponding points with respect to Prandtl number.
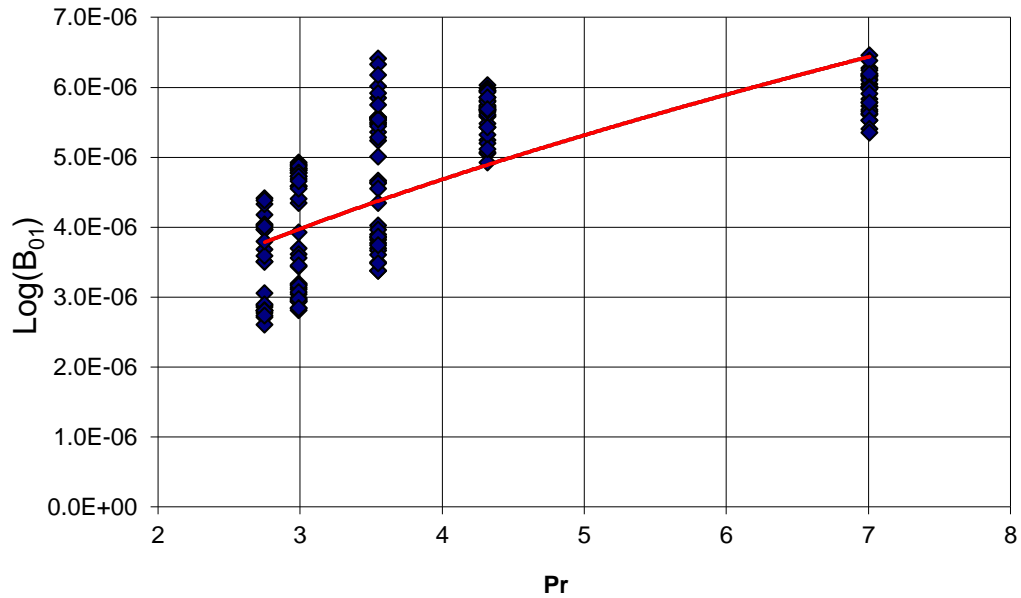
Figure 5.7 : B_{01} with respect to Prandtl number (Pr)

Obtained equation is as follows;

$$\frac{\left\{ dP / dL \right\}}{e^{7x10^{-9}Ta} \, \mathrm{Re}^{1.74}} = C_0 \, \mathrm{Pr}^{0.57} \tag{50}$$

The final equation of predicting annular frictional pressure loss is as following;

$$\frac{dP}{dL} = C_0 e^{7x10^{-9}Ta} \, \mathrm{Re}^{1.74} \, \mathrm{Pr}^{0.57} \tag{51}$$

More than 160 experiments are conducted to develop an understanding of annular frictional pressure losses in a fully eccentric annulus. When the temperature of water in the fully eccentric annulus is increased, pressure gradient decreases. Moreover, as the Reynolds number is increased, the influence of temperature on pressure gradient becomes more severe. Taylor number has no noticeable influence on frictional

pressure losses for all temperature conditions. Regression analysis of the dataset obtained from the experiments is done and a simple empirical frictional pressure losses correlation including temperature effect is proposed. In order to develop a general empirical correlation to estimate frictional pressure losses, three dimensionless parameters such as Reynolds number, Taylor number, Prandtl number – were used and a simple correlation based on the experimental data has been developed.

The values of the coefficients of the regression analysis are;

$$A_0 = 2x10^{-6}, \quad B_{01} = 4.6x10^{-6} \quad \text{and} \quad C_0 = 2x10^{-6} \tag{52}$$

The result in the following correlation for annular pressure gradient is

$$\frac{dP}{dL} = 2x10^{-6} \, \mathrm{Re}^{1.74} \, e^{7x10^{-9} Ta} \, \mathrm{Pr}^{0.57} \tag{53}$$

From uncertainty analysis, it is known that the maximum uncertainty values in Reynolds number, Taylor number and Prandtl number for the present study is 1.8 %, 3.8 % and 0.5 %, respectively. Therefore, the maximum uncertainty in predicting pressure gradient can be calculated as;

$$U^2_{dP/dL} = (1.74)^2 \left(\frac{U_{\mathrm{Re}}}{\mathrm{Re}} \right)^2 + \left(\frac{U_{Ta}}{Ta} \right)^2 + (0.57)^2 \left(\frac{U_{\mathrm{Pr}}}{\mathrm{Pr}} \right)^2 \tag{54}$$

Maximum uncertainty for determining pressure gradient is around 5%. That means the correlation has developed with 95% level of confidence. Comparison of predicted results by correlation and experimental data can be seen in Figure 5.8 with 0.9395 R^2 value (coefficient of determination). Correlation based on three dimensionless parameters such as Reynolds number, Taylor number, Prandtl number is practical to use in the field rather than solving a system of equations.
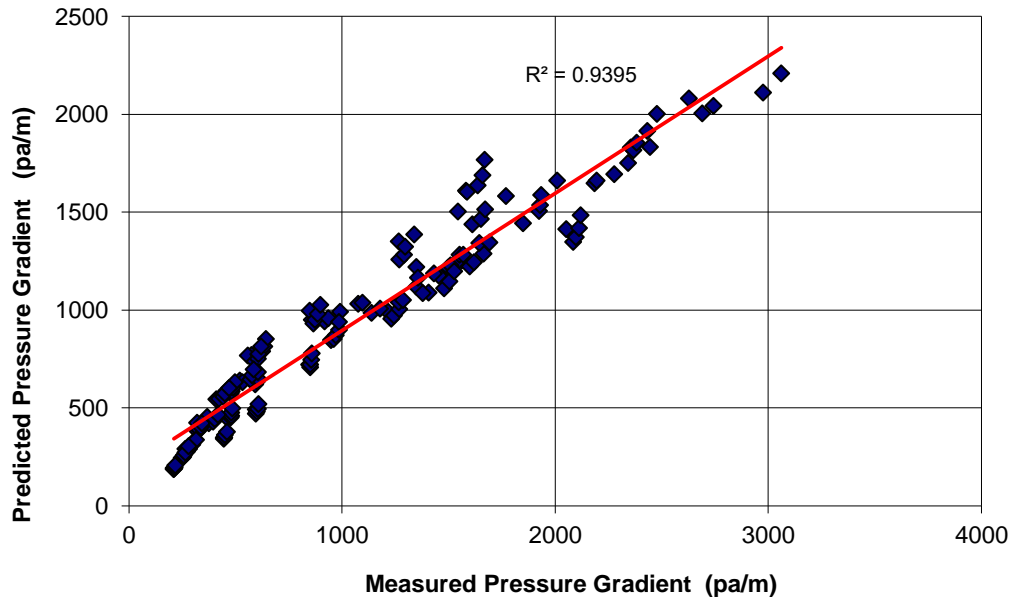
Figure 5.8 : Comparison of experimental annular frictional pressure loss measurements with predicted results obtained by correlation

As a result, the effect of temperature on frictional pressure losses could be estimated using the proposed correlation while rotating inner pipe. Furthermore, it is practical, due to its simplicity, to use the predicted correlation in field studies rather than solving a system of equations numerically to estimate annular frictional pressure losses.

5.2 Numerical Results of Mathematical Model

The mathematical insight of hydraulics applications is far from trivial. Comprehensive understanding of the physical behavior of fluid flow requires getting accurate solutions. Just recently, it has been gradually available to predict all features of the annular flow including its affecting parameters such as flow velocity, rotating cylinder, eccentricity as the numerical approaches have been developing with

technological enhancement. In the present study, a numerical method is proposed and compared its efficiency with a well-known numerical method, which is Newton-Raphson method. It is seen that proposed method takes relatively longer time than Newton's method. Although the proposed method is computationally expensive, it may help researchers to overcome the nonlinearity of challenging problems in order to have the approximate solutiond. In particular, it is hoped for momentum equation of fully developed turbulent flow including inner pipe rotation in curvilinear coordinates such as Bipolar coordinate which is one of the adequate coordinate systems for eccentric annulus geometry. Therefore, the proposed method is used for determining accurate frictional pressure gradient of turbulent flow through the fully eccentric annulus, including the effects of pipe rotation and temperature.

The experimental data should be compared in order to analyze the performance of the mathematical model. First, measured frictional pressure losses is compared with proposed model prediction at the conditions of room temperature and without inner pipe rotation. Figure 5.9 and Figure 5.10 show that the proposed model successively predicted frictional pressure losses for fully eccentric annulus.
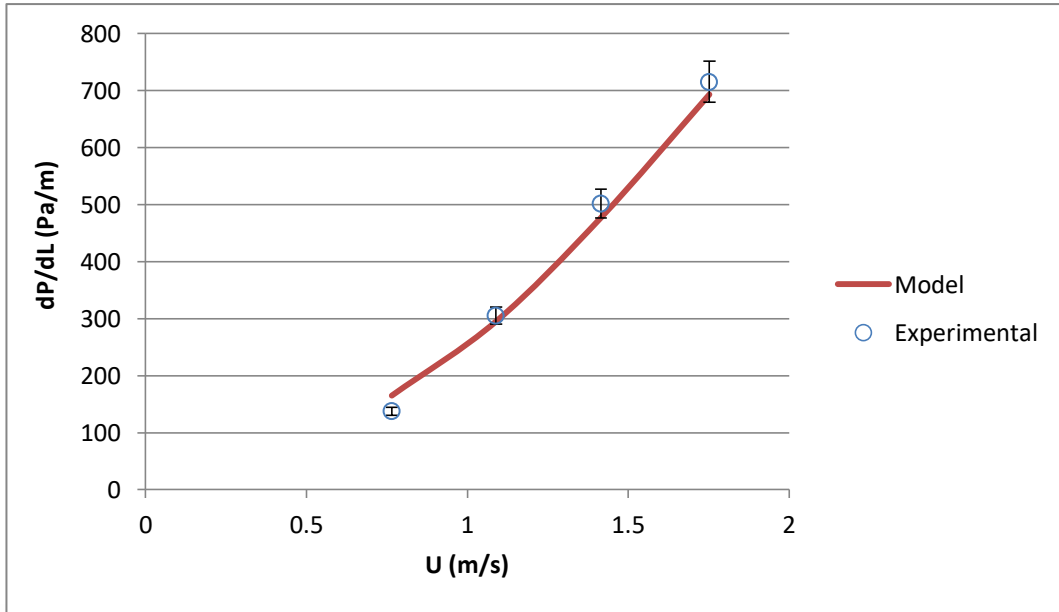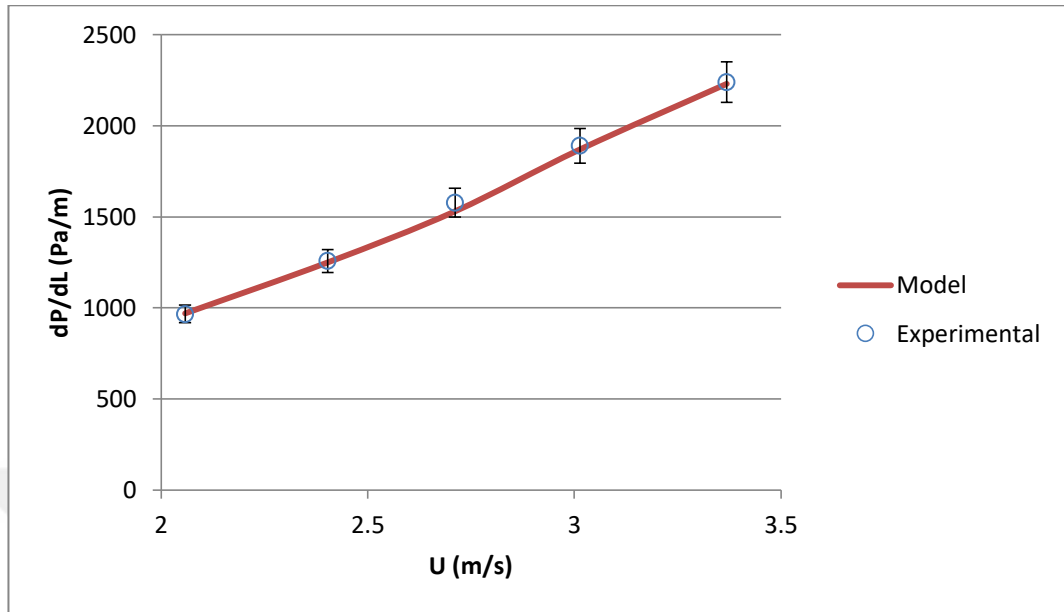
Figure 5.9: For low fluid velocity, comparison of measured and predicted pressure gradient for room temperature without inner pipe rotation
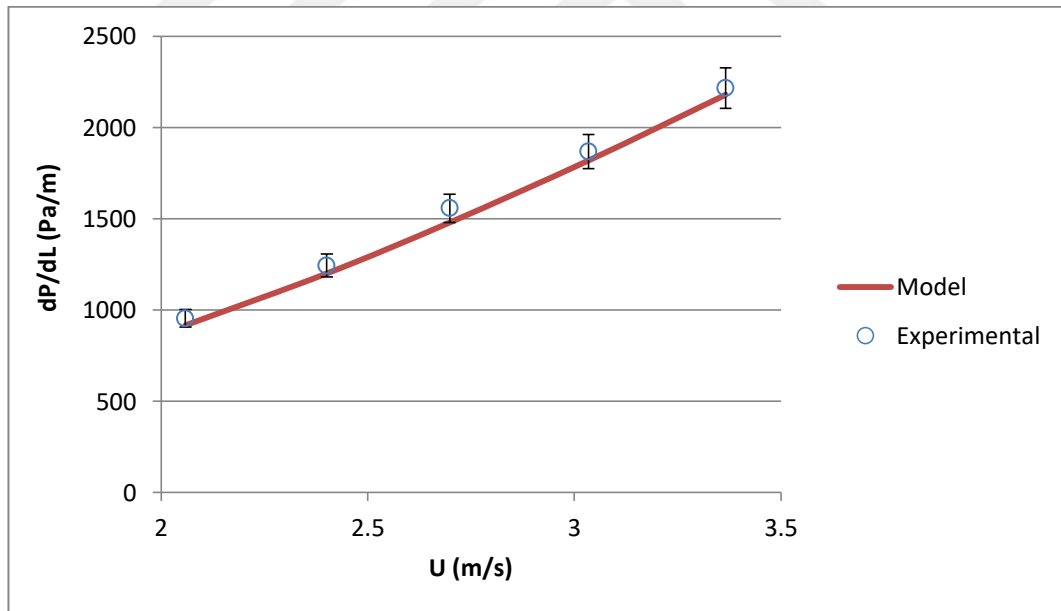
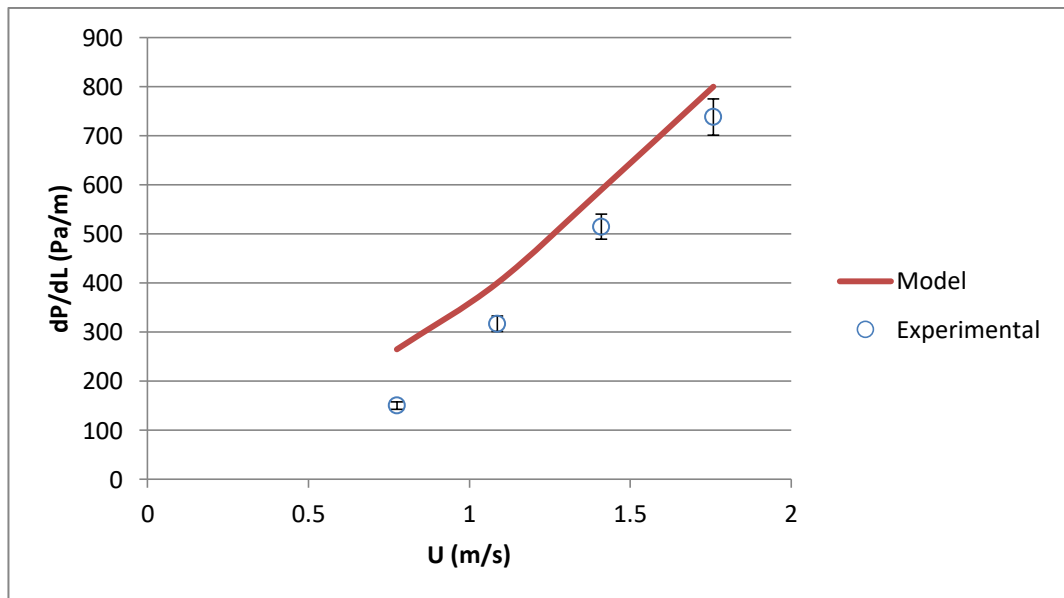**Figure 5.10:** For high fluid velocity, comparison of measured and predicted pressure gradient for room temperature without inner pipe rotation

The proposed model predicted the accurate frictional pressure losses within 5.3% error margin. This shows the model has good accuracy. From now on, temperature and rotation effects can be included and compared. The following figures (Figure 5.11-Figure 5.18) show the pressure gradient for different inner pipe rotation rate.
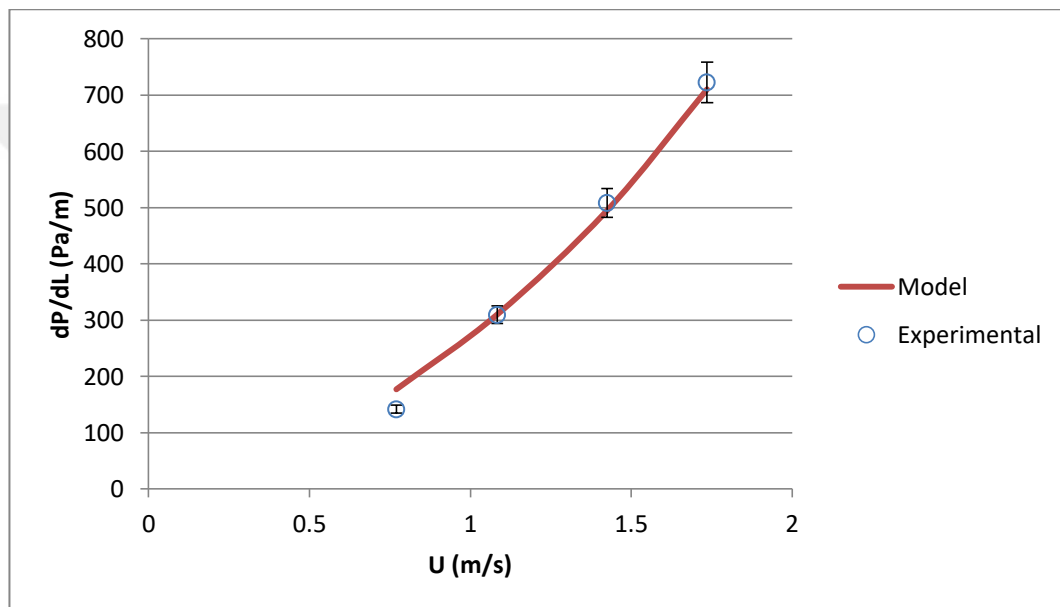
Figure 5.11: For low fluid velocity, comparison of measured and predicted pressure gradient for room temperature and 30 rpm
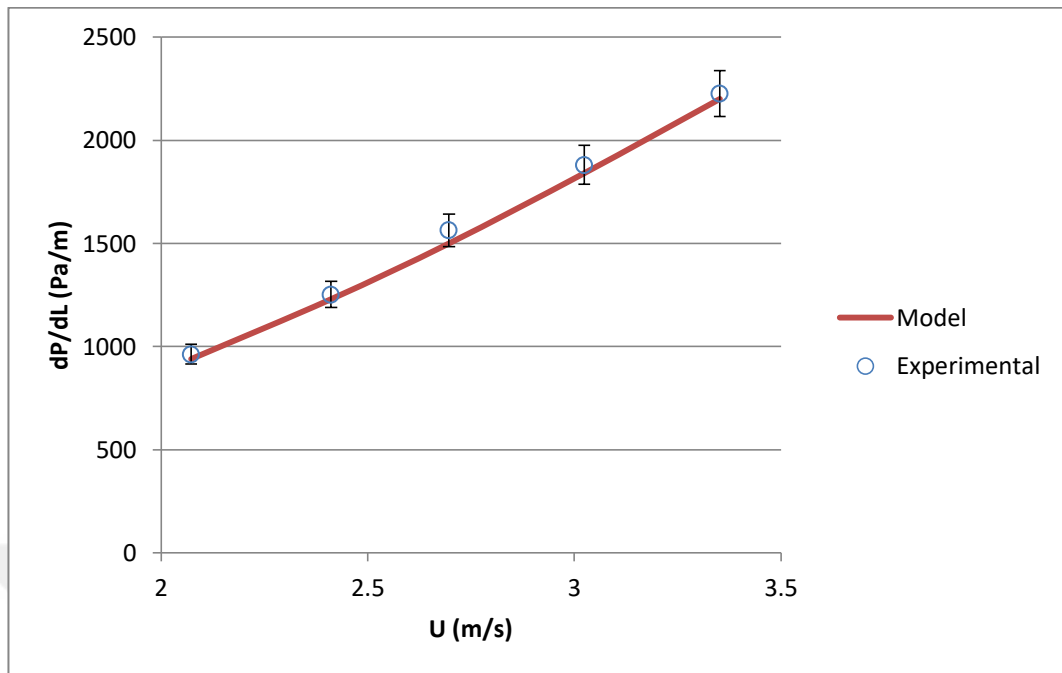
Figure 5.12: For high fluid velocity, comparison of measured and predicted pressure
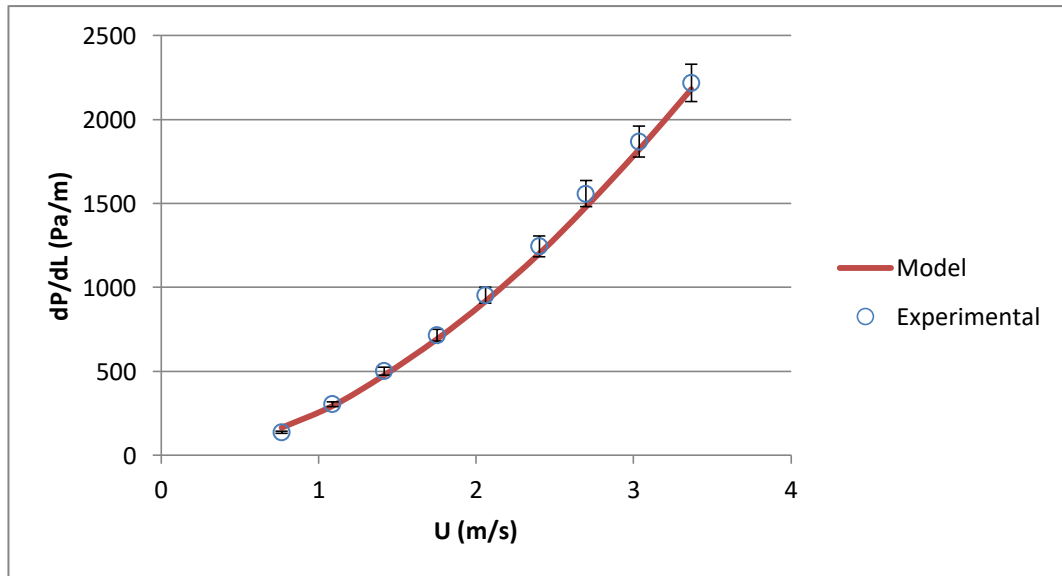
gradient for room temperature and 30 rpm
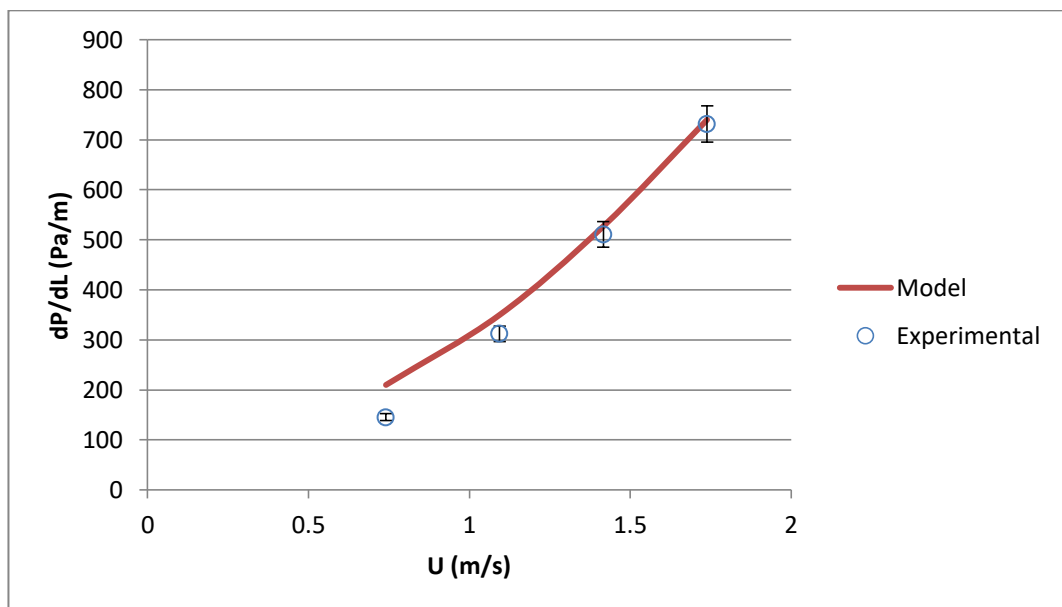
Figure 5.13: For low fluid velocity, comparison of measured and predicted pressure
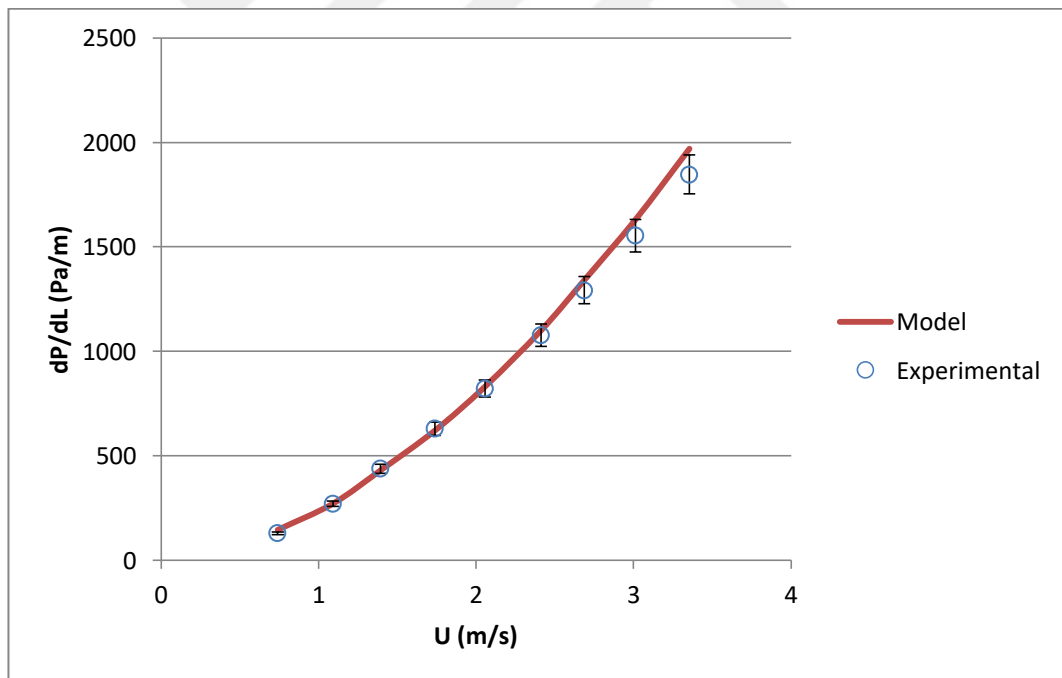
gradient for room temperature and 60 rpm

Figure 5.14: For high fluid velocity, comparison of measured and predicted pressure

gradient for room temperature and 60 rpm

Figure 5.15: For low fluid velocity, comparison of measured and predicted pressure

gradient for room temperature and 90 rpm
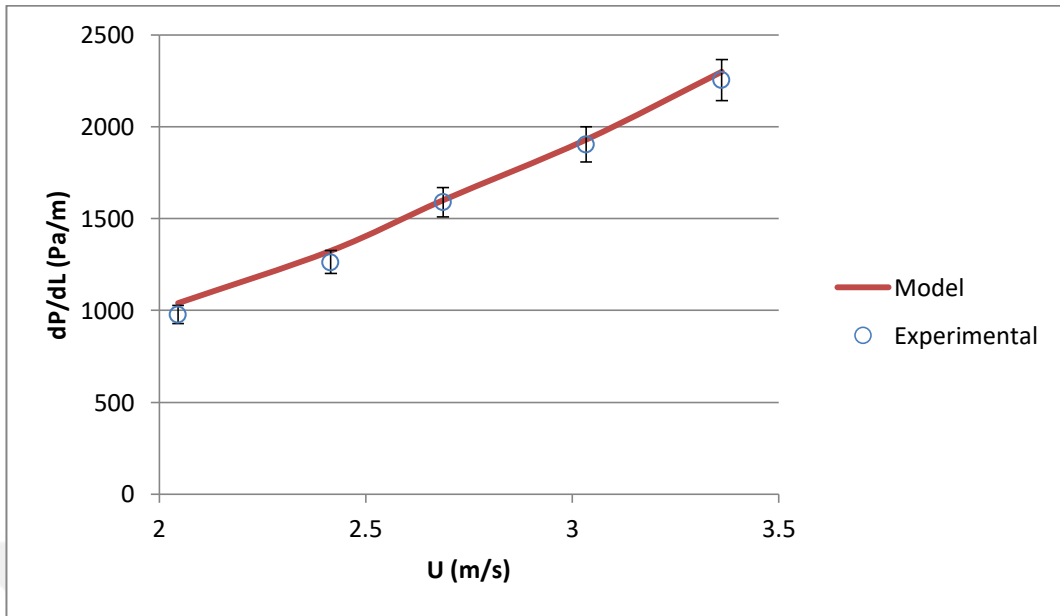
Figure 5.16: For high fluid velocity, comparison of measured and predicted pressure gradient for room temperature and 90 rpm
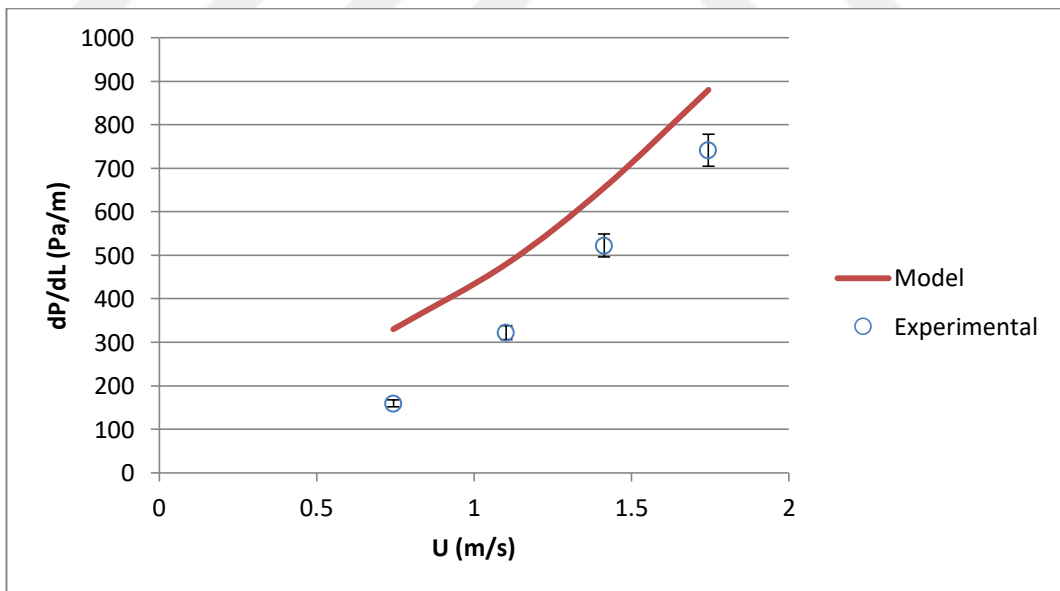
Figure 5.17: For low fluid velocity, comparison of measured and predicted pressure gradient for room temperature and 120 rpm
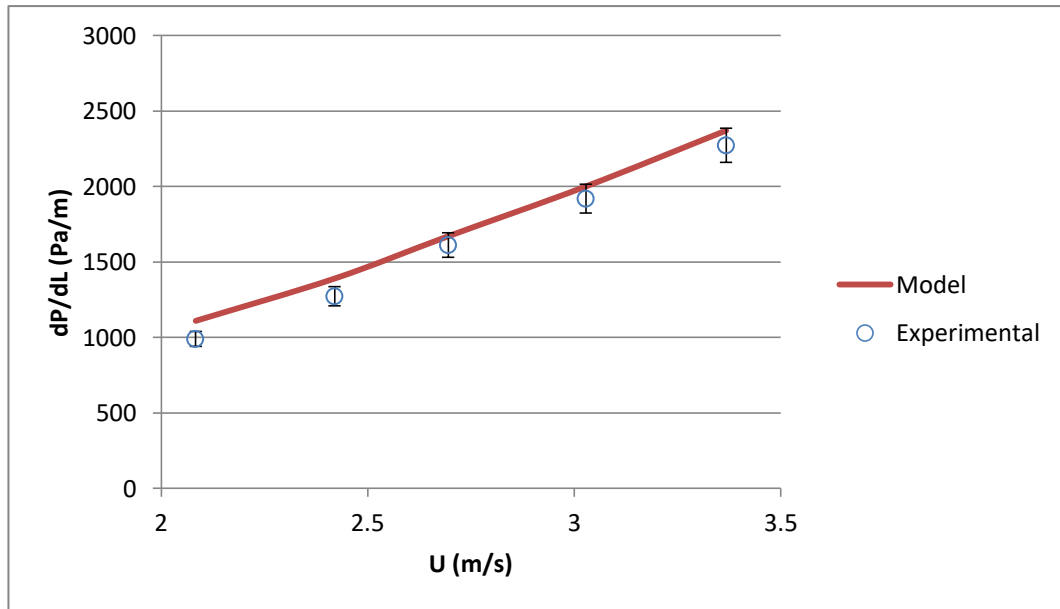
Figure 5.18: For high fluid velocity, comparison of measured and predicted pressure gradient for room temperature and 120 rpm

When the figures above are analyzed, it can be concluded that the model can predict better pressure gradient at higher velocities. At lower velocities and high inner pipe rotation rate, the model prediction performance is getting worse. The reason is the wobbling effect of the inner pipe due to concentric ends. The axial velocity couldn't overcome this effect at lower velocities. Therefore, the discrepancy between the results arises.

Now, it can be jumped to investigate temperature effect on annular flow. The following figures reflect the results of pressure gradient with respect to axial velocity without inner pipe rotation case. In order to see pure temperature effect, the rotational effect shouldn't be interfering. The following figures Figure 5.19- Figure 5.22 show pressure gradient with respect to axial velocity without inner pipe rotation and for different fluid temperature.
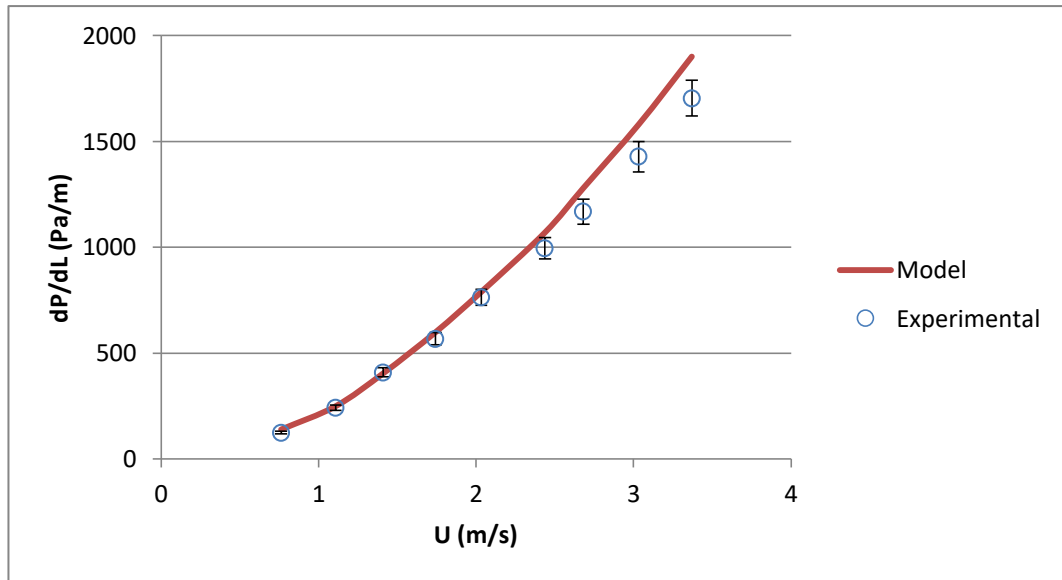
Figure 5.19 : Comparison of measured and predicted pressure gradient for room

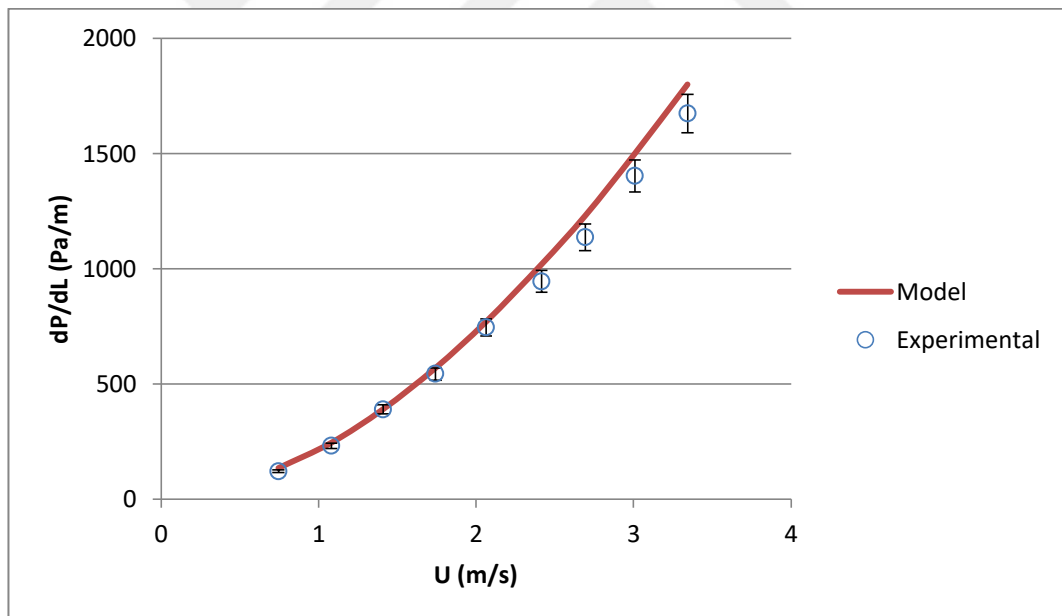temperature without inner pipe rotation at room temperature

Figure 5.20 : Comparison of measured and predicted pressure gradient for room
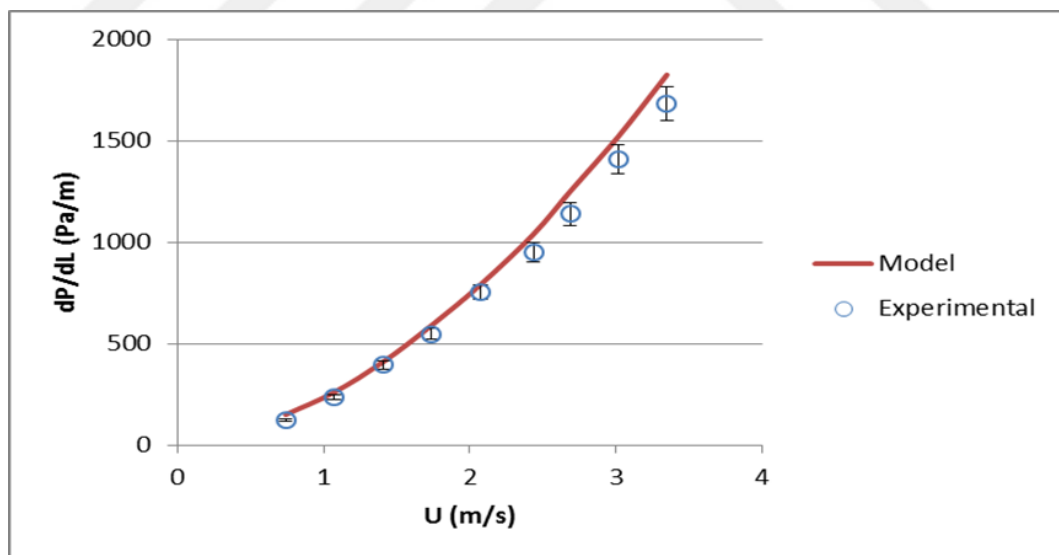
temperature without inner pipe rotation at 40 °C

63

Figure 5.21 : Comparison of measured and predicted pressure gradient for room

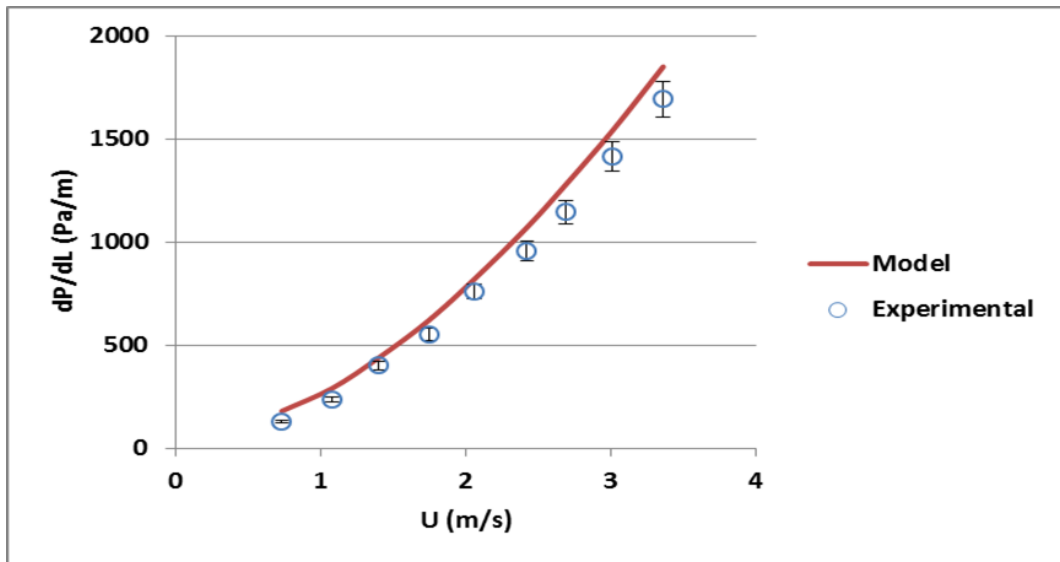temperature without inner pipe rotation at 50 °C

Figure 5.22 : Comparison of measured and predicted pressure gradient for room

temperature without inner pipe rotation at 60 °C

Increasing fluid temperature causes a discrepancy between measured and numerically predicted pressure gradient values. Most probably the reason for the discrepancy is due to plexiglass deformation with temperature. The deformation of the plexiglass causes dislocates the inner pipe relative to the outer pipe. That means eccentricity of the annulus might get different value. Therefore, both theta angle and slot height change with temperature. At higher velocities, the pressure gradient is higher and changing location effect can be seen greater. Although the drawbacks of the temperature and rotation effects on the mathematical model, the model can predict pressure gradient within 7%.

Next, it can be investigated the combined effect of temperature and rotation effects. The following figures represent the comparison of pressure gradient at 60 °C for different inner pipe rotation rates.
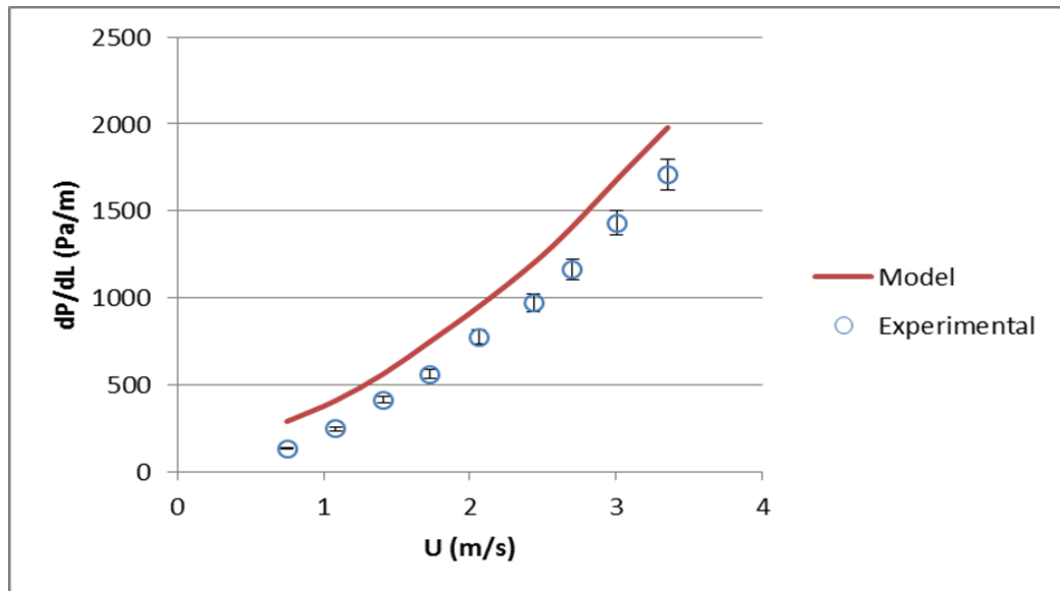

Figure 5.23 : Comparison of measured and predicted pressure gradient for room temperature and 30 rpm at 60 °C

Figure 5.24 : Comparison of measured and predicted pressure gradient for room

temperature and 60 rpm at 60 °C
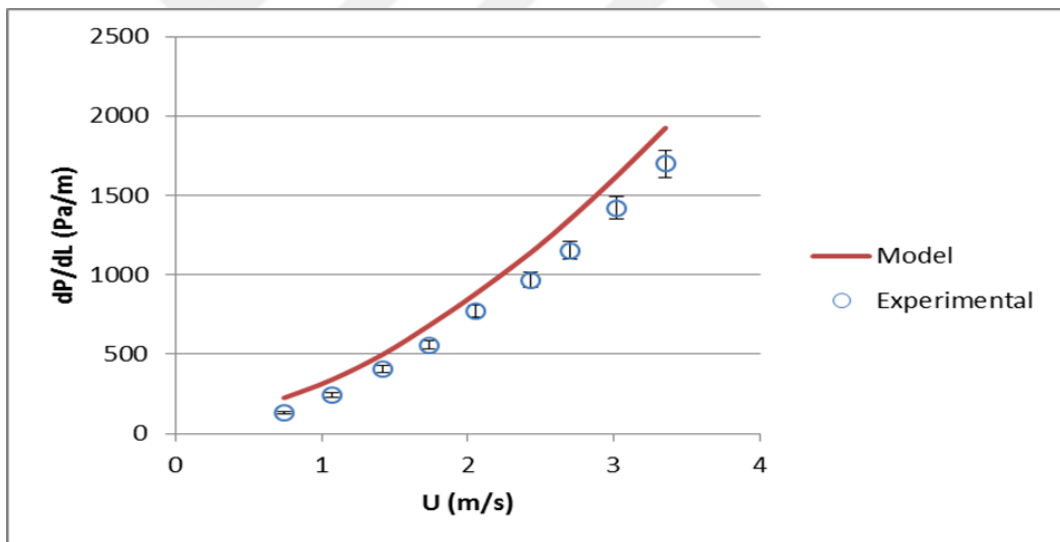
Figure 5.25: Comparison of measured and predicted pressure gradient for room

temperature and 90 rpm at 60 °C

Figure 5.26: Comparison of measured and predicted pressure gradient for room

temperature and 120 rpm at 60 °C

Combined effects trigger the predicting away from the actual value. Deformation with temperature might be greater with inner pipe rotation. The radial force may help to dislocate of the plexiglass which changes eccentricity in return. Nevertheless, even at those extreme conditions for the experiment done in the flow loop, Figures 5.23 - 5.26 indicate that the model still has good accuracy to predict pressure gradient.

5.3 Effect of Temperature and Rotation on Maximum Velocity in Eccentric Annulus

In the previous section, the figures are constructed with average fluid velocity in the fully eccentric annulus and the pressure transmitter is set the system at right degree. However, we know that the velocity profile is changing with the angle due to the eccentric geometry of the annulus. For a comprehensive study, one should see the whole region behavior. One of the adequate coordinate systems for modeling fluid

flow in the eccentric annulus is Bipolar Coordinates. However, modeling turbulent flow has still been a challenge due to its complex nature. Transforming turbulent momentum equation from Cartesian Coordinates to Bipolar Coordinates system results in a huge differential equation which is not easy to solve by current technological enhancement. In order to analyze the effects of temperature and rotation on turbulent flow through the eccentric annulus, one can utilize the present model in this study by changing the radial angle for each increment. Due to symmetry, it is only half of the domain taken. Therefore, the angle is scanned till 180° with an increment of 5°. Some of the velocity profile of the fluid flow inside the annulus is given below and the rest can be found in Appendix C.
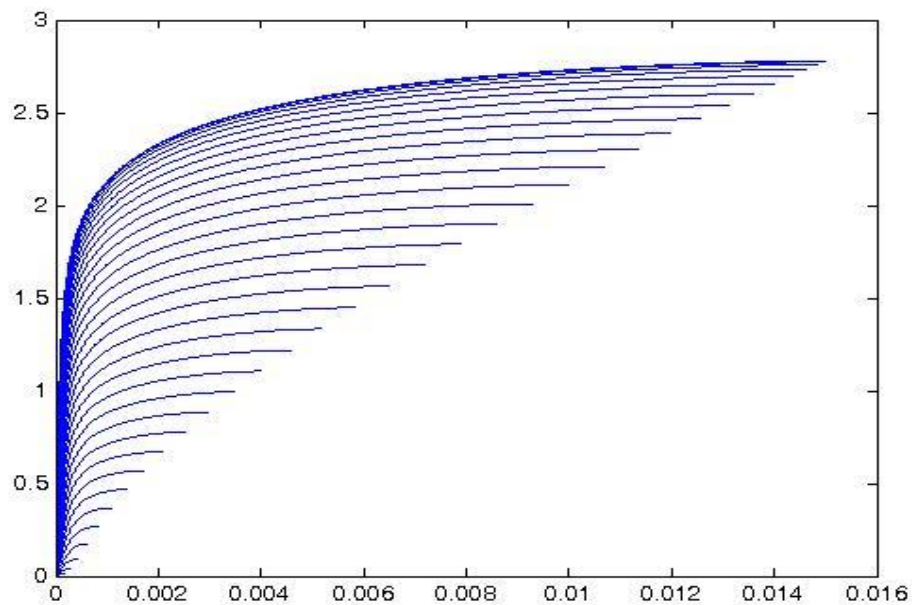
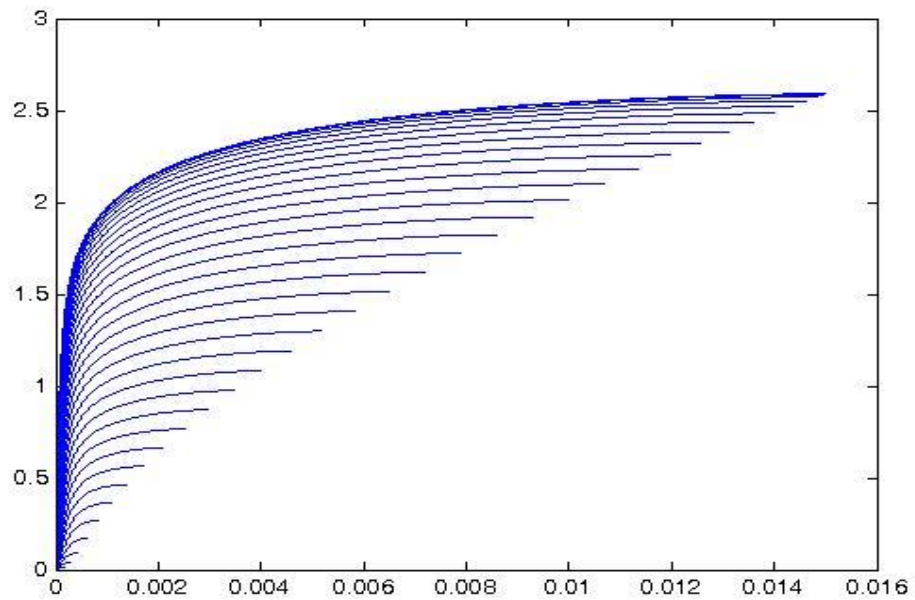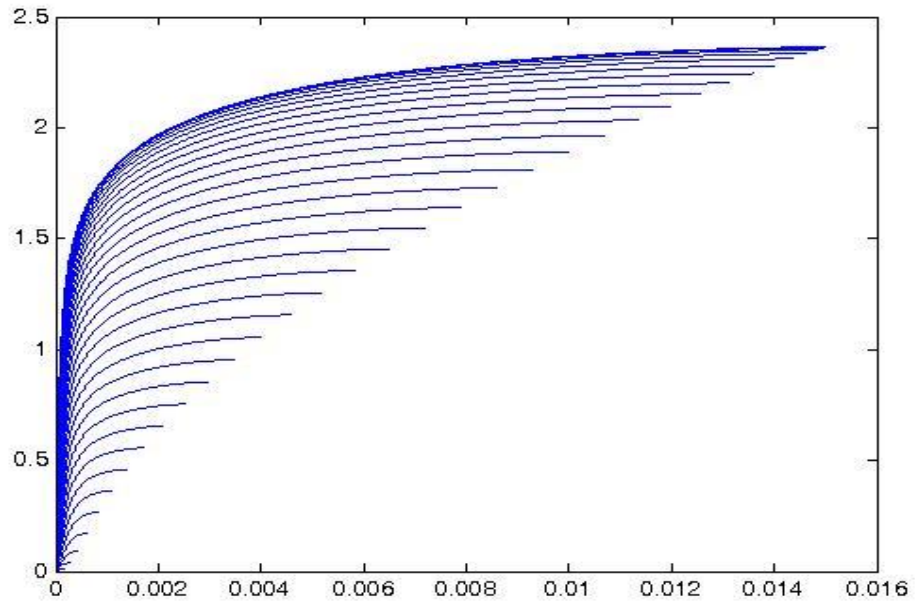**Figure 5.27 :** Velocity profile for half domain of the annulus at each angle at

dP/dL=1000 Pa/m, $\omega = 0$ RPM, and T = 23 °C
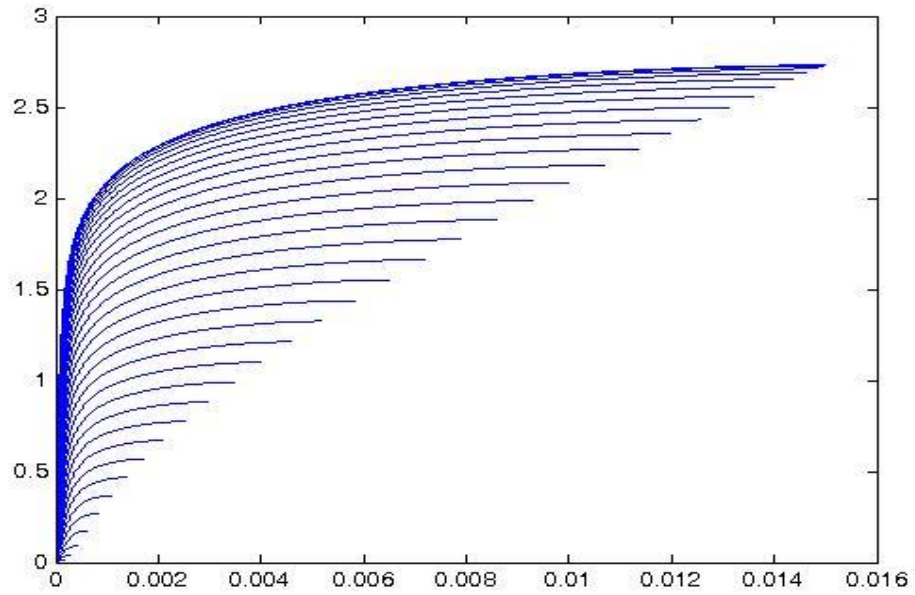
Figure 5.28 : Velocity profile for half domain of the annulus at each angle at

dP/dL=1000 Pa/m, ω = 30 RPM, and T = 23 °C

Figure 5.29 : Velocity profile for half domain of the annulus at each angle at
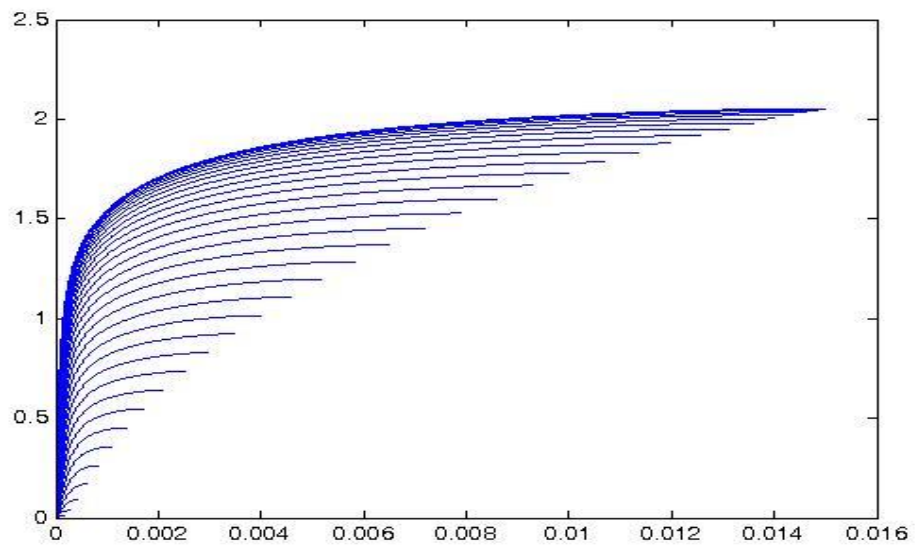
dP/dL=1000 Pa/m, ω = 60 RPM, and T = 23 °C

Figure 5.30 : Velocity profile for half domain of the annulus at each angle at
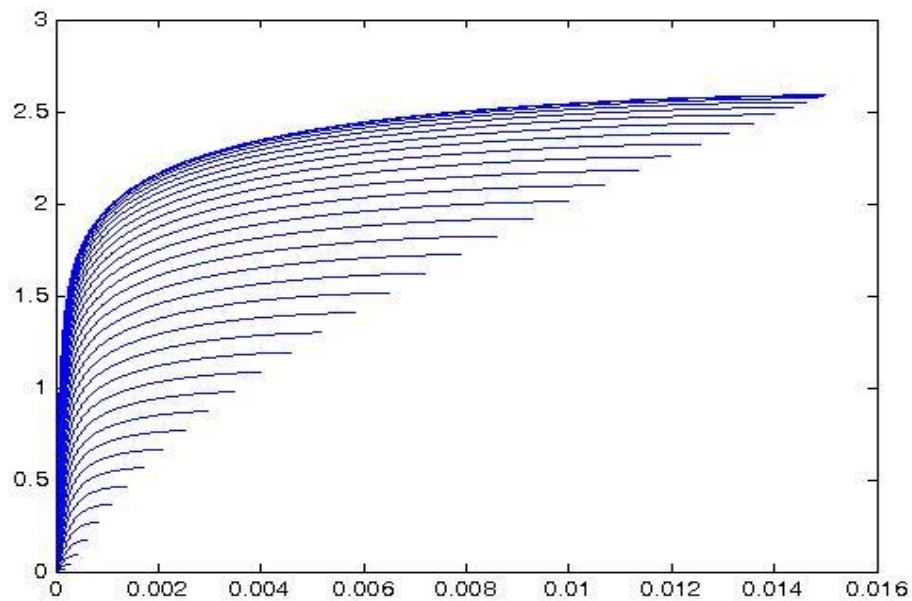
dP/dL=1000 Pa/m, ω = 90 RPM, and T = 23 °C

Figure 5.31 : Velocity profile for half domain of the annulus at each angle at

dP/dL=1000 Pa/m, ω = 120 RPM, and T = 23 °C

As it can be observed from the figures, one can figure out that maximum velocity at the higher slot height. In return, it can be concluded that the maximum velocity is developed at the 0 angle of the annulus where the distance between inner and outer pipe is highest. Another conclusion is rotation decreases maximum velocity in order to have same pressure loss. On the other hand, the temperature should also be checked in order to fully understand the flow performance. The following figures show that velocity profile for the different temperature at same inner pipe rotation and pressure loss.

Figure 5.32 : Velocity profile for half domain of the annulus at each angle at

dP/dL=1000 Pa/m, $\omega = 60$ RPM, and T = 23 °C
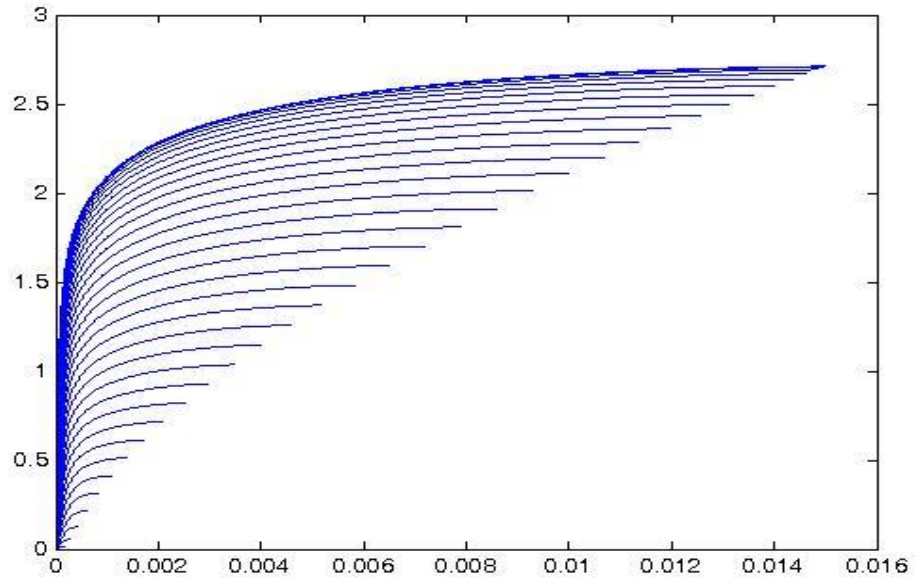
Figure 5.33 : Velocity profile for half domain of the annulus at each angle at
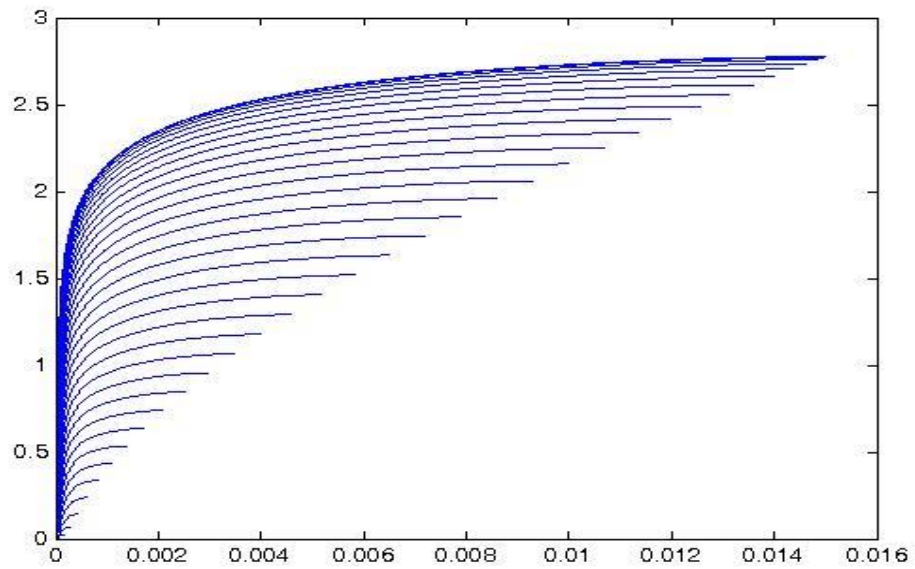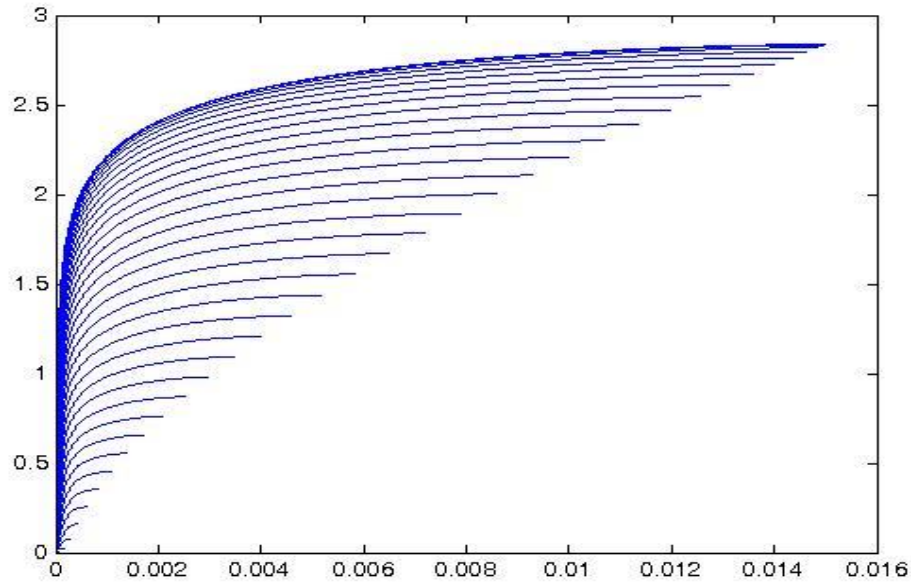
dP/dL=1000 Pa/m, ω = 60 RPM, and T = 40 °C

Figure 5.34 : Velocity profile for half domain of the annulus at each angle at

dP/dL=1000 Pa/m, ω = 60 RPM, and T = 50 °C

Figure 5.35 : Velocity profile for half domain of the annulus at each angle at
dP/dL=1000 Pa/m, ω = 60 RPM, and T = 60 °C

Increasing temperature at same pressure loss causes an increase in maximum velocity. But the effect of temperature on maximum velocity is not seen as dominant as rotation. The reason may be disturbtion of rotation on axial flow. On the other hand, there shouldn't be any external effect on the velocity profile due to temperature. In order to see the details of this phenomena, they should be investigated for same flow rate instead of same pressure loss. The following figures show the effects of temperature and rotation on the maximum velocity of annular flow through the eccentric annulus.
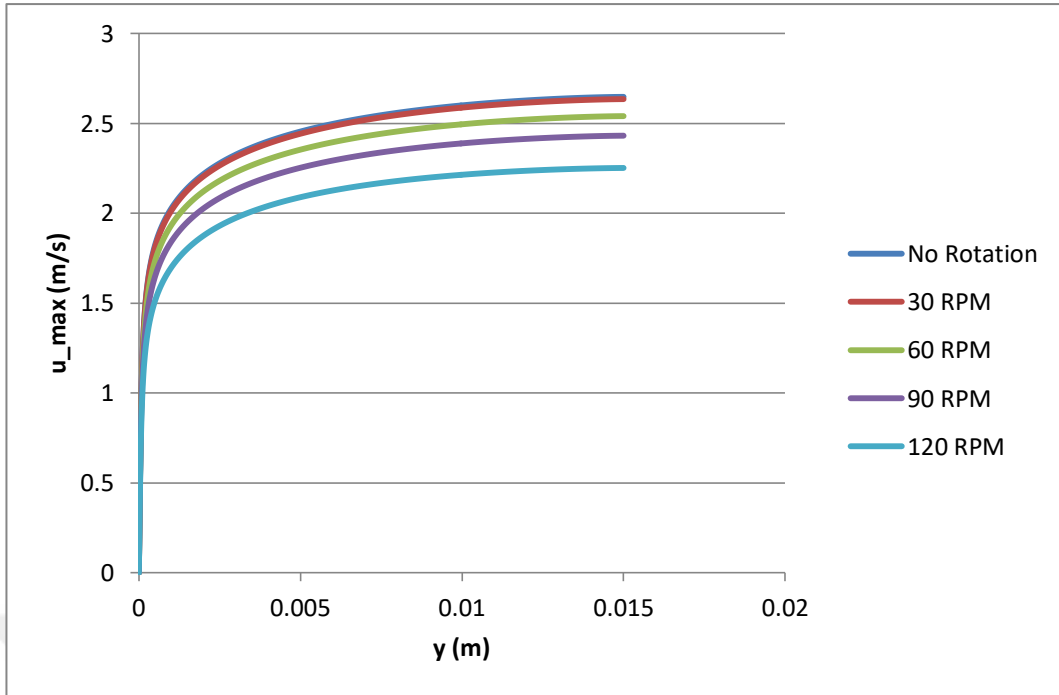
Figure 5.36: Maximum velocity profile for different inner pipe rotation at room temperature for same flow rate
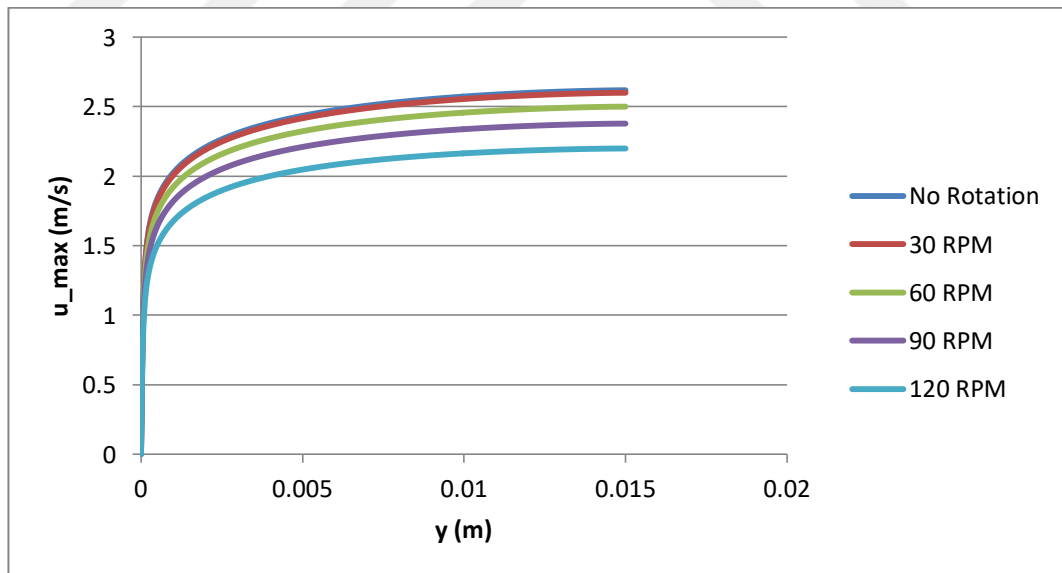
Figure 5.37: Maximum velocity profile for different inner pipe rotation at 40 °C for same flow rate
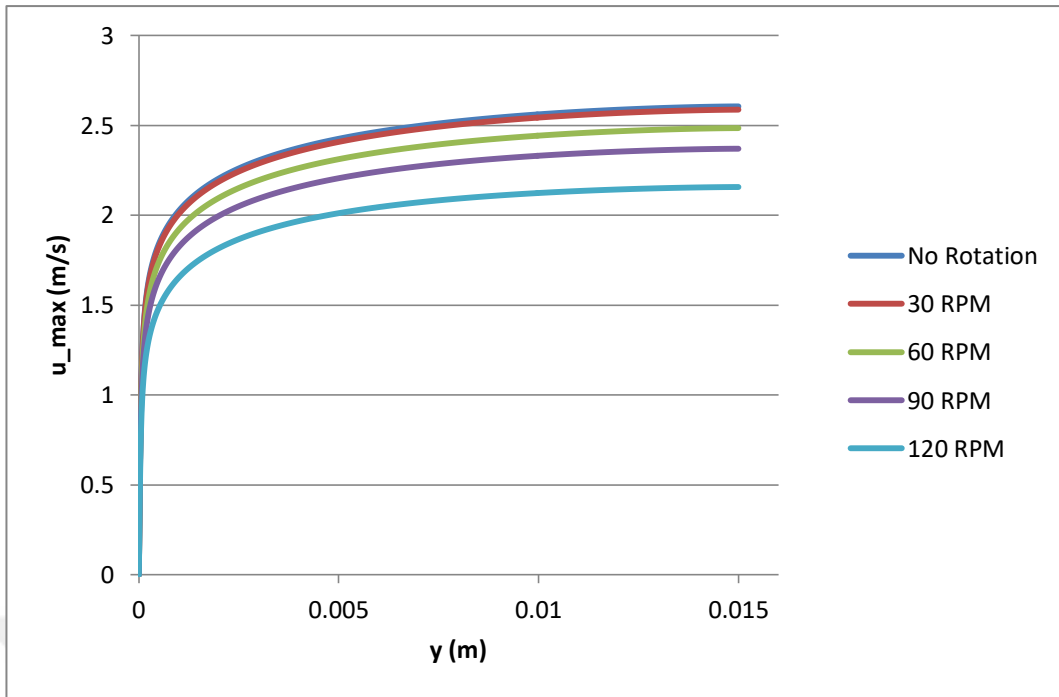
Figure 5.38: Maximum velocity profile for different inner pipe rotation at 50 °C for

same flow rate

Figure 5.39 : Maximum velocity profile for different inner pipe rotation at 60 °C for

same flow rate

75

It is now obvious that inner pipe rotation affects the flow pattern inside the annulus without depending temperature variance. Increasing inner pipe rotati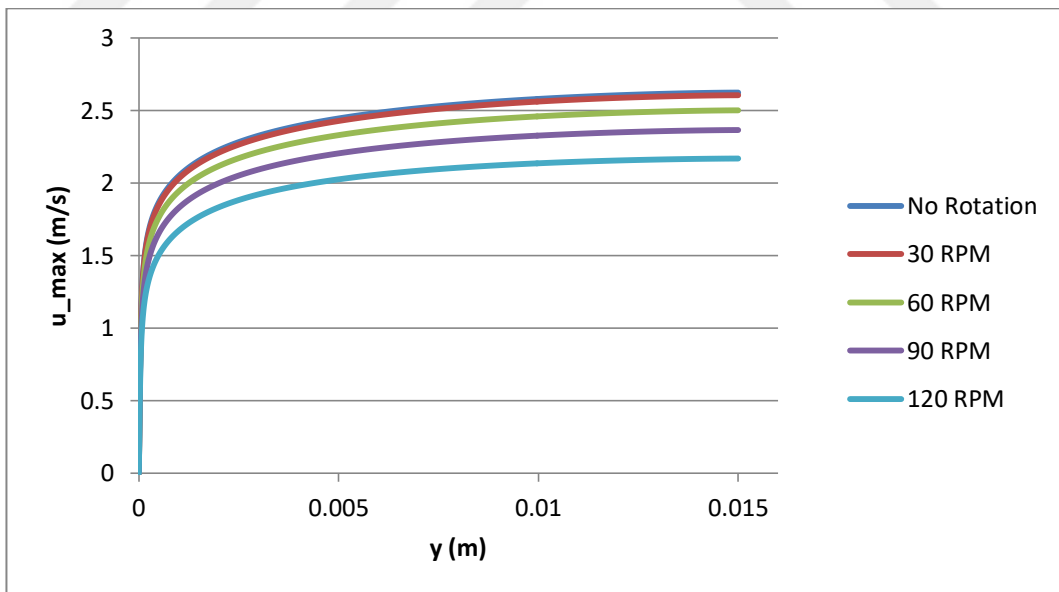on decreases maximum velocity in annulus due to disturbance of radial movement. When the inner pipe rotates, it creates a helical flow which decreases axial flow. Moreover, the wobbling effect also interferes and causes the disturbance which in return decreases maximum velocity. However, the rotation effect is not visible till 30 RPM. After this rotation rate, the effect becomes dominant and change maximum velocity drastically. On the other hand, it can be seen that temperature effect is negligible when the above figures are analyzed carefully. In order to see it explicitly, the following figure should be analyzed as well.
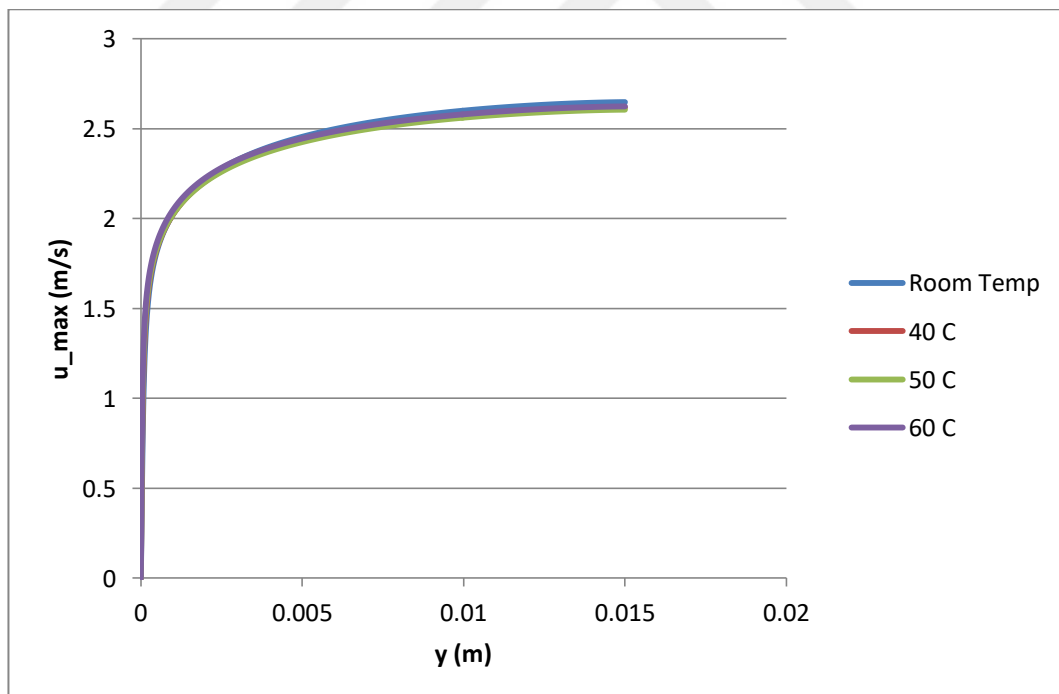
Figure 5.40 : Maximum velocity profile for different temperature without inner pipe rotation

76

As it is seen in the figures, it is clear that temperature has a negligible effect on flow profile in the annulus. Overall, it is observed that increasing inner pipe rotation at constant pressure gradient decreases maximum velocity value. In contrast, increasing the fluid temperature at constant pressure gradient increase maximum velocity value for annulus flow. When the flow rate of the system is set to a constant value, it can be observed that maximum velocity get lower value with increasing inner pipe rotation, however changing temperature doesn't have a significant variation on maximum velocity value. In conclusion, changing inner pipe rotation affects both flow profiles and frictional pressure loss. On the other hand, changing fluid temperature affects only frictional pressure loss. The reason is that temperature plays a significant role determining fluid density and viscosity which is effective on pressure gradient. But, temperature does not interfere any external force on axial flow. In contrast, inner pipe rotation disturbs axial flow and causes distributing the velocity profile in the eccentric annulus. This causes changes in frictional pressure, although there is no viscosity or density variation with motion due to the incompressible and Newtonian fluid that is used in the present experiment.

6. CONCLUSIONS

In order to determine rotation and temperature effects on pressure losses of Newtonian fluid for fully developed turbulent flow in fully eccentric annulus;

- Total of 148 distinct experiments were recorded for different velocity, temperature, and revolution of the inner pipe.

- By experiments, it has been observed that increasing axial velocity causes an increase in frictional pressure loss. On the other hand, increasing fluid temperature give results in decreasing frictional pressure loss. Besides that, inner pipe rotation does not have a significant effect on frictional pressure loss for turbulent flow when we compare other two parameter effects.

- Uncertainty analysis was done and around 5% of error arises due to experimental tools nature.

- A simple correlation – based on three dimensionless parameters (Reynolds number, Prandtl number, and Taylor number) were proposed. It is developed with 95% level of confidence and 0.9395 as the coefficient of determination.

- Two different numerical methods are used to solve Navier-Stokes equations including inner pipe rotation effects and turbulent flow. Proposed approach primarily discretizes the equation using finite difference method and solved iteratively by freezing the nonlinear terms. The other approach "Newton-

78

Raphson method" linearizes the equation at first and then solves iteratively. Although the former is computationally expensive, this numerical technique may allow solving challenging problems. Additionally, the proposed method predicts frictional pressure losses successfully. A mechanistic model is developed using proposed numerical method for fully developed turbulent flow through eccentric annulus including inner pipe rotation. When the developed mechanistic model is compared with experimental measurements, it gives reasonably good agreement.

- Results showed that without rotation and temperature effects, the developed model can determine pressure losses within 7% error margin. However, the discrepancy between experimental and numerical results gets higher when either one or both of rotation and temperature play in role in the system. Nevertheless, the model can determine pressure losses within 16.2% error margin for all cases.

- With the help of numerical solver, many figures were produced in order to understand flow behavior and performance by looking flow profile and maximum velocity values at a constant flow rate or constant frictional pressure losses.

- It is observed that increasing inner pipe rotation at constant pressure gradient decreases maximum velocity, increasing the fluid temperature at constant pressure gradient increase maximum velocity in the eccentric annulus. Maximum velocity gets lower value with increasing inner pipe rotation, however changing temperature doesn't have a significant variation on maximum velocity value when the flow rate is kept in a certain range.

79

- It can be concluded that changing inner pipe rotation affects both flow profiles and frictional pressure loss. On the other hand, changing fluid temperature affects only frictional pressure loss.

REFERENCES

[1] **Boussinesq, J. (1877).** Théorie de l'écoulement tourbillant. Mem. Présentés par Divers Savants Acad. Sci. Inst. Fr, 23(46-50), 6-5.

[2] **Reynolds, O. (1894).** On the dynamical theory of incompressible viscous fluids and the determination of the criterion. Proceedings of the Royal Society of London, 56(336-339), 40-45.

[3] **Prengle, R. S., & Rothfus, R. R. (1955).** Fluid Mechanics Studies-Transition Phenomena in Pipes and Annular Cross Sections. Industrial & Engineering Chemistry, 47(3), 379-386.

[4] **Fredrickson, A., & Bird, R. B. (1958).** Non-Newtonian flow in annuli. Industrial & Engineering Chemistry, 50(3), 347-352.

[5] **Rothfus, R. R., Sartory, W. K., & Kermode, R. I. (1966).** Flow in concentric annuli at high reynolds numbers. AIChE Journal, 12(6), 1086-1091.

[6] **Skelland, A. H. P. (1967).** "Non-Newtonian Flow and Heat Transfer", John Wiley &Sons, Inc. New York.

[7] **Quarmby, A. (1967).** An experimental study of turbulent flow through concentric annuli. International Journal of Mechanical Sciences, 9(4), 205-221.

[8] **Clump, C. W., & Kwasnoski, D. (1968).** Turbulent flow in concentric annuli. AIChE Journal, 14(1), 164-168.

[9] **Meter, D. M., & Byron Bird, R. (1961).** Turbulent Newtonian flow in annuli. AIChE Journal, 7(1), 41-45.

[10] **Hanks, R. W., & Larsen, K. M. (1979).** The flow of power-law non Newtonian fluids in concentric annuli. Industrial & Engineering Chemistry Fundamentals, 18(1), 33-35.

[11] **Leung, J. C. M. (1981).** An Imprawement in the Calculation of Turbulent Friction in Smooth Concentric Annuli1. Journal of Fluids Engineering, 103, 615.

[12] **Nouri, J. M., Umur, H., & Whitelaw, J. H. (1993).** Flow of Newtonian and non-Newtonian fluids in concentric and eccentric annuli. Journal of Fluid Mechanics, 253, 617-641.

[13] **Gücüyener, H. I., & Mehmetoğlu, T. (1992).** Flow of yield-pseudo-plastic fluids through a concentric annulus. *AIChE journal*, *38*(7), 1139-1143.

[14] **Escudier, M. P., & Gouldson, I. W. (1995).** Concentric annular flow with centerbody rotation of a Newtonian and a shear-thinning liquid. International journal of heat and fluid flow, 16(3), 156-162.

[15] Gücüyener, I. H., & Mehmetog, T. (1996). Characterization of flow regime in concentric annuli and pipes for yield-pseudoplastic fluids. *Journal of Petroleum Science and Engineering*, *16*(1-3), 45-60.

[16] Filip, P., & David, J. (2003). Axial Couette–Poiseuille flow of power-law viscoplastic fluids in concentric annuli. Journal of Petroleum Science and Engineering, 40(3), 111-119.

[17] Chung, S. Y., & Sung, H. J. (2005). Large-eddy simulation of turbulent flow in a concentric annulus with rotation of an inner cylinder. International journal of heat and fluid flow, 26(2), 191-203.

[18] Sorgun, M., & Ozbayoglu, M. E. (2010). A Mechanistic Model for Predicting Frictional Pressure Losses for Newtonian Fluids in Concentric Annulus. Petroleum Science and Technology, 28(16), 1665-1673.

[19] Kelessidis, V. C., Dalamarinis, P., & Maglione, R. (2011). Experimental study and predictions of pressure losses of fluids modeled as Herschel–Bulkley in concentric and eccentric annuli in laminar, transitional and turbulent flows. *Journal of Petroleum Science and Engineering*, *77*(3), 305-312.

[20] Deissler, R. G. (1954). Analysis of turbulent heat transfer, mass transfer, and friction in smooth tubes at high Prandtl and Schmidt numbers.

[21] Deissler, R. G., & Taylor, M. F. (1955). Analysis of fully developed turbulent heat transfer and flow in an annulus with various eccentricities. NACA Tech. Note 3451.

[22] Wolffe, R. A., & Clump, C. W. (1963). The maximum velocity locus for axial turbulent flow in an eccentric annulus. AIChE Journal, 9(3), 424-425.

[23] Heyda, J. F. (1959). A Green's function solution for the case of laminar incompressible flow between non-concentric circular cylinders. Journal of the Franklin Institute, 267(1), 25-34.

[24] Jonsson, V. K., & Sparrow, E. M. (1965). Results of laminar flow analysis and turbulent flow experiments for eccentric annular ducts. AIChE Journal, 11(6), 1143-1145.

[25] Jonsson, V. K., & Sparrow, E. M. (1966). Experiments on turbulent-flow phenomena in eccentric annular ducts. Journal of Fluid Mechanics, 25(01), 65-86.

[26] Rehme, K. (1973). Simple method of predicting friction factors of turbulent flow in non-circular channels. International Journal of Heat and Mass Transfer, 16(5), 933-950.

[27] Kacker, S. C. (1973). Some aspects of fully developed turbulent flow in non-circular ducts. Journal of Fluid Mechanics, 57(03), 583-602.

[28] Usui, H., & Tsuruta, K. (1980). Analysis of fully developed turbulent flow in an eccentric annulus. Journal of Chemical Engineering of Japan, 13(6), 445-450.

[29] Tosun, I. (1984). Axial laminar flow in an eccentric annulus: an approximate solution. *AIChE journal*, *30*(5), 877-878.

[30] **Özgen, C., & Tosun, I. (1987).** Application of geometric inversion to the eccentric annulus system. *AIChE journal*, *33*(11), 1903-1907.

[31] **Uner, D., Ozgen, C., & Tosun, I. (1988).** An approximate solution for non-Newtonian flow in eccentric annuli. *Industrial & engineering chemistry research*, *27*(4), 698-701.

[32] **Ogino, F., Sakano, T., & Mizushina, T. (1987).** Momentum and heat transfers from fully developed turbulent flow in an eccentric annulus to inner and outer tube walls. Heat and Mass Transfer, 21(2), 87-93.

[33] **Haciislamoglu, M., & Langlinais, J. (1990).** Non-Newtonian flow in eccentric annuli. Transactions of the ASME. Journal of Energy Resources Technology, 112(3), 163-169.

[34] **Nouri, J. M., & Whitelaw, J. H. (1994).** Flow of Newtonian and non-Newtonian fluids in a concentric annulus with rotation of the inner cylinder. Transactions-American Society Of Mechanical Engineers Journal Of Fluids Engineering, 116, 821-821.

[35] **Erge, O., Ozbayoglu, M. E., Miska, S. Z., Yu, M., Takach, N., Saasen, A., & May, R. (2014).** Effect of drillstring deflection and rotary speed on annular frictional pressure losses. Journal of Energy Resources Technology, 136(4), 042909.

[36] **Erge, O., Vajargah, A. K., Ozbayoglu, M. E., & van Oort, E. (2016, March).** Improved ECD Prediction and Management in Horizontal and Extended Reach Wells with Eccentric Drillstrings. In IADC/SPE Drilling Conference and Exhibition. Society of Petroleum Engineers.

[37] **Rushd, S., Shazed, A. R., Faiz, T., Kelessidis, V., Hassan, I. G., & Rahman, A. (2017, March).** CFD Simulation of Pressure Losses in Eccentric Horizontal Wells. In SPE Middle East Oil & Gas Show and Conference. Society of Petroleum Engineers.

[38] **Coleman, B. D., & Noll, W. (1959).** Helical flow of general fluids. Journal of Applied Physics, 30(10), 1508-1512.

[39] **Walker, R. E., & Al-Rawi, O. (1970, January).** Helical flow of bentonite slurries. In Fall Meeting of the Society of Petroleum Engineers of AIME. Society of Petroleum Engineers.

[40] **Luo, Y., & Peden, J. M. (1990).** Laminar Annular Helical Flow Of Power-Law Fluids Part I: Various Profiles And Axial Flowrates.

[41] **Delwiche, R. A., Lejeune, M. W. D., Mawet, P. F. B. N., & Vighetto, R. (1992, January).** Slimhole drilling hydraulics. In SPE Annual Technical Conference and Exhibition. Society of Petroleum Engineers.

[42] **Marken, C. D., He, X., & Saasen, A. (1992, January).** The influence of drilling conditions on annular pressure losses. In SPE Annual Technical Conference and Exhibition. Society of Petroleum Engineers.

[43] **Cui, H. Q., & Liu, X. S. (1995, January).** Research on helical flow of non-Newtonian fluids in eccentric annuli. In International Meeting on Petroleum Engineering. Society of Petroleum Engineers.

[44] **McCann, R. C., Quigley, M. S., Zamora, M., & Slater, K. S. (1995).** Effects of high-speed pipe rotation on pressures in narrow annuli. SPE Drilling & Completion, 10(02), 96-103.

[45] **Hansen, S. A., Rommetveit, R., Sterri, N., Aas, B., & Merlo, A. (1999, January).** A new hydraulics model for slim hole drilling applications. In SPE/IADC Middle East Drilling Technology Conference. Society of Petroleum Engineers.

[46] **Escudier, M. P., Gouldson, I. W., Oliveira, P. J., & Pinho, F. T. (2000).** Effects of inner cylinder rotation on laminar flow of a Newtonian fluid through an eccentric annulus. International Journal of Heat and Fluid Flow, 21(1), 92-103.

[47] **Wan, S., Morrison, D., & Bryden, I. G. (2000).** The flow of Newtonian and inelastic non-Newtonian fluids in eccentric annuli with inner-cylinder rotation. Theoretical and Computational Fluid Dynamics, 13(5), 349-359.

[48] **Ooms, G., & Kampman-Reinhartz, B. E. (2000).** Influence of drillpipe rotation and eccentricity on pressure drop over borehole with newtonian liquid during drilling. SPE Drilling & Completion, 15(04), 249-253.

[49] **Fang, P., & Manglik, R. M. (2002).** The influence of inner cylinder rotation on laminar axial flows in eccentric annuli of drilling bore wells. International journal of transport phenomena, 4, 257-274.

[50] **Diaz, H., Miska, S., & Takach, N. (2007).** Modeling of ECD in casing drilling operations and comparison with experimental and field data. Archives of Mining Sciences, 52(4), 457-481.

[51] **Tao, L. N., & Donovan, W. F. (1955).** Through-flow in concentric and eccentric annuli of fine clearance with and without relative motion of the boundaries. Trans. ASME, 77(8), 1291-1301.

[52] **Hemphill, T., & Ravi, K. (2005, January).** Calculation of Drill Pipe Rotation Effects on Axial Flow: An Engineering Approach. In SPE Annual Technical Conference and Exhibition. Society of Petroleum Engineers.

[53] **Ravi, K., & Hemphill, T. (2006, January).** Pipe Rotation and Hole Cleaning in Eccentric Annulus. In IADC/SPE Drilling Conference. Society of Petroleum Engineers.

[54] **Alizadehdakhel, A., Rahimi, M., Sanjari, J., & Alsairafi, A. A. (2009).** CFD and artificial neural network modeling of two-phase flow pressure drop. International Communications in Heat and Mass Transfer, 36(8), 850-856.

[55] **Ahmed, R. M., Enfis, M. S., El Kheir, H. M., Laget, M., & Saasen, A. (2010, January).** The Effect of Drillstring Rotation on Equivalent Circulation Density: Modeling and Analysis of Field Measurements. In SPE Annual Technical Conference and Exhibition. Society of Petroleum Engineers.

[56] **Neto, J. L., Martins, A. L., Neto, A. S., Ataíde, C. H., & Barrozo, M. A. S. (2011).** CFD applied to turbulent flows in concentric and eccentric annuli with inner shaft rotation. The Canadian Journal of Chemical Engineering, 89(4), 636-646.

[57] **Sorgun, M., Aydin, I, Ozbayoglu, E., & Schubert, J. J. (2012).** Mathematical modeling of turbulent flows of Newtonian fluids in a concentric annulus with pipe rotation. Energy Sources, Part A: Recovery, Utilization, and Environmental Effects, 34(6), 540-548.

[58] **Bicalho, I. C., dos Santos, D. B. L., Ataíde, C. H., & Duarte, C. R. (2016).** Fluid-dynamic behavior of flow in partially obstructed concentric and eccentric annuli with orbital motion. Journal of Petroleum Science and Engineering, 137, 202-213.

[59] **Erge, O., Ozbayoglu, E. M., Miska, S. Z., Yu, M., Takach, N., Saasen, A., & May, R. (2016).** Equivalent circulating density modeling of Yield Power Law fluids validated with CFD approach. Journal of Petroleum Science and Engineering, 140, 16-27.

[60] **Rooki, R., & Rakhshkhorshid, M. (2016).** Cuttings transport modeling in underbalanced oil drilling operation using radial basis neural network. Egyptian Journal of Petroleum.

[61] **Rooki, R. (2016).** Application of general regression neural network (GRNN) for indirect measuring pressure loss of Herschel–Bulkley drilling fluids in oil drilling. Measurement, 85, 184-191.

[62] **Syrjälä, S. (1996).** Further finite element analyses of fully developed laminar flow of power-law non-Newtonian fluid in rectangular ducts: Heat transfer predictions. International communications in heat and mass transfer, 23(6), 799-807.

[63] **Naccache, M. F., & Mendes, P. R. S. (1996).** Heat transfer to non-Newtonian fluids in laminar flow through rectangular ducts. International journal of heat and fluid flow, 17(6), 613-620.

[64] **Moraga, N. O., Garrido, C. P., & Castillo, E. F. (2013).** Fluid Dynamics and Heat Transfer in Non-Newtonian Annular Cylindrical Solidification of a Binary Alloy. In Proceedings of the World Congress on Engineering (Vol. 3).

[65] **Peixinho, J., Desaubry, C., & Lebouche, M. (2008).** Heat transfer of a non-Newtonian fluid (Carbopol aqueous solution) in transitional pipe flow. International journal of heat and mass transfer, 51(1), 198-209.

[66] **Farias, M. H., Braga, C. V., & de Souza Mendes, P. R. (2009).** Heat transfer coefficients for the laminar fully developed flow of viscoplastic

liquids through annuli. International Journal of Heat and Mass Transfer, 52(13), 3257-3260.

[67] **Sheela-Francisca, J., Tso, C. P., Hung, Y. M., & Rilling, D. (2012).** Heat transfer on asymmetric thermal viscous dissipative Couette–Poiseuille flow of pseudo-plastic fluids. Journal of Non-Newtonian Fluid Mechanics, 169, 42-53.

[68] **Lian-Cun, Z., Xin-Xin, Z., & Chun-Qing, L. (2006).** Heat Transfer for Power Law Non-Newtonian Fluids. Chinese Physics Letters, 23(12), 3301.

[69] **Carmona, A., Pérez-Segarra, C. D., Lehmkuhl, O., & Oliva, A. (2012).** Numerical solutions for the fluid flow and the heat transfer of viscoplastic-type non-Newtonian fluids. In Journal of Physics: Conference Series (Vol. 395, No. 1, p. 012002). IOP Publishing.

[70] **Prasad, K. V., Santhi, S. R., & Datti, P. S. (2012).** Non-Newtonian power-law fluid flow and heat transfer over a non-linearly stretching surface. Applied Mathematics, 3(05), 425.

[71] **Li, B. T., Zheng, L. C., & Zhang, X. X. (2010).** Numerical Investigation on Heat Transfer of Power Law Fluids in a Pipe With Constant Wall Temperature. In World Congress on Engineering, London, UK (Vol. 3, pp. 1864-1866).

[72] **Pinho, F. T., & Coelho, P. M. (2006).** Fully-developed heat transfer in annuli for viscoelastic fluids with viscous dissipation. Journal of non-newtonian fluid mechanics, 138(1), 7-21.

[73] **Yavuz, T., Erol, Ú., & Kaya, M. (2011).** Heat transfer characteristics of laminar annular duct flow with viscous dissipation. Proceedings of the Institution of Mechanical Engineers, Part C: Journal of Mechanical Engineering Science, 225(7), 1681-1692.

[74] **Han, S. M., Woo, N. S., & Hwang, Y. K. (2007, January).** Heat transfer characteristics of non-Newtonian fluid in a rotating annulus. In Thermal Issues in Emerging Technologies: Theory and Application, 2007. THETA 2007. International Conference on (pp. 213-218). IEEE.

[75] **Ahmed, R., and Miska, S., (2008),** Experimental Study and Modeling of Yield Power-Law Fluid Flow in Annuli With Drillpipe Rotation, SPE/IADC Drilling Conference, March 4–6, Orlando, FL, Paper No. SPE 112604.

[76] **Saasen, Arild. (2014)** Annular Frictional Pressure Losses During Drilling— Predicting the Effect of Drillstring Rotation. Journal of Energy Resources Technology136.3 (2014): 034501.

[77] **Al-Shemmeri, T. (2012).** Engineering Fluid Mechanics. Bookboon.

[78] **Bird, R. B., Stewart, W. E., & Lightfoot, E. N. (2007).** *Transport phenomena*. John Wiley & Sons.

[79] Iyoho, A. W., & Azar, J. J. (1981). An accurate slot-flow model for non-Newtonian fluid flow through eccentric annuli. *Society of Petroleum Engineers Journal*, *21*(05), 565-572.

[80] Vaughn, R. D. (1965). Axial laminar flow of non-Newtonian fluids in narrow eccentric annuli. *Society of Petroleum Engineers Journal*, *5*(04), 277-280.

[81] Kell, G. S. (1975). Density, thermal expansivity, and compressibility of liquid water from 0. deg. to 150. deg.. correlations and tables for atmospheric pressure and saturation reviewed and expressed on 1968 temperature scale. *Journal of Chemical and Engineering Data*, *20*(1), 97-105.

APPENDIX A

UNCERTAINTY ANALYSIS

Although viscosity of water is well known for different range of temperature. There exists uncertainity due to temperature measurements uncertainity. A well-known correlation for viscosity of water with temperature as an independent variable can be used [77]

$$\mu(T) = 2.414x10^{-5} \, x10^{\frac{247.8}{T-140}}$$ (A.1)

As it is seen from the correlation, viscosity is only a function of temperature $\mu(T)$. Therefore, the uncertainity analysis gives the following equation;

$$U_\mu^2 = \left(\frac{\partial \mu}{\partial T}\right)^2 U_T^2$$ (A.2)

In order to take derivative of $\mu(T)$, it should be known following equation for simplicity;

If

$$y = a^{f(x)}$$ (A.3)

then

$$\frac{dy}{dx} = \ln(a) f'(x) a^{f(x)}$$ (A.4)

Thus,

$$\frac{d\mu}{dT} = \ln(10)\left(-\frac{247.8}{(T-140)^2}\right)\left(2.414x10^{-5} \, x10^{\frac{247.8}{T-140}}\right)$$ (A.5)

Temperature range is between 20 $^{\circ}$C and 65 $^{\circ}$C in the experiment. Maximum uncertainity error is obtained at 65 $^{\circ}$C where U_{μ} for 65 °C is $2.65x10^{-6}$ and $\mu = 0.0004$. Therefore;

$$\frac{U_{\mu}}{\mu} = 0.63\% \tag{A.6}$$

On the other hand, density of water should be investigated according to small amount of temperature change in order to calculate kinematic viscosity. From a common correlation of density for fluids, density of water can be written;

$$\rho(T) = \frac{999.8}{1+0.0002T} \tag{A.7}$$

where T is in Celcius degree.

Here it is considered that density is only a function of temperature. Therefore uncertainity analysis is;

$$U_{\rho}^2 = \left(\frac{\partial \rho}{\partial T}\right)^2 U_T^2 \tag{A.8}$$

Taking derivative of density with respect to temperature gives the result of;

$$\frac{d\rho}{dT} = \frac{(999.8)(0.0002)}{(1+0.0002T)^2} \tag{A.9}$$

where $U_{\rho} = 0.0095$ and $\rho = 987$ for 65 $^{\circ}$C. Thus, the result is;

$$\frac{U_{\rho}}{\rho} = 0.001\% \tag{A.10}$$

It shows that uncertainity in desity with small change in temperature is negligible.

It was already stated that the flowmeter has maximum 0.55% uncertainty of reading. In order to calculate velocity of the flow loop, the following equation should be used;

$$\Phi = VA = V\frac{\pi}{4}(D_o - D_i)^2 \tag{A.11}$$

Taking into account of manufacturing uncertainity of inner and outer diameter of plexiglass tube, the uncertainity analysis gives the following equation;

$$\left(\frac{U_\Phi}{\Phi}\right)^2 = \left(\frac{U_V}{V}\right)^2 + (2)^2\left(\frac{U_D}{D}\right)^2 \tag{A.12}$$

However, the flowmeter is assumed to have constant; therefore the equation should be rearranged to;

$$\left(\frac{U_V}{V}\right)^2 = \left(\frac{U_\Phi}{\Phi}\right)^2 + (2)^2\left(\frac{U_D}{D}\right)^2 \tag{A.13}$$

By using milimetric calliper, it was observed that there was a 0.7 % uncertainity reading. Therefore, the equation becomes;

$$\left(\frac{U_V}{V}\right)^2 = (0,0055)^2 + (4)(0,007)^2 \tag{A.14}$$

$$\left(\frac{U_V}{V}\right) = 0,015 = 1,5\% \tag{A.15}$$

It can be jumped to the uncertainity analysis of dimensionless parameters. Firstly, Reynolds number was already presented at equation (1) in Chapter 3. The equation of the uncertainity of Re can be written as following;

$$\left(\frac{U_{Re}}{Re}\right)^2 = \left(\frac{U_V}{V}\right)^2 + \left(\frac{U_D}{D}\right)^2 + \left(\frac{U_\nu}{\nu}\right)^2 \tag{A.16}$$

$$\left(\frac{U_{Re}}{Re}\right)^2 = (0,015)^2 + (0,007)^2 + (0,0063)^2 \tag{A.17}$$

$$\left(\frac{U_{Re}}{Re}\right) = 0,018 = 1,8\% \tag{A.18}$$

Next is uncertainity analysis for Taylor number. Uncertainity equation for Taylor number is given by;

$$\left(\frac{U_{Ta}}{Ta}\right)^2 = (4)^2\left(\frac{U_R}{R}\right)^2 + (2)^2\left(\frac{U_\omega}{\omega}\right)^2 + (-2)^2\left(\frac{U_\nu}{\nu}\right)^2 \tag{A.19}$$

By using tacometer, it was observed that there is a fluctuation around 0.5 rpm. The maximum uncertainity value exists at 30 rpm.

$$\left(\frac{U_{Ta}}{Ta}\right)^2 = (16)(0,0035)^2 + (4)\left(\frac{0,5rpm}{30rpm}\right)^2 + (4)(0,0063)^2 \qquad \text{(A.20)}$$

$$\left(\frac{U_{Ta}}{Ta}\right) = 0,038 = 3,8\% \qquad \text{(A.21)}$$

Prandtl number of water with respect to temperature is well known. It was previously stated that thermocouple has 0.75% of uncertainity reading. Maximum discrepancy corresponds to 65 $^{\circ}$C in the present experiment range. Therefore, it can easily concluded that Prandtl number has around 0.5 % uncertainity with 0.5 $^{\circ}$C difference.

APPENDIX B

NARROW SLOT ANALYSIS FOR A FULLY ECCENTRIC ANNULUS

Representatio of eccentric narrow slot approach is illustrated Figure B.1.
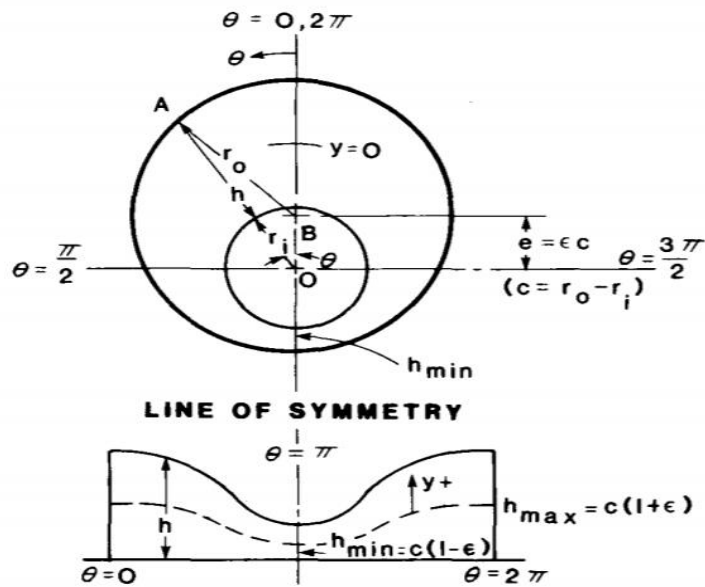
Figure B.1 : equivalent slot of eccentric annulus and displays of parameters

In order to find the relation between h, ro, and ri, cosine law is applied as;

$$r_o^2 = (h + r_i)^2 + (r_o - r_i)^2 - 2(r_o - r_i)(h + r_i)\operatorname{Cos}\theta \tag{B.1}$$

Expanding all the paranthesis;

$$0 = h^2 + 2hr_i + r_i^2 - 2r_or_i + r_i^2 - 2\operatorname{Cos}\theta(r_oh + r_or_i - r_ih - r_i^2) \tag{B.2}$$

Rearrange for h;

$$h^2 + 2h(r_i - \operatorname{Cos}\theta(r_o - r_i)) - 2r_i(r_o - r_i)(1 + \operatorname{Cos}\theta) = 0 \tag{B.3}$$

Solving quadratic equation for h leads to;

$$h_{1,2} = \frac{\left[2(\operatorname{Cos}\theta(r_o - r_i) - r_i) \pm \sqrt{\begin{array}{c}[2(\operatorname{Cos}\theta(r_o - r_i) - r_i)]^2 \\ -8r_i(r_o - r_i)(1 + \operatorname{Cos}\theta)\end{array}} \right]}{2} \tag{B.4}$$

Simplifying and neglecting the negative h values leads to;

$$h = \frac{1}{2}\sqrt{r_o^2 - (r_o - r_i)^2 \operatorname{Sin}^2\theta} - r_i + (r_o - r_i)\operatorname{Cos}\theta \tag{B.5}$$

APPENDIX C

NUMERICAL RESULTS OF FULLY DEVELOPED TURBULENT WATER FLOW IN ECCENTRIC ANNULUS FOR EACH ANGLE VALUE

Following figures has produced by the present proposed model's numerical simulation. The M-code was developed and run for each cases. Researchers who are interested in can be observe different flow behavior and velocity profile at different inner pipe rotation, temperature and pressure gradient. Due to symmetry of the annulus, it was only simulated half of the domain which correcponds to 180°. As it can be seen at Figure B.1, the highest point of the channel is at 0°. The height of the channel is zero at 180° because the annulus in the present study is fully eccentric annulus. The following figures are scanned full range of zero rotation to 120 rpm and room temperature to 60 °C at pressure gradient of 1000 Pa/m.
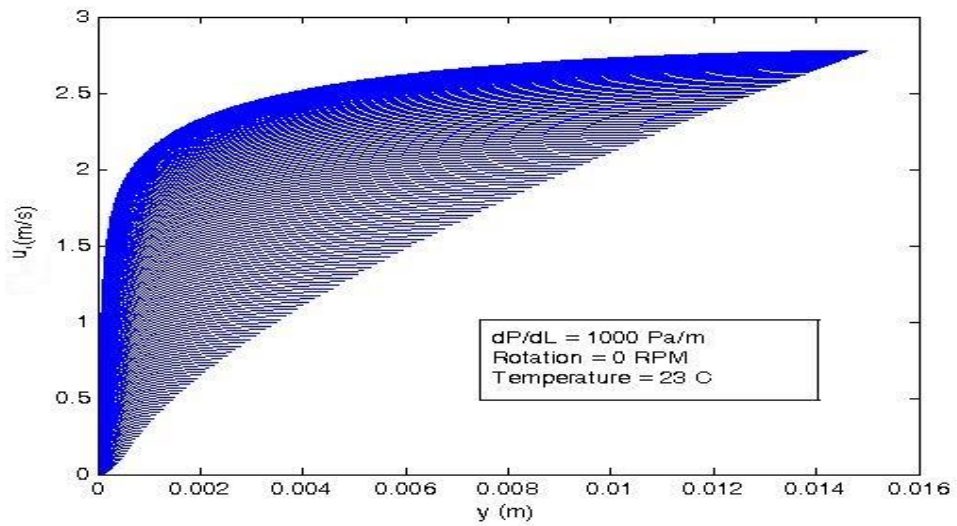
Figure C.4 : Velocity profile for half domain of the annulus at each angle at

dP/dL=1000 Pa/m, ω = 0 RPM, and T = 23 °C
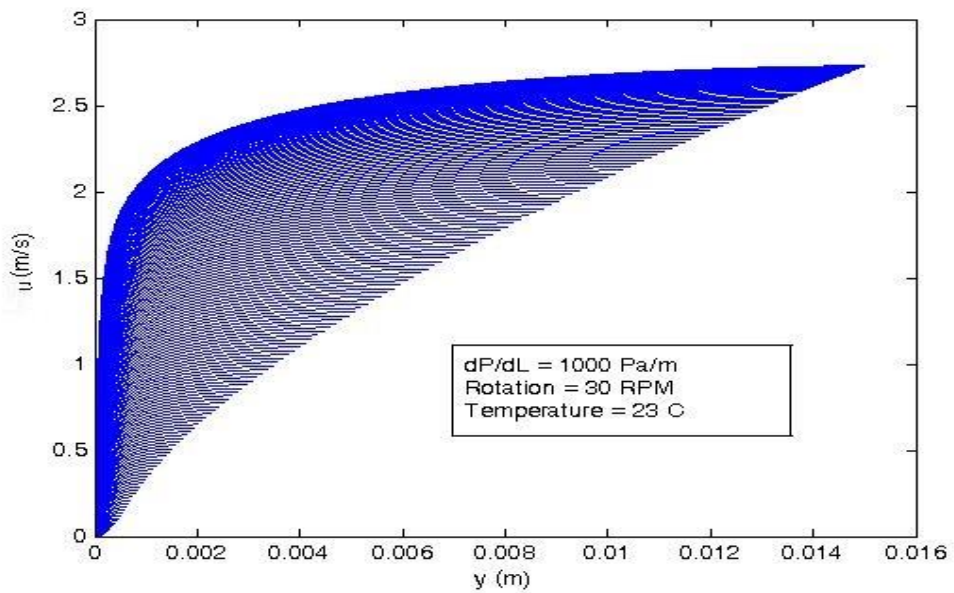
Figure C.10 : Velocity profile for half domain of the annulus at each angle at

dP/dL=1000 Pa/m, ω = 30 RPM, and T = 23 °C
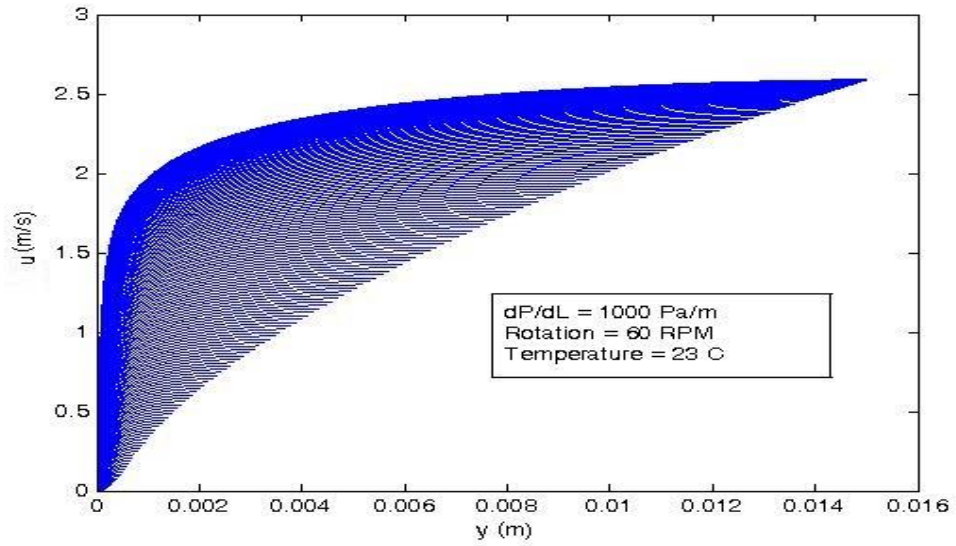
Figure C.16 : Velocity profile for half domain of the annulus at each angle at
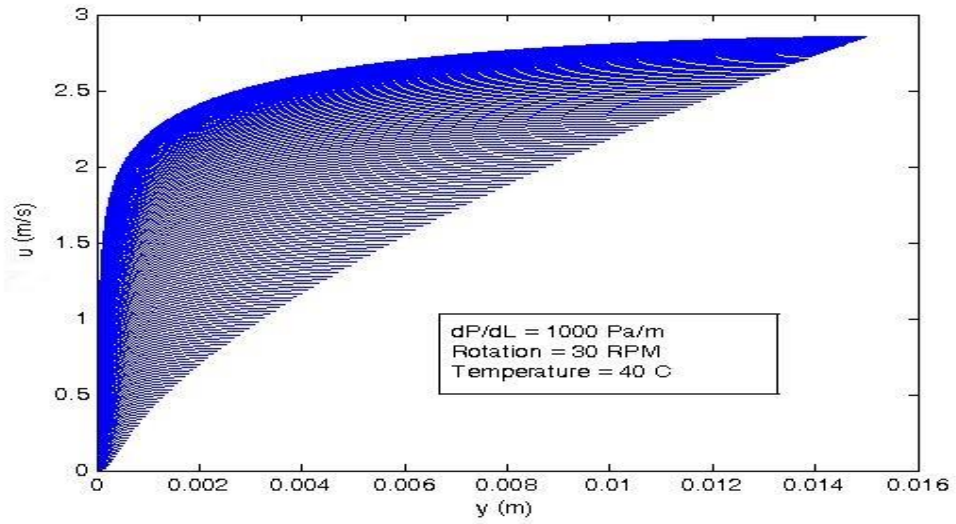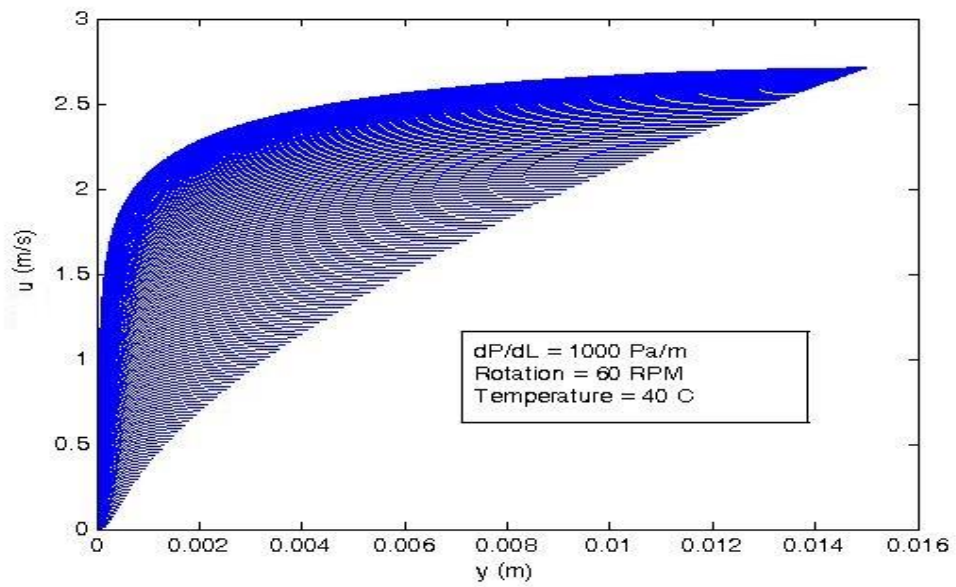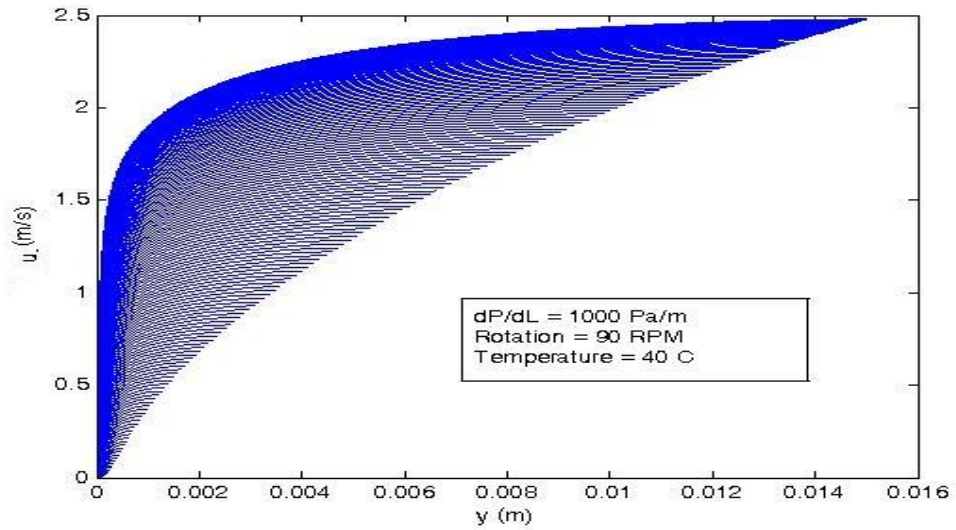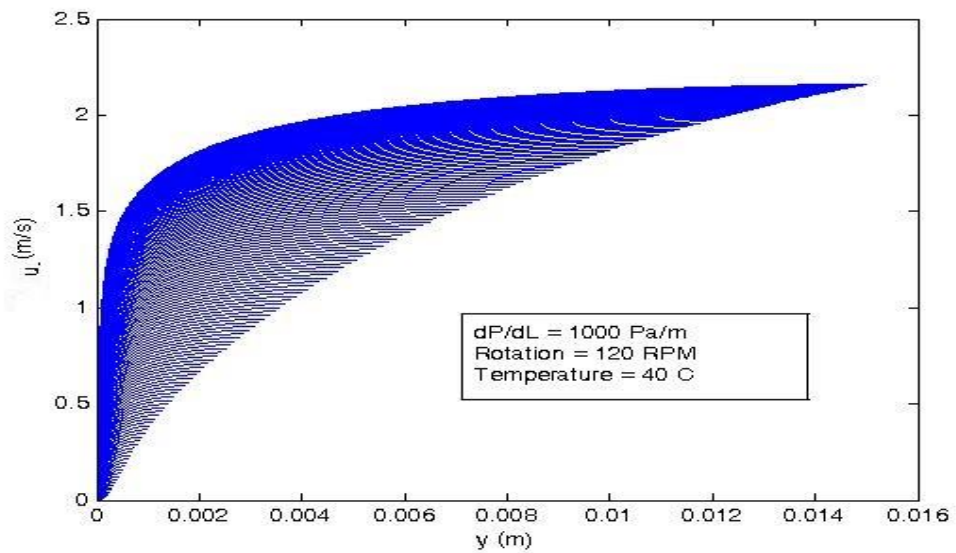
dP/dL=1000 Pa/m, ω = 60 RPM, and T = 23 °C
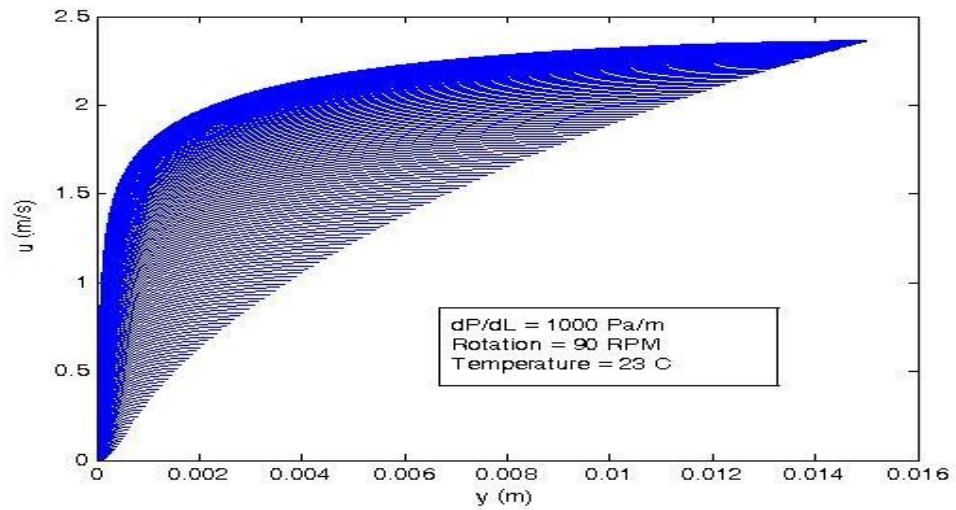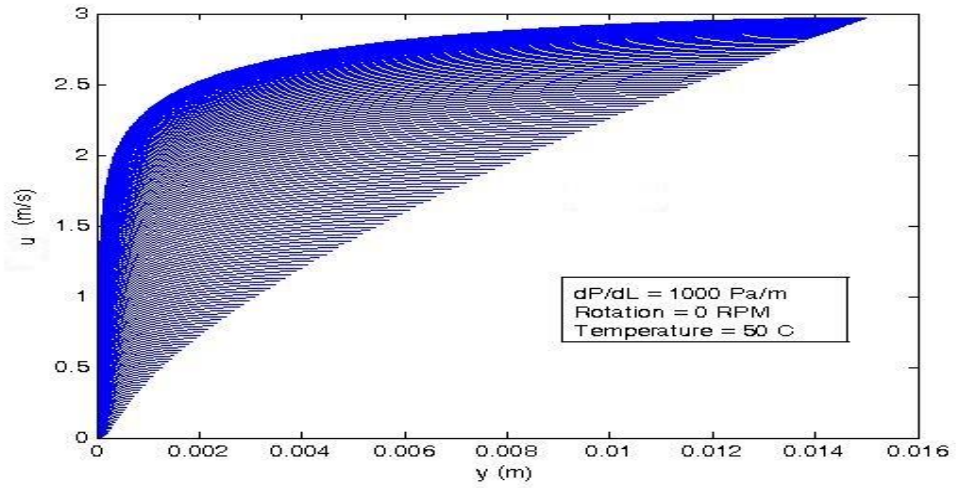

Figure C.21 : Velocity profile for half domain of the annulus at each angle at

dP/dL=1000 Pa/m, ω = 90 RPM, and T = 23 °C
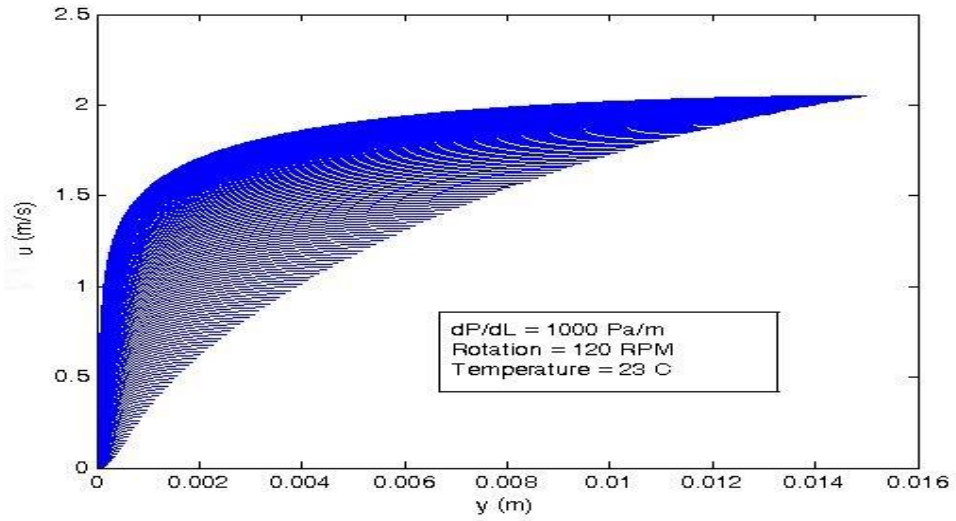
Figure C.25 : Velocity profile for half domain of the annulus at each angle at

dP/dL=1000 Pa/m, $\omega = 120$ RPM, and T = 23 °C
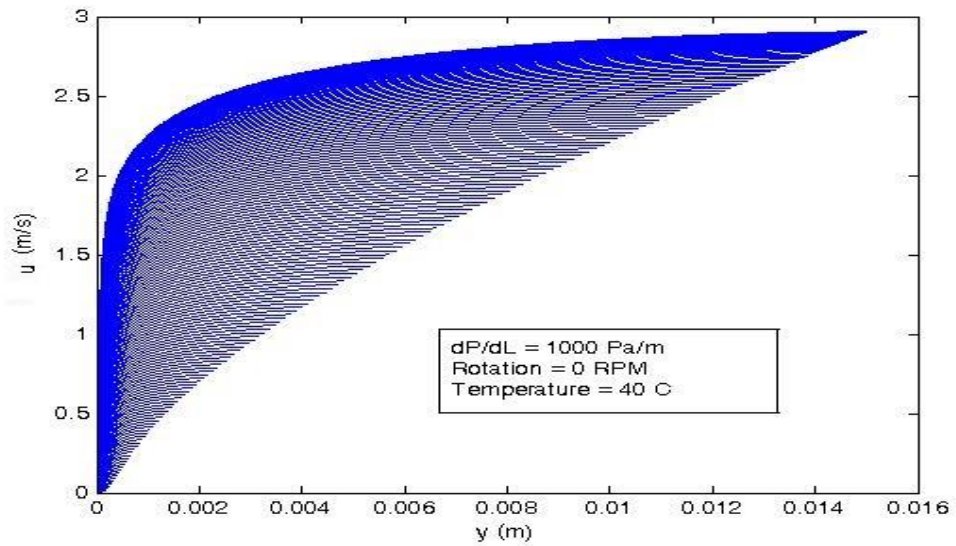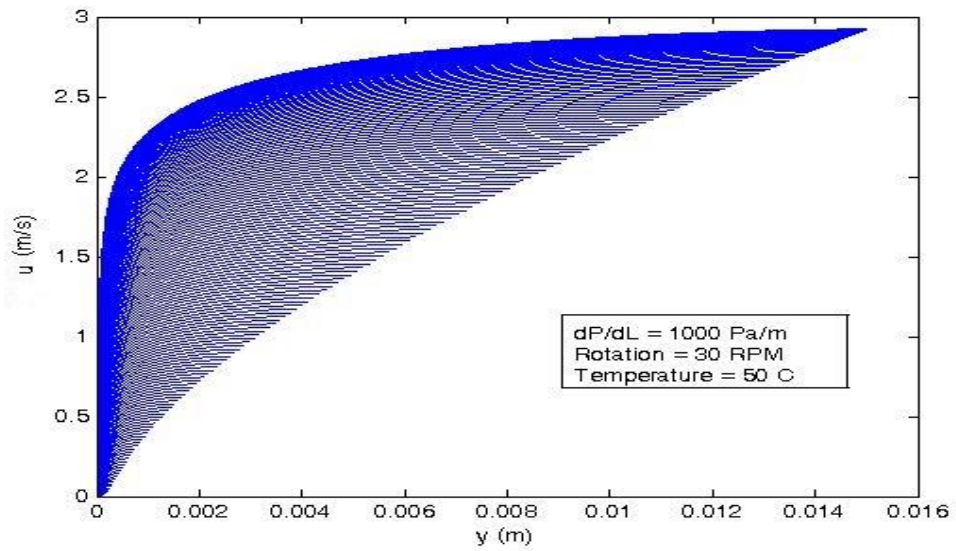

Figure C.31 : Velocity profile for half domain of the annulus at each angle at

dP/dL=1000 Pa/m, $\omega = 0$ RPM, and T = 40 °C

Figure C.37 : Velocity profile for half domain of the annulus at each angle at

dP/dL=1000 Pa/m, ω = 30 RPM, and T = 40 °C
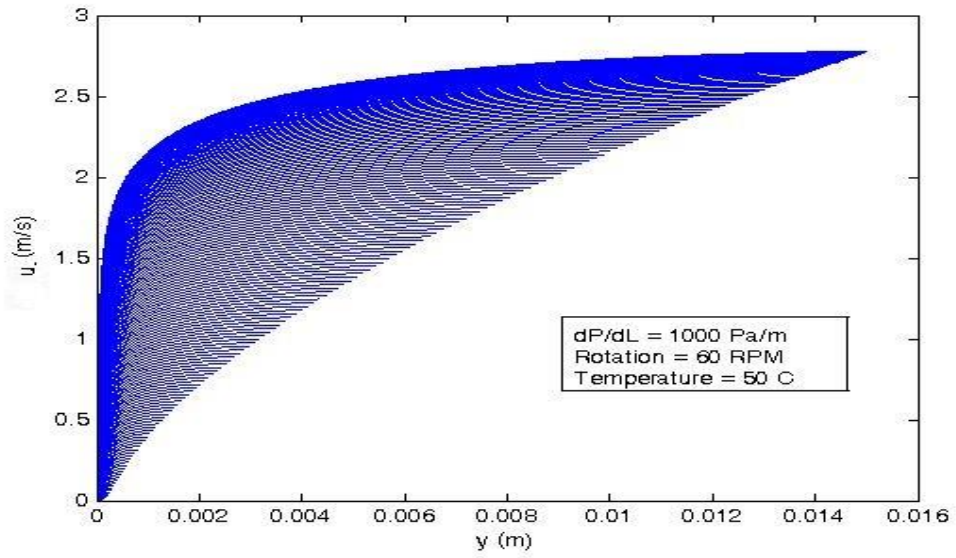

Figure C.43 : Velocity profile for half domain of the annulus at each angle at

dP/dL=1000 Pa/m, ω = 60 RPM, and T = 40 °C

Figure C.48 : Velocity profile for half domain of the annulus at each angle at

dP/dL=1000 Pa/m, ω = 90 RPM, and T = 40 °C

Figure C.52 : Velocity profile for half domain of the annulus at each angle at
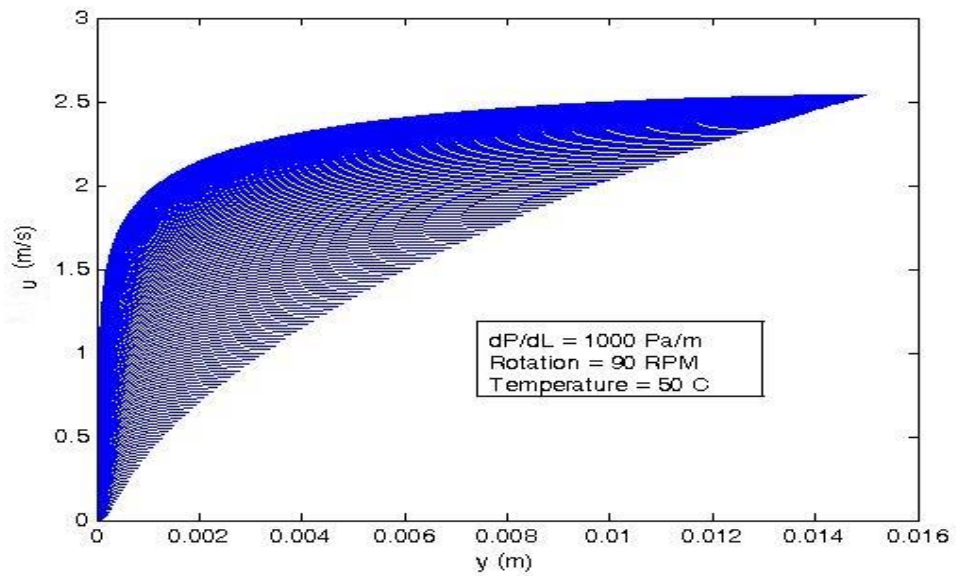
dP/dL=1000 Pa/m, ω = 120 RPM, and T = 40 °C

Figure C.58 : Velocity profile for half domain of the annulus at each angle at
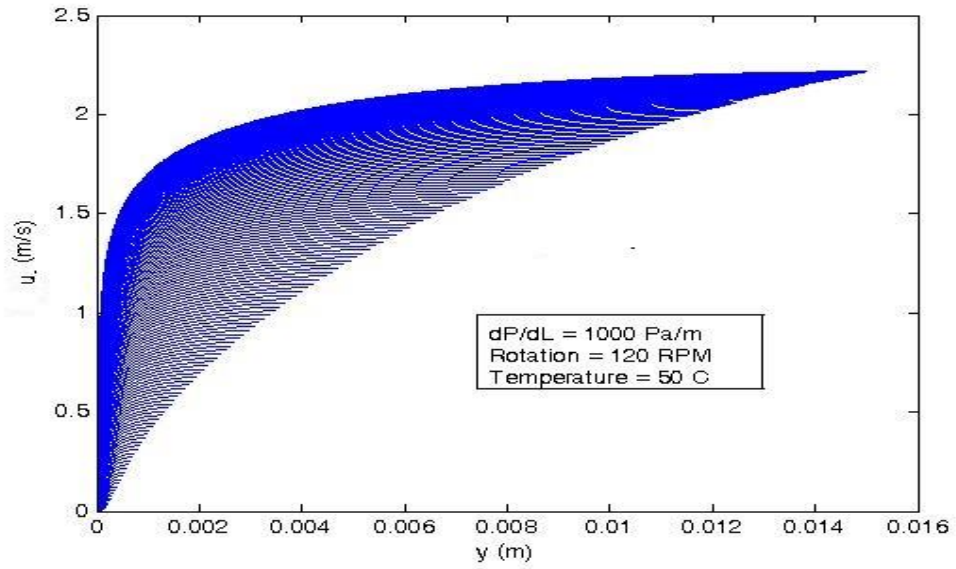
dP/dL=1000 Pa/m, ω = 0 RPM, and T = 50 °C

Figure C.64 : Velocity profile for half domain of the annulus at each angle at
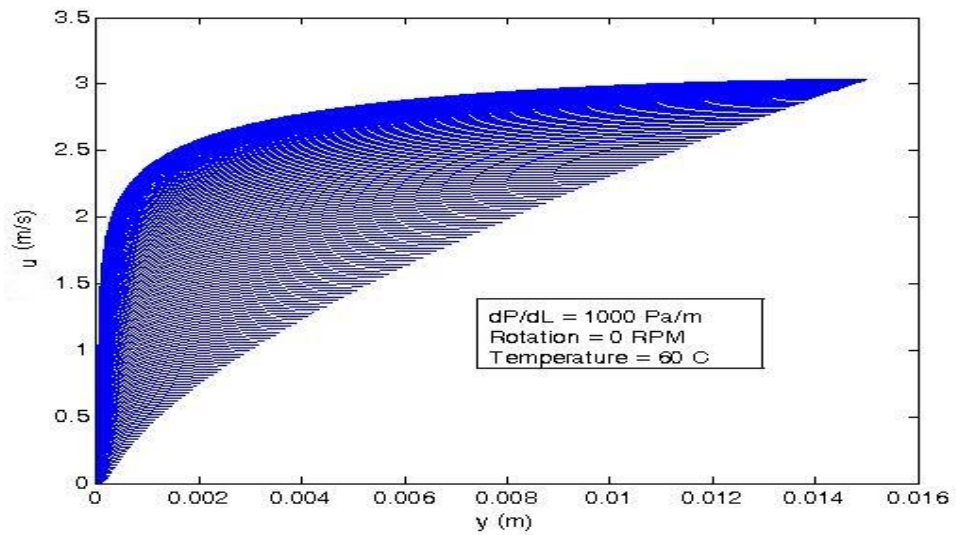
dP/dL=1000 Pa/m, ω = 30 RPM, and T = 50 °C

Figure C.70 : Velocity profile for half domain of the annulus at each angle at

dP/dL=1000 Pa/m, ω = 60 RPM, and T = 50 °C

Figure C.75 : Velocity profile for half domain of the annulus at each angle at

dP/dL=1000 Pa/m, ω = 90 RPM, and T = 50 °C

Figure C.79 : Velocity profile for half domain of the annulus at each angle at

dP/dL=1000 Pa/m, ω = 120 RPM, and T = 50 °C
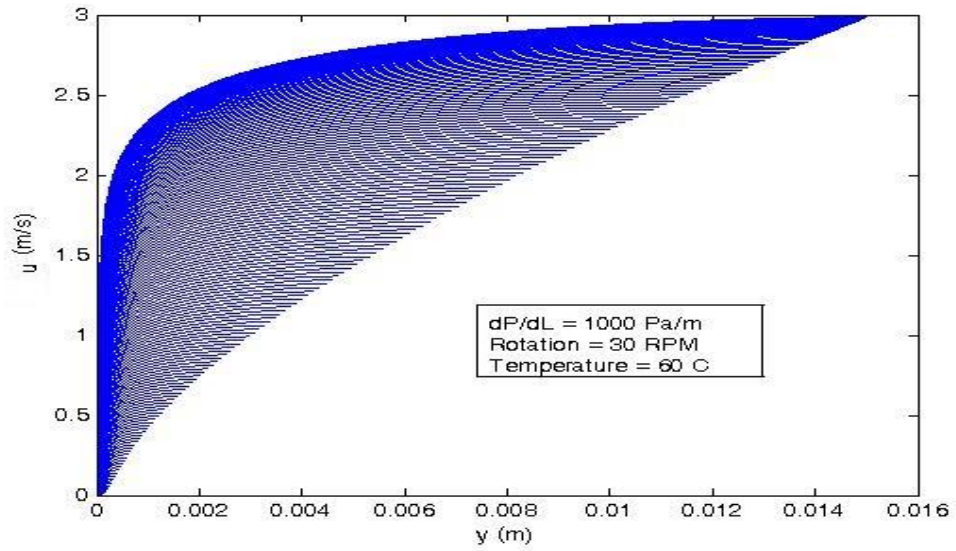

Figure C.85 : Velocity profile for half domain of the annulus at each angle at

dP/dL=1000 Pa/m, ω = 0 RPM, and T = 60 °C

Figure C.91 : Velocity profile for half domain of the annulus at each angle at

dP/dL=1000 Pa/m, ω = 30 RPM, and T = 60 °C

Figure C.97 : Velocity profile for half domain of the annulus at each angle at

dP/dL=1000 Pa/m, ω = 60 RPM, and T = 60 °C

Figure C.102 : Velocity profile for half domainof the annulus at each angle at
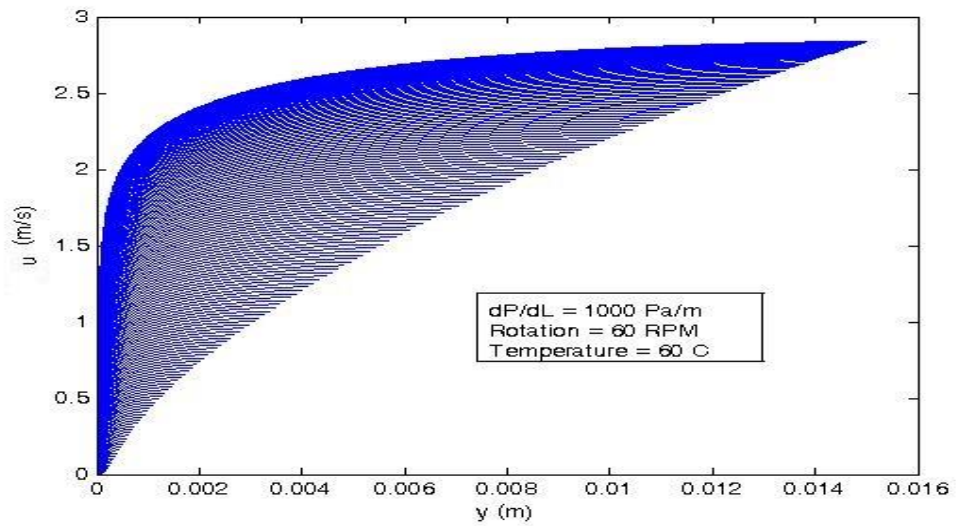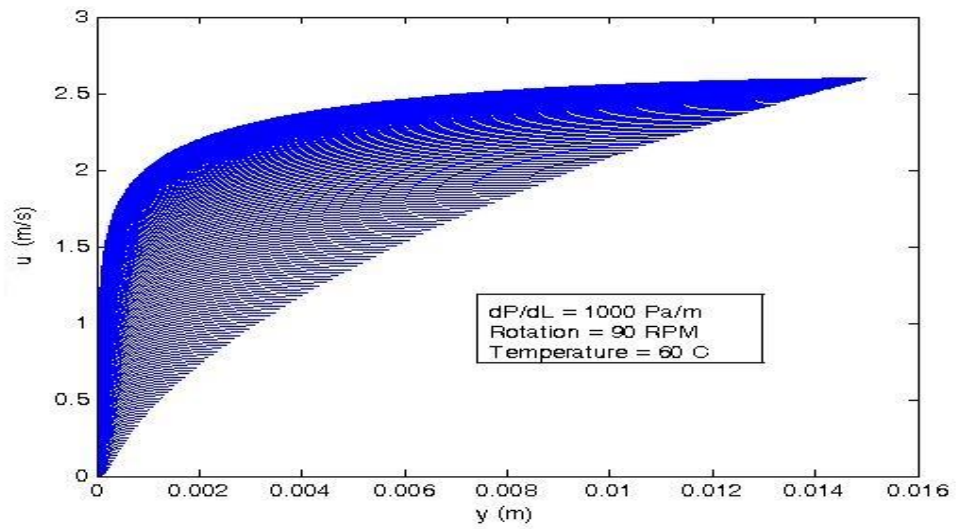
dP/dL=1000 Pa/m, ω = 90 RPM, and T = 60 °C
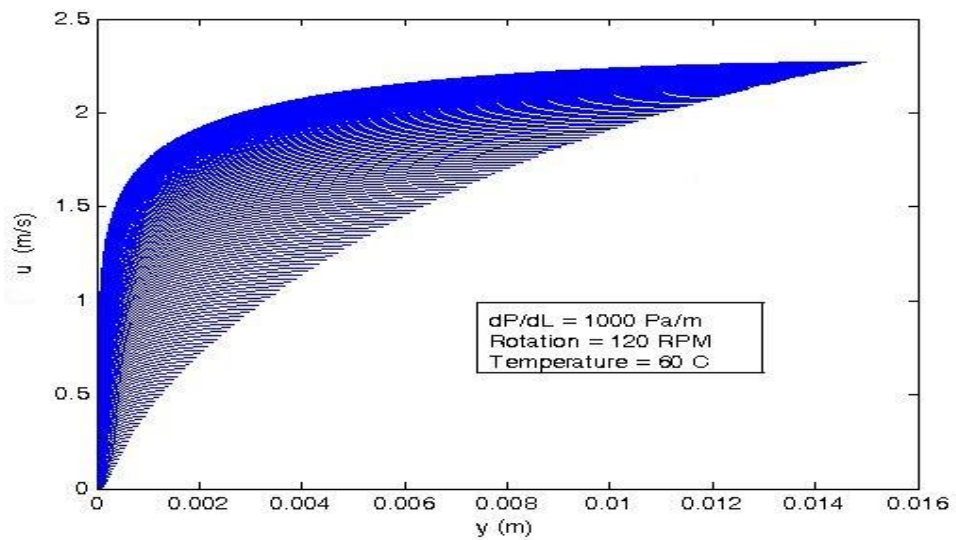

Figure C.106 : Velocity profile for half domain of the annulus at each angle at

dP/dL=1000 Pa/m, ω = 120 RPM, and T = 60 °C

CIRRUCILUM VITAE

Erman Ülker
erman.ulker@ikc.edu.tr

Personal Information

- **About**   : Physicist, Aerospace Engineer, Occupational Health and Safety Expert, Researcher
- **Birthday**   : March 12th 1982
- **Gender**   : Male
- **Marital Status** : Married
- **Nationality**   : Turkish

Graduate

- **2013 -:** PhD. Civil Engineering, IKCU, Turkey
- **Supervisor :** Assoc. Prof. Dr. Mehmet Sorgun
- **2010 - 2012 :** PhD Aerospace Engineering, University of Arizona, USA GPA: 3.5/4.0 (Not completed)
- **2008-2010 :** M.Sc. Aerospace Engineering, University of Arizona, USA GPA: 3.556/4.0
- **Thesis :** Boundary Layer Solvers for Binary Reacting Mixtures of Oxygen and Nitrogen, and for 5-Species Model of Air
- **Supervisor :** Prof. Dr. Anatoli Tumin

Undergraduate

- **2000-2005 :** Physics, AIBU, Bolu, Turkey (GPA : 3.32/4.0)
- **Thesis :** Destruction or Construction of Brain Waves under Effects of Electromagnetic Waves from Cellulars
- **Supervisor :** Prof. Dr. Atilla Kilic

Scientific Articles and Activities

Articles

- Jill Klentzman, Erman Ulker and Anatoli Tumin , 2012, "Projection of the Solution of the Linearized Navier-Stokes Equations in Reacting High Speed Boundary Layers onto Discrete Modes," 42nd AIAA Fluid Dynamics Conference and Exhibit, New Orleans, Louisiana, June 25-28, 2012, AIAA-2012-3149.

- Erman Ulker, Jill Klentzman and Anatoli Tumin , 2011, "Stability of Boundary Layers in Binary Mixtures of Oxygen and Nitrogen," 49th AIAA Aerospace Sciences Meeting including the New Horizons Forum and Aerospace Exposition, Orlando, Florida, Jan. 4-7, 2011, AIAA-2011-370.

- Sorgun, Mehmet, and Erman Ulker. "Modeling and Experimental Study of Solid– Liquid Two-Phase Pressure Drop in Horizontal Wellbores With Pipe Rotation." Journal of Energy Resources Technology 138.2 (2016): 022902.

- Ulker, E., & Sorgun, M. (2016). Comparison of computational intelligence models for cuttings transport in horizontal and deviated wells. Journal of Petroleum Science and Engineering, 146, 832-837.

- Sorgun Mehmet,Ülker Erman (2016). İki Boru Arasindaki Kati Madde Taşiniminin Hesaplamali Akişkanlar Dinamiği İle Modellenmesi. Deu Muhendislik Fakultesi Fen Ve Muhendislik, 18(54), 455-455., Doi: 10.21205/deufmd.2016185413

- Ulker, E., Sorgun, M., Solmus, I., & Karadeniz, Z. H. (2017). Determination of Newtonian Fluid Flow Behavior Including Temperature Effects in Fully Eccentric Annulus. Journal of Energy Resources Technology, 139(4), 042001.

Conferences

- Erman Ulker , Jill Klentzman and Anatoli Tumin, 2011, "The effect of chemistry and transport models on the inviscid stability of boundary layers in binary mixtures of oxygen and nitrogen," 64th Annual Meeting of the APS Division of
Fluid Dynamics Volume 56, Number 18, Baltimore, Maryland, November 20–22, 2011.

- Jill Klentzman, Erman Ulker and Anatoli Tumin "The role of the frozen relative Mach number on the stability of boundary layers in chemical non-equilibrium," 64th Annual Meeting of the APS Division of Fluid Dynamics Volume 56, Number 18, Baltimore, Maryland, November 20–22, 2011.

- Jill Klentzman , Erman Ulker and Anatoli Tumin, "Inviscid Stability Analysis of Chemically Reacting Boundary Layers in Binary Gas Mixtures," 63rd Annual Meeting of the APS Division of Fluid Dynamics, Volume 55, Number 16, Long Beach, California, November 21–23, 2010.

- AIAA 2011 Hawaii

- Erman Ulker, Mehmet Sorgun, 2015 "Boru Rotasyonlu Yatak Kuyulardaki Katı-Sıvı Çift Fazlı Akışkanın Basınç Kaybı Modellemesi Ve Deneysel Çalışması", XIX. Ulusal Mekanik Kongresi, Trabzon, Ağustos 2015

- Mehmet Sorgun, Erman Ulker, 2015 "Predicting Pressure Loss for Liquid-Solid Flow in Annulus Using CFD", Applied and Computational Mechanics, Izmir, August 2015

- Ülker Erman,Sorgun Mehmet,Karadeniz Ziya Haktan,Solmuş İsmail (2016). Pressure Losses Measurements Considering Temperature and Pipe Rotation in Annulus. ACE International Congress On Advances In Civil Engineering, İstanbul, September 2016.

- Ülker Erman, Ali Pamukçu, Mehmet Sorgun (2017). Predicting Pressure Loss For A Newtonian Fluid In Annulus Under Effects Of Temperature And Rotation Variation By Artificial Neural Network. IWA-PPFW, İzmir, May 2017

- Ülker Erman, Sıla Övgü Korkut Uysal, Mehmet Sorgun (2017). A Numerical Study Of Turbulent Flow Inside Fully Eccentric Annulus With Inner Pipe Rotation. ICAAMM, İstanbul, July 2017

Research Area at Past

- Hypersonic flow
- Chemically equilibrium/non-equilibrium flow
- Thermally equilibrium/non-equilibrium flow
- Computational fluid dynamics (CFD)
- heat and mass transfer
- numerical studies of fluid flow

Research Area at Present

- Geothermal drilling in high temperature and pressure
- Mathematical modelling of flow behavior

- Hydraulics
- Optimization of flow properties
- Deep drilling

Awards

- **Primary-Secondary –High Schoo:** Governmental scholarship
- **2000**   **:** Prime Minister scholarship
- **2005**   **:** Honor student
- **2007**   **:** Government scholar for foreign education from Ministry of Education
- **2009**   **:** Scholarship for PhD program from University of Arizona

Work Experiences

- **2005 - 2006 :** Owner and Manager at Oz Idil Educational Service
- **2006 – 2008 :** Formal governmental scholar at Ministry of Education
- **2008-2012   :** Research Assistan in University of Arizona
- **2012-2013   :** Officer in R&D department in Directory of Ministry of Education
- **2013 -**: Research Assistant at IKCU, Turkey

Computer Knowledge

- **Programs   :** Matlab, Maple, Mathematica, SolidWorks, Ansys, Visual Basic
  Studio, Linux Suse, Origin, Abaqus, Microsoft Office, Webmatrix,
  Dreamweaver, WordPress,
- **Language   :** Fortran, C#

Language

- Turkish (Fluent)
- English (Fluent)
- Spanish(Basic)